EFFECTIVE MANAGEMENT OF THE RIPARIAN ZONE VEGETATION TO SIGNIFICANTLY REDUCE THE COST OF CATCHMENT MANAGEMENT AND ENABLE GREATER PRODUCTIVITY OF LAND RESOURCES

C Everson • M Gush • M Moodley •
C Jarmain • M Govender • P Dye

WRC Report No. 1284/1/07

Water Research Commission

EFFECTIVE MANAGEMENT OF THE RIPARIAN ZONE VEGETATION TO SIGNIFICANTLY REDUCE THE COST OF CATCHMENT MANAGEMENT AND ENABLE GREATER PRODUCTIVITY OF LAND RESOURCES

by

C Everson[1], M Gush[1], M Moodley[1], C Jarmain[2], M Govender[1] and P Dye[1]

[1] CSIR Natural Resources and the Environment, Private Bag X01, Scottsville, Pietermaritzburg, 3209

[2] CSIR Natural Resources and the Environment, P.O. Box 320, Stellenbosch, 7599

REPORT TO THE WATER RESEARCH COMMISSION ON THE PROJECT "*CAN EFFECTIVE MANAGEMENT OF RIPARIAN ZONE VEGETATION SIGNIFICANTLY REDUCE THE COST OF CATCHMENT MANAGEMENT AND ENABLE GREATER PRODUCTIVITY OF LAND RESOURCES?* (WRC PROJECT NO K5/1284)

Report No: 1284/1/07

ISBN: 978-1-77005-613-8

AUGUST 2007

Acknowledgements

The research in this project was funded by the Water Research Commission, for whose assistance we are sincerely grateful. The Department of Water Affairs and Forestry are thanked for funding in the earlier and later stages of the project. Mondi are thanked for allowing access to their catchment and for contributions in kind (labour, management operations and data). Temesgren Zewotir, from the University of KwaZulu-Natal, for his assistance with the statistical analysis of the streamflow data. We also wish to acknowledge contributions made by members of the steering committee:

Dr R	Dube	*Water Research Commission (current chairman)*
Dr S	Mkhize	*Water Research Commission (past chairman)*
Dr R.	Knight	*University of the Western Cape, Dept of Botany*
Mr A	Khan	*Working for Water*
Mr C	Ruiters	*DWAF*
Mr J	Bosch	*CSIR, Natural Resources and the Environment*
Prof G	Jewitt	*University of KwaZulu-Natal*
Prof P	Roberts	*Forest Industries Association*
Mr P	Gardiner	*Mondi Forests*
Dr N	Lecler	*SASRI*
Prof S	Lorentz	*University of KwaZulu-Natal*
Ms N	Mkhize	*DWAF*
Ms A	Muir	*DWAF*
Mrs L	McKune	*Water Research Commission (secretary)*

The following people provided valuable technical assistance to the trial:

Phillip Vilakazi, Robert Ndedla, Zaheer Rasool, Joshua Xaba, Lucas Ngidi, Vivek Naiken and Alistair Clulow.

Executive Summary

1. MOTIVATION

The concept of the influence of riparian saturated zones in moderating land use impacts on catchment water yields potentially holds great significance to water conservation in forestry catchments, and the overall efficiency of water use by plantation forests. What is unclear is the size and significance of this moderating influence. The purpose of this research project is to investigate the links among vegetation, saturated zone dynamics, and runoff generation for the different classes of riparian zone, and to test the hypothesis that riparian zone vegetation has a significantly variable effect on catchment yields.

2. PROJECT OBJECTIVE

To investigate the links among vegetation saturated zone dynamics and runoff generation for the different classes of riparian zone, and to test the hypothesis that riparian zone vegetation has a significantly variable effect on catchment water yields.

Specific objectives:

- To quantify the influence of stands of *Acacia mearnsii* growing at different distances from the stream channel on soil water storage and streamflow.
- To determine the effect of the re-colonization of the riparian zone by natural vegetation on streamflow.

3. BACKGROUND

The Working for Water programme, funded by the Department of Water Affairs and Forestry, is a multi-million Rand project aimed at clearing alien invasive vegetation from South African river courses. The rationale behind this programme is that the clearfelling of invasives will help to restore the water balance and biological diversity in many of South Africa's most important water yielding catchments. Invaders such as black wattle (*Acacia mearnsii*) impact negatively on water yield from catchments and on natural communities by reducing the biotic diversity. However, the effects of clearfelling these invading trees have not been quantified adequately enough to enable planning of clearing operations to optimise water yield. Neither are there conclusive data to substantiate the benefits of these clearings. Data from catchment experiments in South Africa extend over a period of at least 50 years and have shown that afforestation with alien trees decreases streamflow (Van Der Zel and Kruger, 1975; Van Wyk, 1977, 1987; Bosch and von Gadow, 1990). However, there are only a few studies that have been undertaken to investigate the effect of clearing of indigenous and invasive vegetation in riparian zones. Those that have been undertaken have all shown increases in streamflow (Nanni, 1972; Dye and Poulter, 1995a; Scott and Lesch, 1995, 1996). Of particular interest in this study was the difference in impacts of trees close to streams and those further away from streams.

Re-colonisation of cleared areas with natural vegetation will also have an impact on water yield. In order to quantify the long-term effects of clearfelling invasives one has to compare streamflow responses following clearfelling with those after re-colonisation has taken place.

Commercial forestry companies are required by legislation to leave riparian areas unplanted. The rationale behind this legislation is to reduce the negative impact of trees on streamflow. This practice results in the loss of thousands of hectares of the most productive forestry land. Foresters argue that if they were able to quantify water-use of trees planted at different distances from easily available water resources, they would be able to optimise the water used by commercial forests. Keeping riparian areas clear of weeds is very costly for land owners and they need to know what return in terms of water is achieved for their efforts.

The need to objectively define riparian zones has led to the development of a classification system for stream channels, in which three categories are defined on the basis of the presence and persistence of saturated soil and stream flow in the watercourse. Thus, type A-section channels are associated with ephemeral streams in the upper reaches of a watercourse, and are not associated with a permanent body of saturated soil. Type-B-section channels occur further downstream, and are characterized by ephemeral flow, and a fluctuating water table. Type-C-section channels occur further down stream, and are characterized by permanent channel flow.

With the introduction of the new National Water Act (NWA) (Act No 36 of 1998) in South Africa, there has also been an urgent need to quantify the benefits to downstream users of clearing riparian areas of alien invasives.

4. METHODS

The study catchments were situated at the Mistley-Canema Estate (Mondi Forests) in the Seven Oaks district, approximately 70 km from Pietermaritzburg. Both type A and B class riparian zones were present in the catchment. The experiment was carried out by progressively clearing wattle trees from the riparian to upslope regions from January 2000 to October 2005. This sequence of clearfelling was designed to allow quantification of the relative water-use of trees closer to streams and their impacts on the soil water and streamflow (with emphasis on low flow). A V-notch weir was built in the catchment to provide precise measurements of streamflow. This enabled us to quantify the effects of clearfelling the riparian and upslope areas on the catchment water yield.

4.1 General climatic variables

Rainfall was monitored at three sites in the catchment area using tipping bucket rain gauges.

A Campbell Scientific automatic weather station, located near the Mondi lookout tower, was used to measure ambient temperature, relative humidity, rainfall (0.1 mm), windspeed and direction at hourly intervals during the study.

4.2 Streamflow

Streamflow was monitored continuously in the main catchment using a 457.2 mm, 90° V-notch weir with a Belfort Streamflow recorder modified with an MCS 250-01 streamflow encoder. This was later replaced with an Ott Streamflow recorder and pressure transducer.

4.3 Ground Water Monitoring

The Department of Water Affairs installed eight boreholes (drilled to bedrock) in February 2000. The boreholes were located along the soil water monitoring transects. Two deep boreholes (60 m +) were drilled at the upper and lower reaches of the catchment to monitor the deep aquifer. Depth to the bedrock varied between approximately 6 m near the stream to 14 m at the top of the slope.

4.4 Soil water dynamics

Intensive soil water monitoring instrumentation networks were established along a north-south aspect. Twenty-five aluminium access tubes were installed to a depth of 2.0 m, roughly equidistant apart along the transect, so that soil water content could be measured with a neutron probe. The measurements were made at six depth intervals within each access tube.

To measure soil water potential, fifty-six tensiometers arranged in fourteen nests of four tensiometers each were installed at strategic locations along the common transect within the B zone of the catchment. A further fourteen nests of tensiometers were installed in a spatially distributed system within the A-Zone. Each nest had three instruments located at soil depths of approximately 0.3, 0.6 and 1.5 m. At six of these nests neutron probe access tubes were installed to soil depths approaching 6 m.

Five additional nests of watermark sensors manufactured by the Irritol Corporation were installed along a single transect within the A-Zone in October 2003 and this was extended into the B-Zone and riparian area during November 2004.

The drainage line in the A-zone was further instrumented with runoff plot to measure surface and subsurface runoff.

4.5 Evaporation Monitoring

Sapflow by trees was measured using the heat pulse velocity technique (Dye *et al.*, 1992). Evaporation of the recolonised natural grassland in the cleared riparian strip was monitored using the Bowen ratio energy balance technique (Everson *et al.*, 1998). The FAO 56 formulation was used to calculate the potential evaporation.

4.6 Catchment scale modelling

The SWAT and ACRU models were used to predict the relative impacts of changes in management practices and vegetation, on water quantity. The aim of this aspect of the project was to conduct a verification of the SWAT and ACRU models using the Two Streams Catchment data and to carry out long-term simulations on the impact on streamflow of *Acacia mearnsii* on the hydrology of the study catchment.

5. RESULTS AND DISCUSSION

Annual rainfall totaled 1071 mm, 898 mm, 1171 mm, 659 mm, 727 mm and 1139 mm for the 1999/2000, 2000/2001, 2001/2002, 2002/2003, 2003/2004, and 2004/2005 seasons (hydrological year Oct-Sep) respectively. The five year study period was therefore characterised by both dry and wet conditions as the long-term average for the area is 853 mm.

Annual streamflow for the study period averaged only 33.5 mm, with highs of 46.1 and 91.8 mm in the high rainfall years. In the driest year (2002/2003 – MAP of 659.1 mm) the stream discharge was only 6.7 mm. Streamflow was only a small fraction of the annual rainfall, with the average rainfall:runoff ratio (Rr) = 3.4%.

Evaporation of the recolonised natural grassland in the cleared riparian strip showed that grassland evaporation ranged between 3 and 6.5 mm day^{-1}, showing the large contribution of the grassland to water use within the catchment during the summer periods. Clear trends of low evaporation in the dry winter period followed by peak rates in mid summer were shown by these data. It is during the winter period, when the grass has senesced, that the wattle trees used more water. These data do however illustrate the very high water use (summer maxima > 6 mm day^{-1}) of the predominantly dense *Setaria megaphylla* vegetation in the riparian strip.

Soil water potential within the Two Streams catchment was found to be strongly seasonal. During summer matric potential was high due to abundant rainfall but decreased rapidly from the onset of winter (usually at the end of March). By the end of July the soil was at its driest limit. Matric potential, especially within the topsoil, decreased gradually in response to drainage and evaporative drying. Hillslope topographic position and aspect also had a notable influence on soil water dynamics. The A-Zone which was characterised by the absence of a permanent water table was consistently found to be the driest part of the hillslope segment. The B-Zone was on average much wetter. An interesting finding is that during summer when rainfall is high, the deeper soil depth within the B-Zone was consistently found to be drier than higher up the soil profile, but a reversal in this trend occurs from the onset of winter where the deeper parts of the soil appear to be wetter. This suggests that during summer, which is often associated with short-duration high intensity rainfall episodes, much of this water does not percolate completely to the deeper layers but rather moves laterally in the near-surface horizon to augment streamflow. Interflow during summer therefore appears to be a significant flow pathway in this catchment. This process could also be aided by the presence of macro-pores and channels in the topsoil formed by the mechanical action of the roots of trees as well as the incorporation of organic matter and the presumably more intense faunal activity. On average, the south facing slope was wetter than the north facing slope with comparatively lower matric potentials owing mainly to differences in evaporative demands.

Compared to elsewhere in the catchment (upslope B and A-Zone), the soil within the riparian zone was much wetter. On average the soil in the riparian strip at a depth of 1.20 m remained close to saturation and at 2.0 m the soil was permanently saturated, even during winter. Seasonal fluctuations in water potential are more accentuated for the upper part of the riparian soil (0 - 0.80 m) as it is this part of the soil environment that would be subject to the greatest evaporative demands. Even so the water potential of the topsoil only reached a minimum of -40 kPa during mid-winter. The rate at which the water potential of the topsoil decreased following the onset of winter was also much lower than in the upslope B and A-zone portions of the catchment. These findings offer support for the generally accepted view that riparian zones are an integral component of the catchment responsible for the regulation of streamflow and that these systems need to be protected to ensure adequate water supply.

The removal of the 7.5 ha of trees from the riparian zone in May 2000 clearly had a positive impact on the runoff from the treated catchment. Notably, the stream continued to flow throughout the five winter periods of the study following the riparian treatment. This contrasts with the pre-clearing period when the stream only began flowing in late summer. Our data indicated that evaporation in the riparian zone was approximately 1-2 mm day^{-1} during the winter months. However, wattle tree transpiration during August was generally above 3 mm day $^{-1}$. It is these seasonal differences in evaporation between the dormant grassland and evergreen exotic trees which result in streamflow reductions, as summer evaporation rates of the trees and grasses were similar.

The annual evaporation estimated by subtraction in the water balance equation, varied widely from 700.7 mm in 2003/2004 to 1120.7 mm in 2001/2002. The average evaporation was 884.7 mm, while the average annual FAO 56 reference evaporation was 1234 mm annum^{-1}. The evaporation was a very high percentage of the annual rainfall (mean = 94.5%). In the 2002/2003 year this percentage was 106.9%, indicating that the evaporation exceeded rainfall.

The impact of the clearing of **all** the trees by January 2004 was a 44% increase in streamflow. This was equivalent to 75 000 cubic meters for the catchment. The relative contribution of the riparian zone compared to the upslope region during the period when both areas were cleared (January 2004 to May 2006) was 16 mm and 78 mm respectively (the riparian zone therefore contributing 21% to annual streamflow). Since the riparian zone represented only 11% of the total catchment area (7.5 ha versus 65 ha, Table 3.1), the significance of the riparian zone to streamflow generation was clearly demonstrated.

6. CONCLUSIONS

The data collected in this study have demonstrated the impact of both riparian and upland wattle on the streamflow of a small catchment in the KwaZulu-Natal midlands. The results show that the streamflow reduction resulting from the combined effects of the riparian and upslope wattle trees is a decrease in runoff of approximately 44%. Both the ACRU and SWAT models have been successfully validated using the Two Streams catchment data sets. The models showed a streamflow reduction of about 75 mm $annum^{-1}$, when compared with natural grassland. The modelled data were in close agreement with the measured data.

7. EXTENT TO WHICH THE CONTRACT OBJECTIVES HAVE BEEN MET

The objective of this research was to investigate the links among vegetation, saturated zone dynamics and runoff generation for the different classes of riparian zone and to test the hypothesis that riparian zone vegetation has a significantly variable effect on catchment water yields.

After six years of intense hydrological monitoring the impacts of clearing the riparian and upslope vegetation have been quantified. In addition, a valuable data set has been created which makes an excellent platform for future research. A difficult aspect of the project was the short calibration period and failure of the control catchment weir. Clearly further monitoring in this catchment is warranted to advance our understanding of riparian zone dynamics.

8. CAPACITY BUILDING & TECHNOLOGY EXCHANGE

At the beginning of this project expertise in riparian zone hydrological behaviour in South Africa resided with a very small group of scientists. The thrust of this project into the understanding of riparian zone processes and the consequent management implications has given impetus to the development of skills in riparian zone management. By collaborating with the School of BEEH at the University of KwaZulu-Natal through Prof Lorentz and Prof Peter Roberts, the project team has gained valuable experience in this important area of hydrological research. Initially Ms G King (geohydrologist) and Ms Naledi May (potential MSc student) were included in the project team. Ms King left SA permanently for the USA and Ms May moved to another DWAF project. However, a great amount of knowledge and skill development has been transferred into the larger team consisting of Colin Everson, Mags Moodley, Mark Gush, Marilyn Govender, Caren Jarmain, Vivek Naiken, J Xaba, Alistair Clulow and Lucas Ngidi.

Students from the School of BEEH have also been exposed to learning from the project on a regular basis as part of their training in Hydrology.

9. RECOMMENDATIONS

Recent studies and modelling of forestry water use has shown that our best estimates of tree water use, and in particular dry season water use, are not within acceptable error margins (Gush *et al.*, 2002). One of the main reasons is the inability of hydrological models (such as ACRU, and others) to accurately simulate the deeper soil water processes. This limitation of the models stems from our lack of understanding of tree root behaviour and its effect on soil water in deeper soil layers. The impact of tree water use on deeper soil water stores has wider consequences such as the impact of trees on critical low flows, the impacts of trees on ground water resources during prolonged droughts and the impacts of trees in riparian zones. In a wider context it has an impact on effective and efficient allocation and management of water resources (in particular forestry, but also all other streamflow reduction activities). The Two Streams catchment experiments have been used to study the impact of trees on soil hydrological processes. The experiments now provide a good opportunity for studies to extend our understanding of other processes such as low flows and deeper soil water dynamics. The Two Streams catchment is one of the few remaining small catchment research areas in South Africa. With six years of intense hydrological monitoring this fallow catchment presents an ideal opportunity to study the impact of a newly planted crop. The motivation for these studies is based on a number of needs: *1*. The need for increased food and timber production has led to dramatic increases in irrigated and forestry lands in South Africa. Agriculture and forestry face increased competition for water by industries, municipalities and other groups. This ever-growing demand for water makes it imperative that water resource management procedures and policies be wisely implemented and improved. To do this, we need to improve our understanding of the impacts of different crops on the water balance of catchments. *2*. DWAF is deeply concerned by the need to link afforestation schemes to low flows in streams and rivers, since the allocation of land use and re-allocation (changes in land use) depend on accurate estimates of tree water use impacts on low flows and ground water resources. *3*. Allocation of water to stream flow reduction activities must take into account the difference in water use between forests and other crops and natural vegetation. Information on these is urgently required. *4*. A recent study on the comparative water use of Eucalypts and Black Wattle trees in the Natal midlands at Seven Oaks (Jarmain and Everson, 2002) showed that total evaporation exceeds rainfall during the exponential growth phase of the trees (for example, the four year accumulated evaporation at the eucalyptus site exceeded the rainfall by 75%). Studies in the Mpumalanga area (Dye *et al.*, 1997) have also demonstrated the reliance of Eucalyptus trees on soil water stored at depths beyond 8 m. This raises concerns over the impact of deep-rooted trees "mining" the soil water and ground water reserves. The effect of excess evaporation over rainfall is ultimately transmitted into reductions in streamflow.

Data from the Mokubulaan research catchments in Mpumalanga (Scott and Lesch, 1997), showed a five-year lag in streamflow recovery following clearfelling of *Eucalyptus grandis*, suggesting that abstraction of soil water from deep profiles may cause significant lags in streamflow response to management activities within the catchment. Currently authorisations for water use are based on generalised curves estimated from tree water use over entire rotations (Gush *et al.*, 2002), which does not account for periods of high water use. In addition the model used did not account for soil water at depths greater than 1.2 m. Gush *et al.* (2002) concluded that our understanding of the hydrological processes with regard to the water use of trees from deep profiles is inadequate. Specifically, potential errors in low flow estimates are in the order of 50% or more, which could have serious consequences for downstream users during times of low flows. Clearly, a better understanding of the hydrological processes of deep-rooted trees is needed to improve the granting of licenses to water users and for water allocation.

10. DATA

All processed data have been catalogued and stored at Environmentek, CSIR, c/o Department of Agrometeorology, UNP, P/Bag X01, Scottsville, 3209.

Contact person: Dr. C.S. Everson.

These data are held on non-flexible diskette. All data can be supplied to researchers and managers on CD-R diskettes.

11. PUBLICATIONS

Everson C.S, Gush M.B, Dye P., Moodley, M., Jarmain C. and Govender M. (2003).The influence of *Acacia mearnsii* (Black Wattle) on the water yield of a first order catchment. Poster presentation, WfW symposium, Cape Town.

Table of Contents

List of figures

List of tables

CHAPTER 1: INTRODUCTION

Wetlands are a common feature of all landscapes, manifesting themselves as ponds, springs, seeps, bogs and mires to mention just a few. Of interest in this report is the interconnection of wetlands through river channels (with riverbanks), which can be broadly defined as riparian habitats. The economic and ecological importance of wetlands is well recognised internationally. Despite this recognition, it is estimated that over 50% of South Africa's wetlands have already been destroyed. The main cause has been the drainage of wetlands for crops and pastures, overgrazing, planting of alien trees in riparian zones and urban development. Since wetlands play such a vital role in the hydrology of catchments (attenuation of floods, prevention of soil erosion, removal of pollutants, plus many more) their importance and function has been recognised in the National Water Act of 1998. In the Act riparian habitat is defined as the physical structure and associated vegetation for the areas associated with a water course which are commonly characterised by alluvial soils and which are inundated or flooded to an extent and with a frequency sufficient to support vegetation with a species composition and physical structure distinct from the "drier" adjacent land areas.

Riparian habitats often represent the deepest, most fertile soils in a catchment, and the high soil water contents make them ideal for plant establishment and growth. For these reasons areas of riparian zones which show temporary periods of wetness normally produce the highest growth rates of commercially planted trees, making them vulnerable to exploitation by the forest industry. Areas in the seasonal and permanent zones where anaerobic saturated conditions exist may limit the growth of non adapted tree species. Since growing trees in the riparian zone results in a decrease in riparian functioning (through increased water use and loss of biodiversity), the forest industry has adopted a proactive approach to optimise water use, primarily by protecting the riparian zone (Woodborne, Robertson & February 2003). This delineation of riparian zones has recently been described in "A practical field procedure for the identification and delineation of wetlands and riparian areas" (Department of Water Affairs and Forestry, undated). Policy and legislation around riparian zone management has been disjointed and has varied considerably over the years. However, the National Water Act (No. 36 of 1998), Section 21 c (impeding or diverting the flow of water in a watercourse) and 21 (i) (altering the bed, banks, course or characteristics of a watercourse) addresses matters impacting on a watercourse. To determine the boundary of a watercourse one needs to delineate a wetland or river to determine the extent of the watercourse. This helps to evaluate the proposed impact of the activity on the watercourse. From here DWAF can recommend that the activity be moved outside the watercourse and set conditions to protect the watercourse. Protection of the water course could require a buffer zone, which may be beyond the limits of the watercourse. The advantage of staying outside a watercourse is that no water use licences for 21 c or i of the National Water Act (No. 36 of 1998) would be required.

Because of the loss of these highly productive riparian areas to the forest industry, riparian zone management has become an important issue in water conservation in South Africa and water resource managers are under increasing pressure to assess the impact of different land uses and management practices on catchment water yield. The need to exclude plantation trees from riparian zones is widely accepted within the forest industry, but it is also recognised that not all riparian zones in a catchment are equally effective in influencing catchment yields.

Since riparian soils are often the wettest and most fertile within a catchment, and are therefore extremely productive, there is strong interest in moving away from the use of a standard width throughout the catchment, and rather to identify the required limits to the riparian zones on the basis of more objective criteria. This need has led to the development of a classification system for stream channels (P.J. Robert, *pers comm.* [1]), in which three categories are defined on the basis of the presence and persistence of saturated soil and stream flow in the watercourse (Figure 1.1). Thus, type A-section channels are associated with ephemeral streams in the upper reaches of a watercourse, and are not associated with a permanent body of saturated soil (Figure 1.2). Type B-section channels occur further downstream, and are characterized by ephemeral flow, and a fluctuating water table defining the surface of a body of permanent saturated soil water (Figures 1.1 and 1.2). This saturation is indicated by soil indicators such as discernible mottling and gleying. Type C-section channels occur further down stream, and are characterized by permanent channel flow. Theoretical analyses of these different riparian zones have led to the conclusion that riparian vegetation alongside type A-section channels has minimal impact on catchment water yields, and therefore does not require exclusion status. Catchment yields are believed to be especially sensitive to vegetation influences along type B-section channels, since changes in plant water use can greatly alter the surface area of saturated soil, and hence the amount of saturation overland flow of that region of the stream. Type C channel sections are characterized by perennial flow and often less fluctuation in the surface area that generates saturation overland flow. Although the absolute amount of streamflow reduction is probably less in B-sections than in C-sections, the biological and hydrological impacts may be greater in the B-section, as the stream could go from some flow to no flow. This is in contrast to C-sections, which may only experience a reduction in flow due to the greater volumes concerned. The reader is referred to the practical field guide (DWAF, undated) for a complete description of the procedures used to delineate riparian zones/wetlands in forestry plantation catchments.

[1] Prof P Roberts- Forest Industries Association

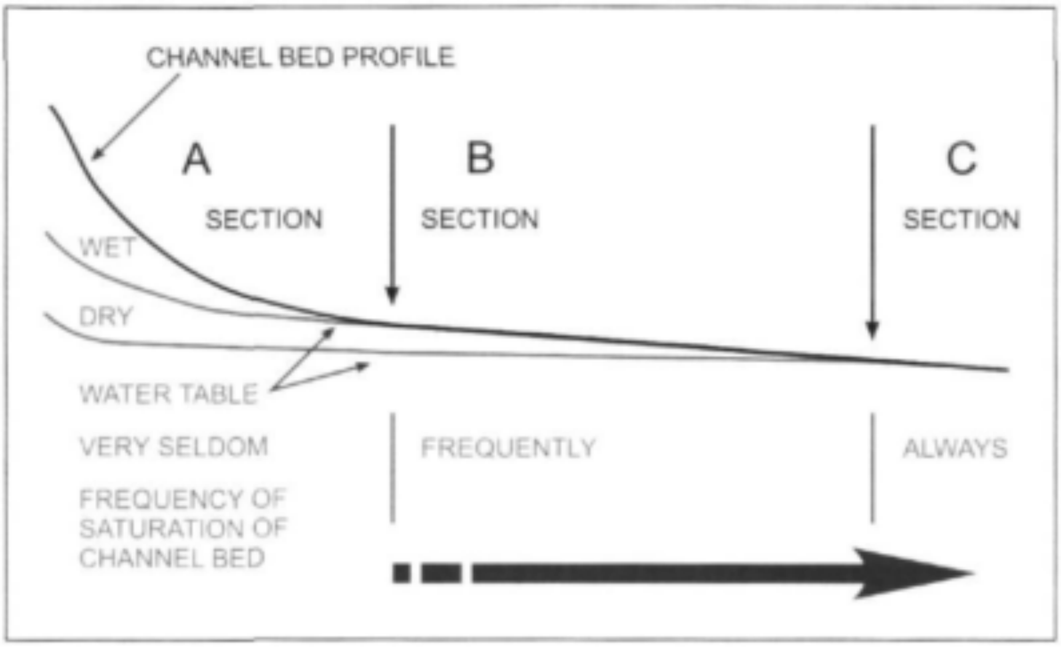

Figure 1.1 Longitudinal profile of a river bed showing classification of channel sections (DWAF undated).

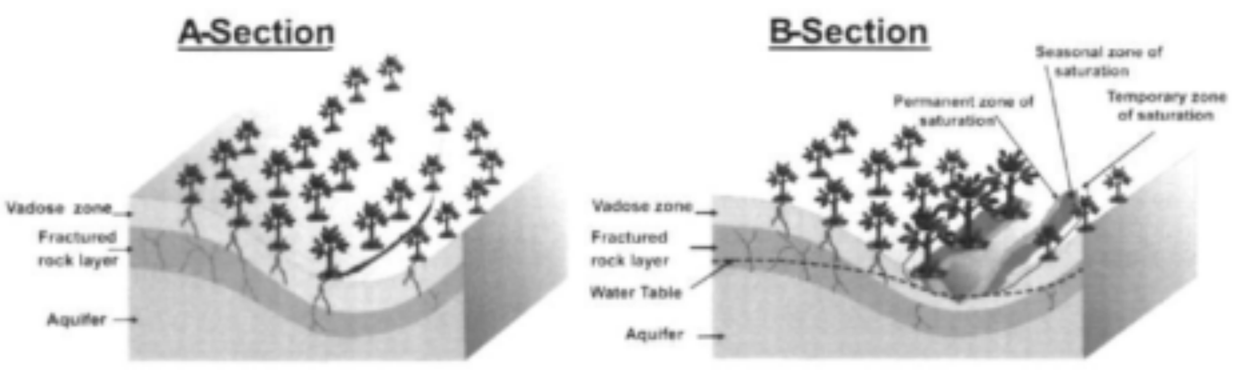

Figure 1.2 Diagrammatic representation of A and B riparian sections in a catchment.

This concept of the influence of riparian saturated zones in moderating land use impacts on catchment water yields potentially holds great significance to water conservation in forestry catchments, and the overall efficiency of water use by plantation forests. What is unclear is the size and significance of this moderating influence. The purpose of this research project was to investigate the links between vegetation, saturated zone dynamics, and runoff generation for the different classes of riparian zones, and to test the hypothesis that different riparian zone vegetation (wattle trees and grasses) have significantly different effects on streamflow.

1.1 Experimental Approach

Two approaches have been adopted in this study namely,

1. Hillslope soil water dynamics measured before and after a change to riparian or hillslope vegetation, to record the effects of the treatment on the soil and streamflow regime.
2. A modelling study to see the data from above in the context of the complete catchment. The streamflow models tested in this study are the Agricultural Research Catchment Unit (ACRU) and the Soil Water Assessment Tool (SWAT).

1.2 Project objective

To investigate the links among vegetation, saturated zone dynamics and runoff generation for the different classes of riparian zone, and to test the hypothesis that riparian zone vegetation has a significantly variable effect on catchment water yields.

Specific objectives:

- To quantify the influence of stands of *Acacia mearnsii* growing at different distances from the stream channel on soil water storage and streamflow.
- To determine the effect of the re-colonization of the riparian zone by natural vegetation on streamflow.

1.3 Funding

The original "Two Streams" project (funded by WfW), was planned for three-years and was started in 1999 and ended in March 2002. This project was the focus of intensive research by the CSIR's hydrology group at Pietermaritzburg and the scale of the research expanded greatly in these first three years. The construction of gauging weirs, drilling of boreholes and instrumentation of the catchment took longer than originally anticipated. Because of these problems it became clear during the 2000 year that additional support would be needed in order gain maximum benefit from the funds already invested. Thus a second proposal to support this research and extend the measurements into an "A-section" was submitted to the WRC and approved in April 2001. This funding extended the monitoring into early 2003.

Following a short calibration period, all the trees in the "B" riparian zone were cleared in July 2000. Eighteen months of data were collected to assess the impact of this clearfelling on runoff and hillslope hydrological processes. The plans to remove all the trees from the entire catchment in 2002 were delayed by technical problems experienced by Mondi with stripping the bark and the trees were only finally felled from the catchment by December 2003. Although this allowed extended monitoring of the recovery of the riparian zone, it shortened the monitoring period of the cleared catchment. The continuation of the monitoring of the project in 2003 /2004 and subsequent data analysis and write up in 2005 was therefore requested from WfW and the project was awarded an extension to 2005. These funds were transferred to the WRC who continued to manage the project.

CHAPTER 2: THE STUDY AREA

The Mistley-Canema estate (Mondi Forests) in the Seven Oaks district is situated in the KwaZulu-Natal midlands (Figure 2.1). The Bioresource Group (BRG) (Camp, 1997), is "moist midlands mistbelt". The area is generally hilly, rolling country, with a high percentage (46%) of arable land. The climate is humid; with an annual rainfall ranging from 800 mm to 1280 mm. Heavy mists are a common and important feature, providing additional moisture, particularly to forests. The mean annual temperature is 17°C. Climate hazards include occasional droughts, usually of short duration, occasional hail and frost which vary from slight to severe. Hot "berg winds", followed by cold fronts, make for unpredictable conditions, particularly in spring and early summer (Camp, 1997).

Figure 2.1 The locality of the Seven Oaks district in the KwaZulu-Natal midlands.

The natural vegetation of the area was previously *Themeda triandra* grassland. Only a few relic patches remain, as the high potential of the arable areas has meant that little value has been placed on the natural veld. The potential of the soils of the area is high, in spite of the fact that the inherent nutrient status is very low. Particular problems are P-fixation and Al-toxicity. The soils are highly leached and the area is suited to intensive farming systems. Forestry is ecologically suitable and is the most widespread land use, with gum (eucalyptus spp.), pine and wattle being the species of choice. Sugar cane is grown on sites where drainage of cold air is good, ensuring that no frost or only light frost occurs.

2.1 Study Site

Two small catchments, planted with 13-year-old wattle were selected as the study site. The catchments are situated at the Mistley-Canema Estate (Mondi Forests) in the Seven Oaks district, approximately 70 km from Pietermaritzburg (30.67°S, 29.19°E). The catchment on the Mistley Estate at Seven Oaks has both type A and B class riparian zones (Figure 2.2).

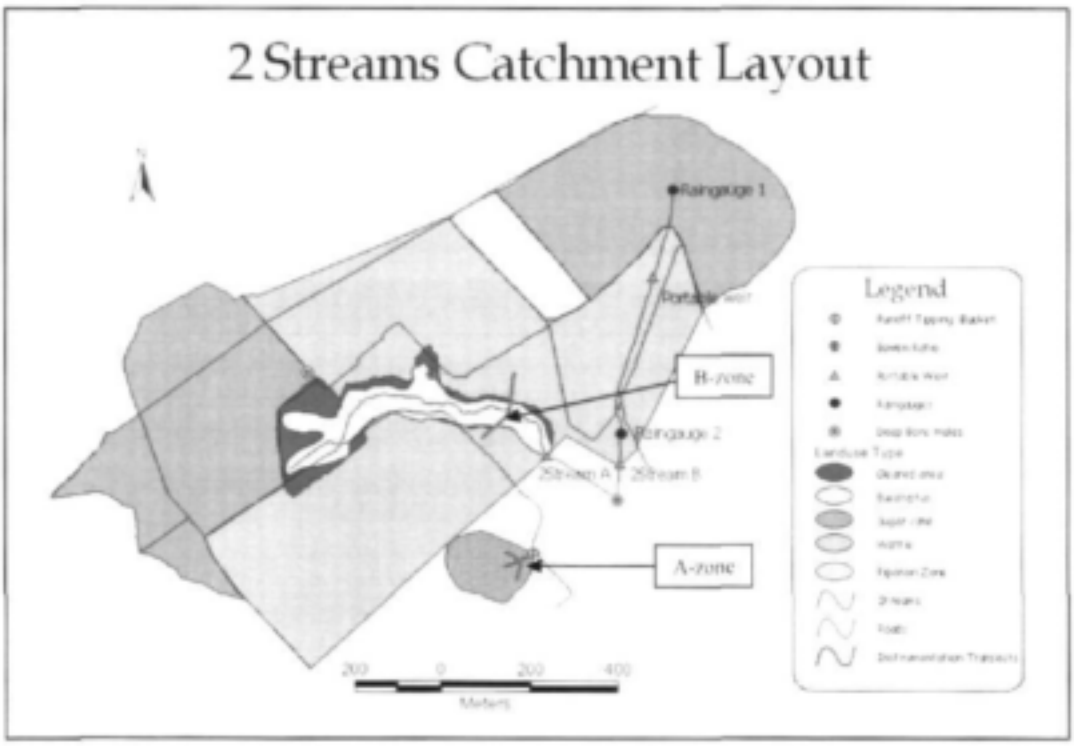

Figure 2.2 Map showing the position of the various monitoring stations on the North and South hillslope study transects.

The catchment details (boundaries, streams, roads, weirs, rain gauges, landuse, and monitoring sites) were mapped using a Trimble geographical positioning system, with accuracy better than 0.20 m and captured into Arc View GIS coverages (Figures 2.2 & 2.3). A profile of the monitoring transect for the B-zone was also created (Figure 2.4). The position of the riparian zone was delineated using the new riparian classification that delineates according to the presence of both a permanent and temporary water table. The Two Streams catchment has been classified as a typical "B-stream", where the contact of the water table and the stream is not permanent as in "C class" streams. A-zones were identified in the upper catchment where no permanent water table exists (Figure 2.5) and were characterised as a shallow drainage line with a lack of any indicators of saturation in the soil profile.

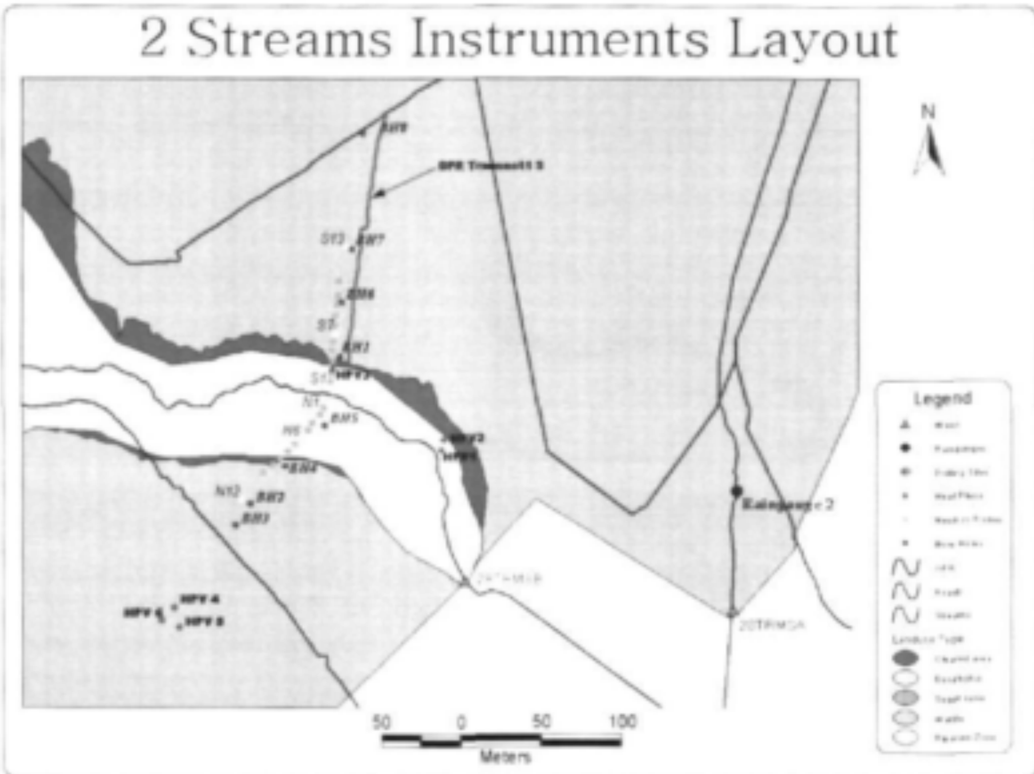

Figure 2.3 Map showing the position of the various monitoring stations on the North and South hillslope study transects.

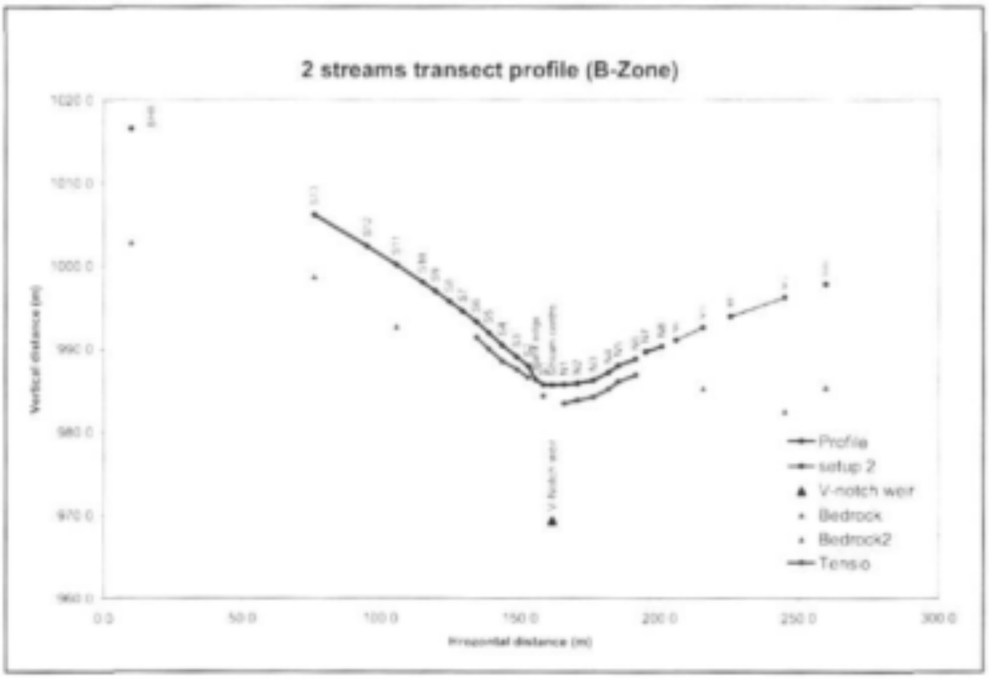

Figure 2.4 Transect profile of monitoring stations for the two streams catchment B-section channel.

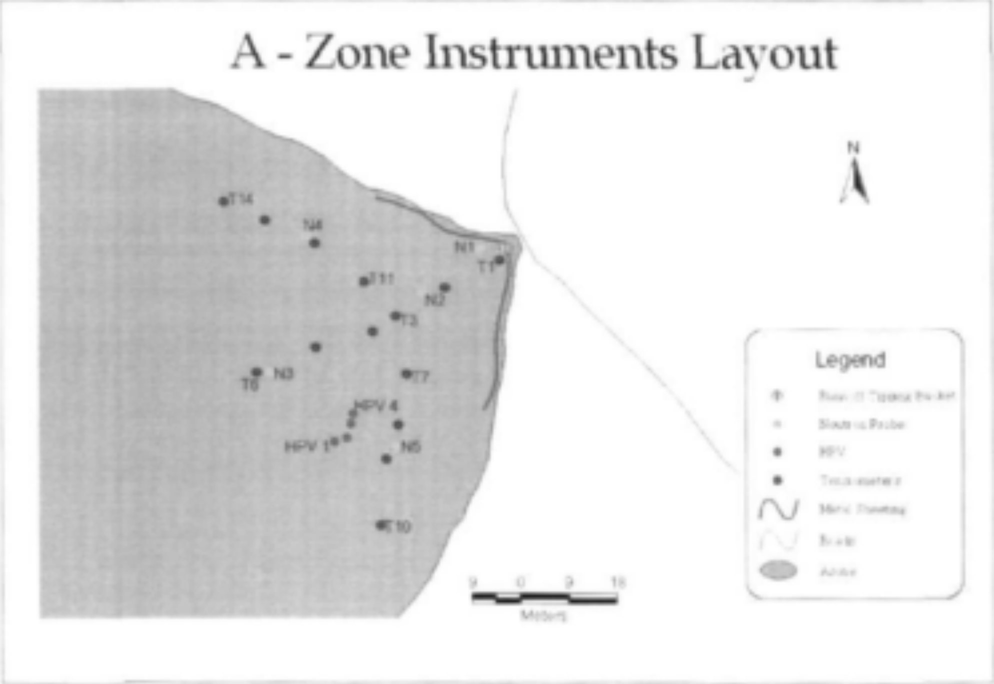

Figure 2.5 Map showing the position of the various monitoring stations on the A-section hillslope transects.

CHAPTER 3: MATERIALS AND METHODS

3.1 Rainfall

Rainfall was monitored at three sites in the catchment area (see Figure 2.2 for locations) using tipping bucket raingauges (MCS-160) with a 0.2 mm resolution. Gauging sites consisted of an upper site at an altitude equivalent to the top of the catchment, and a lower site at a similar altitude to the weir. A further raingauge was situated under the forest canopy within the A-zone. These gauges facilitated the collection of rainfall data across the altitude gradient of the study area. In general there was good correlation between the upper and lower gauges. The experimental set-up included an additional raingauge which was located below the *Acacia mearnsii* (wattle) canopy in the A-zone site. This was used to evaluate intercepted water losses.

3.2 General climatic variables

A Campbell Scientific automatic weather station, located near the Mondi lookout tower, was used to measure ambient temperature, relative humidity, rainfall (0.1 mm), windspeed and direction at hourly intervals during the study.

3.3 Streamflow

The experimental framework consists of a V-notch weir built in the river of the catchment to be cleared. A second weir was established on an adjoining stream to act as a control. Streamflow has been monitored continuously in the main catchment using a 457.2 mm; 90° V-notch weir with a Belfort Streamflow recorder modified with an MCS 250-01 streamflow encoder. This was later replaced, after theft of the original instruments, with an Ott Streamflow recorder and pressure transducer supplied by DWAF. The calibration of the weir was carried out by DWAF staff and appropriate rating tables were provided. Unfortunately the control catchment weir installed by DWAF had an underground leak and could not be used for paired catchment analysis of the effects of the different management treatments. For this reason both statistical (see section 4.2 - breakpoint analysis) and modelling approaches were used.

3.4 Ground Water Monitoring

Eight boreholes (drilled to bedrock) were installed by DWAF in February 2000. The boreholes were positioned along the soil water monitoring transects. Two deep boreholes (60 m +) were sunk at the upper and lower reaches of the catchment to monitor the deep aquifer. Depth to the bedrock varied between approximately 6 m near the stream to 14 m at the top of the slope for the shallow boreholes.

3.5 Soil water dynamics

In February 2000 soil water monitoring instrumentation networks, spanning the topographic extent of the B-zone were established along a north-south aspect (Figure 2.3). Twenty aluminium access tubes were installed roughly 20 m apart to a depth of 2.0 m along the transect (Figure 2). A Campbell neutron moisture meter was used for the determination of soil water content at these points. Weekly count ratios were routinely taken from these sites at 0.30 m depth intervals to 1.8 m. The neutron probe was calibrated against gravimetric samples (Figure 3.1). The relationship between the count ratios and mass water content (g/g) was found to be significant with a R^2 of 0.75. The linear equation y = 0.225 X – 0.111X where X is the count ratio was used to convert count ratios to mass water content. The mass water content values were then converted to volumetric water content using previously determined values of the soil bulk density. From these data the total profile water contents (mm / 1.8 m) were calculated for each access tube along the 200 m transect. Five neutron probe access tubes were also installed within the A-zone site to an approximate depth of 5.5 m to measure the water content of the soil at deeper levels at this site.

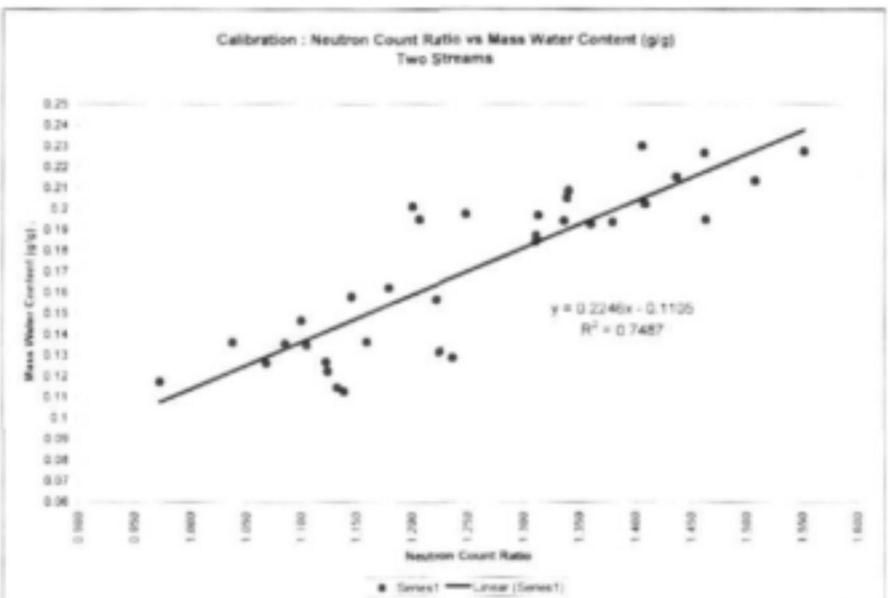

Figure 3.1 Calibration relationship of the neutron probe count ratios vs mass water content (g/g).

Since soil water retention is an important parameter that regulates the storage and movement of water and ultimately plant growth, it was considered important to gain insight into this parameter as it relates to hillslope dynamics. Water at any given point in the soil can be associated with a specific energy state. This is influenced by gravity, the forces arising from the presence of solutes in the soil solution and the forces generated by the mutual attraction of the soil water and the solid matrix. In practice it is difficult to evaluate each of these components separately. Because of this the total soil water potential is more easily obtained by measuring another related property or properties such as hydrostatic pressure, vapour pressure or elevation. A useful measure is the soil matric potential, which relates the soil water pressure against that of the atmosphere. In unsaturated soils the soil water pressure is sub-atmospheric due to capillary forces and hydration envelopes on the solid matrix. In saturated soils on the other hand, as would by definition be the case beneath a water table, the pressure is positive.

To measure soil water potential, fifty-six tensiometers arranged in fourteen nests of four tensiometers each were installed at strategic locations along the common transect within the catchment (Figure 2.3). The four tensiometers within each nest were installed at roughly 0.3 m, 0.6 m, 0.9 m and 1.8 m depths. Briefly, each tensiometer comprised of a porous ceramic cup connected to a de-aired water filled tube terminated on the upper end by a differential pressure transducer. The porous ceramic allows for the exchange of water between the tensiometer and the surrounding soil environment until a state of equilibrium is reached. The pressure transducer senses the difference between the ambient air pressure and the soil water potential and emits a voltage signal that is recorded by a CR10X datalogger every 12 minutes. A calibration relationship, derived for each pressure transducer before the start of this study, allowed for the conversion of the voltage signal to soil water potential, which was then corrected for the depth of the ceramic below the soil surface.

A further fourteen nests of tensiometers were installed in a spatially distributed system within the A-Zone. Each nest had three instruments located at soil depths of approximately 0.3, 0.6 and 1.5 m. At six of these nests neutron probe access tubes were installed to soil depths approaching 6 m. Measurements of water content at 0.30 m depth intervals were made using the neutron probe. The drainage line in the A-zone was further instrumented with a surface and subsurface runoff plot. A tipping bucket connected to a Hobo event logger measured the amount of surface runoff from the plot while rapid interflow was collected in specially designed buckets that also acted as sediment traps.

For reasons expanded upon later in this report, five additional nests of watermark sensors manufactured by the Irritol Corporation were installed along a single transect within the A-Zone in October 2003 and were extended into the B-Zone and riparian areas during November 2004. These sensors contain electrical resistance circuitry embedded within a specially designed granulated matrix. Since the pore-size distribution of the matrix is known a measure of water potential is obtained from the soil water content which in turn is related to electrical resistance. The manufacturer offers a calibration relationship between electrical resistance and soil water potential. Whereas tensiometers cease operating beyond a matric potential of -80 to -90 kPa, watermark sensors have a far greater operating range, typically in the order of 0 to -200 kPa, although for drier conditions these sensors need to have their calibration verified. Watermark sensors are, however, temperature dependent so soil temperature, which is considered in the calibration relationship, needed to be measured. All sensors were mounted at the end of a 25 mm PVC conduit within which was added a copper-constantan thermocouple to obtain a measure of soil temperature. To install the sensors a 30 mm diameter shaft was first augured to the required sensor depth. Slurry containing the recently excavated soil was then poured down the shaft before installing the sensor. This was necessary to minimise the risk of air gaps, between the sensor and surrounding soil. All sensors were wired via an AM416 Campbell multiplexer to a CR10X datalogger programmed to record soil water potential every 12 minutes. The advantage of this system, beyond that of a greater operating range, was that once installed, no further maintenance of the sensors was required, unlike with tensiometers.

Undisturbed soil cores, retained within a 50 mm x 75 mm stainless steel sleeve, were collected from the B- and riparian zones in order to measure water retention properties, bulk density and saturated hydraulic conductivity. Three depths (0, 0.50 m and 1.5 m) were sampled in the B-Zone and two depths (0 and 0.50 m) in the riparian zone. An equivalent set of disturbed samples was collected for the measurement of particle size, pH and organic carbon. Water retention and saturated hydraulic conductivity were measured on the same cores. This meant that the bulk density of each core had to be determined beforehand as any loss of soil when measuring the saturated hydraulic conductivity, could have compromised the accuracy of the results. Considering that the mass of the stainless steel sleeve used to retain the sample was known, only the field mass water content of each core needed to be determined in order to calculate its equivalent oven-dry mass and thus its bulk density. This measurement was carried out on the excess soil removed during the trimming of each core. The cores were saturated overnight and equilibrated at matric potentials of 0, -1, -2, -3, -4, -5, -6, -8, -10 kPa using sand bath tension tables and at -30, -60 and -100 kPa using pressure plate apparatus.

After equilibration at a matric potential of -100 kPa, the steel sleeve containing the sample was lengthened, by taping an empty duplicate sleeve to the upper end. The cores were then re-saturated overnight and fitted with a plastic funnel that contained a wire mesh upon which the base of the sample rested. Saturated hydraulic conductivity was measured by the constant head method (Klute and Dirksen 1986) with a hydraulic head of 50 mm.

The bulk density (ρ_b) and the mass water content of the sample (θ_m) at each matric potential were used to calculate the volumetric water content (θ_v) using the relationship$\theta_v = \theta_m \times \rho_b/\rho_w$ (where ρ_w = density of water). During trimming of the cores a portion of the excess soil was air-dried, crushed to pass a 2 mm sieve, and poured into pre-weighed rubber rings (9.5 mm high, 52 mm i.d.). The samples were leveled within the rings, capillary saturated for 24 h and desorbed on a 15 bar pressure plate at a matric potential of -1500 kPa. After reaching equilibrium the content from each ring was removed and its mass water content determined by oven drying. This mass water content and the bulk density of the core from which the sample was obtained were used to make the conversion to volumetric water content. This procedure was used to reduce the time that would have been required to equilibrate the large cores at -1500 kPa matric potential. Readily available water (RAW) and plant available water (PAW) were calculated for each treatment as the amount of water retained between matric potentials of -10 and -100 kPa and -10 and -1500 kPa respectively (Smith *et al.*,1995).

The water retention data were fitted by the van Genuchten (1980) (VG) model, $\theta = \theta_r + (\theta_s - \theta_r)[1 + (\alpha.h)^n]^{-m}$, where θ is the actual volumetric water content, θ_s is the saturated water content, θr is the residual water content usually taken as the water content at the wilting point (-1500 kPa), *h* is the water potential, α is a curve fitting parameter, the inverse of which relates to the air entry potential, and m and n are dimensionless parameters related to the pore size distribution (van den Bergh *et al.*, 1997). It has been suggested by van Genuchten (1980) that the parameter m may be evaluated by the relationship m = 1 - 1/n, which reduces the number of parameters that must be determined from five to four. Beginning with the measured water retention curve and an initial estimate of the parameters, a non-linear least squares approach was used to iteratively find an equation that maximized the sum of squares associated with the model while minimizing the residual sum of squares. The residual sum of squares represents the degree of bias or lack of fit and the contribution of random errors. In this study the RETC code (van Genuchten *et al.*,1991) was used to parameterise the mean water retention curve determined from four replicates.

3.6 Evaporation Monitoring

Direct measurements of sapflow by trees were measured using the heat pulse velocity technique. Evaporation of the recolonised natural grassland in the cleared riparian strip was monitored using the Bowen ratio energy balance technique.

3.6.1 A description of the heat pulse velocity technique

3.6.1.1 Theory of the heat pulse velocity technique

The heat pulse velocity (HPV) technique measures the velocity of a heat pulse propagating through a tree using the compensation technique (Huber and Schmidt, 1937; Swanson, 1974 cited by Dye *et al.*, 1992). Two probes containing temperature sensors are aligned with the axis of a plant stem and inserted radially to equal depths in the xylem. A heater probe is similarly inserted at a fixed distance upstream from the midpoint between the two temperature probes. A common configuration locates the heater 0.5 cm from the upstream temperature and 1.0 cm from the downstream probe. The temperature rise in the thermistor probe as a result of the application of the heat pulse is measured at the distances X_u (upstream) and X_d (downstream) from the heater probe. When both temperature probes have warmed to the same degree, the heat pulse has moved 0.25 cm from the heater (i.e. the midpoint between the probes). According to Swanson (1983) (cited by Olbrich, 1994), the velocity of the heat pulse (u in m s^{-1}) is calculated as:

$$u = \frac{(X_u + X_d)}{2t} \qquad (3.1)$$

where t (in second) is the time it takes for the temperature at X_u and X_d to become equal (Dye *et al.*, 1992) or for the Wheatstone bridge voltage to return to the initial balance point after the heater is pulsed (Olbrich, 1994), where $(X_u + X_d)/2$ refers to the probe separation (Olbrich, 1994). Both X_u and X_d are regarded as positive quantities.

The heat pulse velocity is corrected for wound size or width according to Swanson and Whitfield (1981):

$$u' = p + qu + ru^2 \qquad (3.2)$$

where *p*, *q* and *r* are correction coefficients derived for the wound size, diameter of Teflon probes (thermistor probes) and probe separation distance.

Finally, the sap flow (*v*), is calculated from the corrected heat pulse velocity (*u'*) (Marshall, 1958):

$$v = \rho_b (m_c + c_{dw})\, u' \qquad (3.3)$$

where ρ_b is the dry wood density (kg m^{-3}), m_c the fractional water content of the sapwood on a dry weight basis (unitless), and c_{dw} the specific heat capacity of dry wood (0.33 J kg^{-1} °C^{-1}) (Dunlap, 1912 cited by Dye *et al.*, 1992).

The various sap fluxes (*v*) measured at different depths below the bark of a tree, are regarded as representative of a ring of sapwood centered at the probe depth. The total sap flux per tree is therefore calculated as the sum of the partial areas (a concentric ring area with limits mid-way between successive thermistors) multiplied by their associated sap fluxes. The sap flux per tree can be converted into sap flux per unit area, using the tree espacement.

The wound size for each set of probes is measured at the end of the experiment. The sections of the tree trunk containing the probe implantation holes are cut out. Then each block containing the probe implant holes is cut longitudinally at the depth at which the thermistors were implanted. The area is then shaved smoothly with a microtome after which the wound width is identified by decolourisation, and measured to the nearest 0.1 mm. Measurements are taken midway between the position of the heater probe and the two thermistor probes. From these measurements, the average wound width is calculated for each tree. The assumption is generally that the same wound size existed for the duration of the experiment. The wood density is also calculated at the end of the experiment, using a fresh sample of sapwood.

3.6.1.2 *The heat pulse velocity equipment*

The heat pulse velocity system consists of a datalogger and a set of probes consisting of two thermistor probes and one heater probe. Teflon probes, each with a thermistor imbedded, are connected in a Wheatstone bridge configuration by using the datalogger. A heat pulse is generated when a current is supplied for 0.5 to 1 s to the heater probes. The data recorder then estimates the time it takes for the bridge to return to the initial balance point, following the heat pulse.

3.6.1.3 *Patching of heat pulse velocity data*

Tree transpiration data loss during a field experiment can result from low battery voltages, corrosion of heater probes, and cracks around heater and thermistor probes and subsequent large wound widths.

Dye *et al.* (2001) found good agreement between daily sapflow (total transpiration) measured with the HPV technique and the product of the average daily water vapour pressure deficits $e_s - e$

and the daylight hours, for a number of tree species. This relationship has been used previously by Dye *et al.* (2001) to accurately patch missing sap flow data.

3.6.1.4 Application of the heat pulse velocity technique for measurement of A. mearnsii tree transpiration

The heat pulse velocity technique (Huber and Schmidt, 1937; Swanson, 1974 cited by Dye *et al.*, 1992) was used to calculate the transpiration (sapflux) of trees within the riparian zone and upslope sites. Four 12-channel heat pulse dataloggers (custom made) were used to measure the velocity at which a heat pulse moves through a tree stem at different depths below the cambium. Measurements were made at hourly intervals. Swanson (1983) found that radial differences in the sapflux occur, and suggested that sets of probes be implanted to different depths within the sapwood (e.g. d1 to d4) (Fig. 3.2). Four sets of probes (a set consisting of a heater probe and two thermistor probes) were therefore installed at different depths (9, 14, 21, 28 mm) below the cambium of each *A. mearnsii* tree studied. This ensured that the variation in sap flux over the sapwood was covered and reflected in the tree transpiration measured.

As the accuracy of the sapflux measurements and heat pulse velocity depends on the distance between the probes, a drill jig with three aligned holes was used to install the probes accurately and parallel to each other. The heater probe was installed in the centre hole, and the two thermistor probes were installed at 5 mm below and 10 mm above the heater probe (Fig. 3.2).

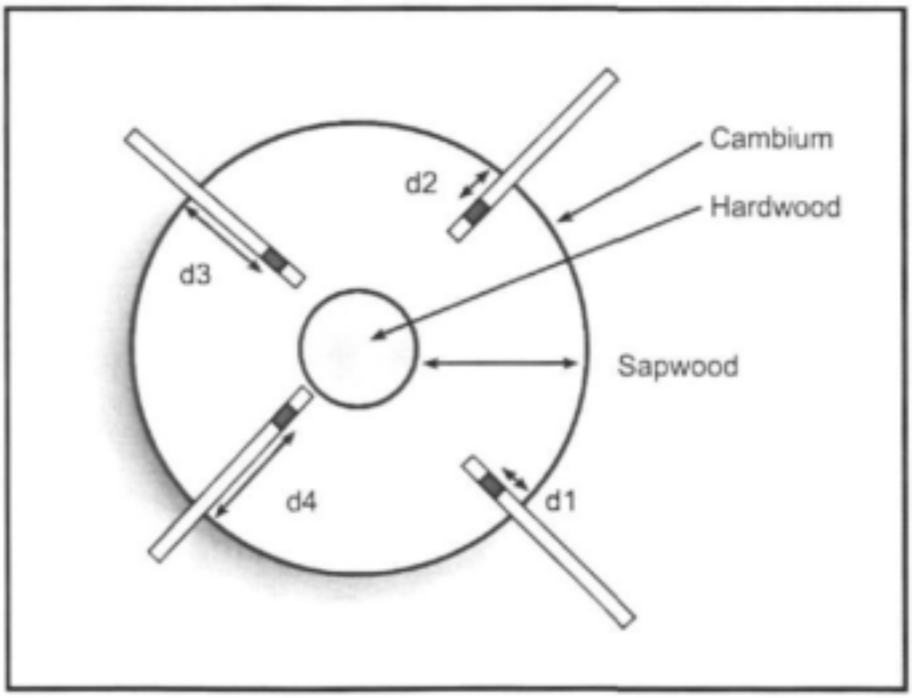

Figure 3.2 Schematic of the implantation of sets of probes at different depths below the cambium, into the stem of an *Acacia mearnsii* tree.

An early finding in this study was that wattle trees (in contrast to eucalypts and pines) reacted strongly to the presence of heat pulse probes inserted in the sapwood. Severe resin exudation around the probes, as well as growth distortions in the sapwood, required that the sample trees be changed every two to three months. Each new cycle of measurement started with a survey of tree diameters to choose four new sample trees that represented four size classes of tree. After the probes were installed and the data logger programmed for hourly readings during daylight hours, the equipment was left to run automatically, and checked at fortnightly intervals. Once growth distortions were visible in the trunk, the probes were removed and implanted into new sample trees. After felling the old sample trees, A-section of trunk was cut and brought back to the laboratory to determine the sapwood properties required to convert heat pulse times to whole-tree sap flow. A Hobo sensor provided a continuous record of temperature and air humidity on the south-facing slope.

3.6.2 Bowen ratio energy balance technique

3.6.2.1 Theory

The Bowen Ratio Energy Balance technique estimates the components of the energy balance and therefore the total evaporation above a surface.

The simplified energy balance (Eq. 1) above a surface is given by:

$$R_n - G = \lambda E + H \tag{3.4}$$

where R_n is the net irradiance, G soil heat flux density, λE latent heat flux density and H sensible heat flux density, all in Wm^{-2}. Solution of equation 1, requires the measurement of the available energy flux density (R_n - G) and the air temperature and water vapour pressure profile differences above a surface. The available energy flux density at a surface is partitioned into latent heat flux density (energy driving evaporation), and sensible heat flux density (energy heating the air). The latent heat flux density is a function of the water vapour pressure profile difference and the sensible heat flux density a function of the air temperature profile difference.

3.6.2.2 Instrumentation

The various components of the energy balance were measured with a 023 A Bowen ratio energy balance system (Campbell Scientific, Inc.). The net irradiance is measured with a net radiometer, installed above the vegetation (Figure 3.3). The soil heat flux density in the upper 80 mm depth of soil was calculated from the average soil temperature and soil water content over 80 mm, and the average soil heat flux at 80 mm. Two Bowen ratio arms with air temperature sensors and air intakes for water vapour pressure measurements were installed above the plant canopy. The lower arm was installed at least 1 m above the vegetation surface with the separation distance between the arms of approximately 1 m. The air temperature profile difference was calculated from the air temperatures measured with fine wire, type-E thermocouples (resolution 0.006°C) located at the end of each Bowen ratio arm. The water vapour pressure difference between the arms was calculated from water vapour pressure measured with a dew-10 hygrometer (resolution 0.01 kPa), *via* air intakes situated at the end of each Bowen ratio arm.

The required measurements were performed with a CR23X datalogger installed in the riparian zone. Measurement intervals were 1 s for the air temperature and water vapour pressure profile differences, and 10 s for the net irradiance, soil heat flux and temperature and soil water content. These frequent measurements were subsequently averaged or totalled over 20 minute periods and output to a storage module.

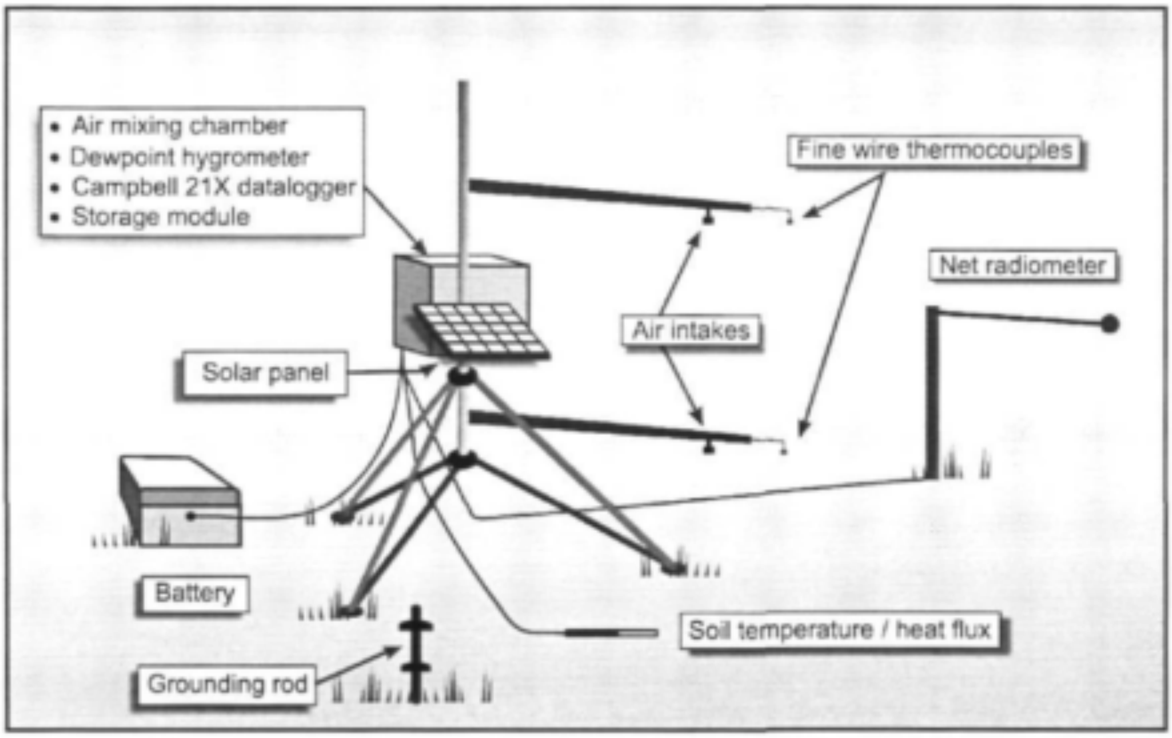

Figure 3.3 A diagrammatic representation of the Bowen ratio system.

3.6.2.3 Installation of Bowen Ratio Energy Balance equipment

The Bowen ratio sampling arms and net radiometer were mounted onto a 6 m mast. The sampling arms of the Bowen Ratio Energy Balance system were orientated due north/south to avoid partial shading of the thermocouples on the arms, while the net radiometer was positioned north/south to prevent sensor shading. The air sensed by sensors mounted on these arms was representative of the surface studied. The lower arm was installed low enough that the bulk vegetation surface environment was not sensed, whereas the upper arms were installed low enough not to sense a different environment upwind. In order to ensure that the air temperature and water vapour profile differences measured were within the resolution of the sensors, a separation distance of at least 1 m between the Bowen ratio sampling arms was maintained, with the height of the lower Bowen ratio arms at approximately 1 m above the vegetation.

As the moist upland grassland surface was uniform, the surface soil heat flux density was estimated using a single pair of soil heat flux plates and two pairs of averaging thermocouples. The soil heat flux plates were installed at 80 mm below the soil surface, the averaging thermocouples at 20 mm and 60 mm below the surface, and the soil water content reflectometer within the upper 80 mm of soil.

3.6.3 Reference Evaporation (FAO 56)

The FAO56 model (Allen *et al.*, 2004), provides a means of calculating reference and crop evapotranspiration from meteorological data and crop coefficients. The effect of climate on crop water requirements is given by the reference evapotranspiration (ET_o), and the effect of the crop by the crop coefficient K_c. Actual crop evapotranspiration (ET_c) is calculated by multiplying ET_o by K_c:

$$ET_c = K_c * ET_o \quad (3.5)$$

The calculation of ET_o is based on the Penman-Monteith combination method, and represents the evapotranspiration of a hypothetical reference crop (short grass). The technique uses standard climatic data that can be easily measured or derived from commonly collected data. Differences in the canopy and aerodynamic resistance of the crop being simulated, relative to the reference crop, are accounted for within the crop coefficient (K_c). K_c serves as an aggregation of the physical and physiological differences between crops. Two calculation methods to derive crop evapotranspiration (ET_c) from ET_o are possible. The first approach integrates the relationships between evapotranspiration of the crop and the reference surface into a single coefficient (K_c). The second approach splits K_c into two factors that separately describe the evaporation (K_e) and transpiration (K_{cb}) components (Allen *et al.*, 2004).

3.7 Site Management

Following a short calibration period, all the trees in the "B" riparian zone were cleared in July 2000. The trees in the entire catchment were scheduled to be removed in April 2002 by Mondi but due to operational setbacks this was rescheduled for September 2002. The northern portion of the catchment was cleared, but due to difficulties with stripping of the bark this operation was stopped by Mondi. The final clearing of the B-section of the catchment was completed in April 2004. The A-section was cleared in August 2004 (see Table 3.1 for the cleared areas). The project team and Mondi also agreed to leave the catchment fallow for a year following the completion of the clearing. This was to allow for the extension of the calibration period which was interrupted due to forestry management influences. A time line of these management operations is presented in Figure 3.4.

Table 3.1 Details on the area (ha) and perimeter (m) of the areas clear-felled during the study (May 2000 to January 2004).

Total Clearfelling	Area (ha)	Perimeter (m)	Notes
Clearfelling 1	7.5	1937.7	RZ area cleared May 2000.
Clearfelling 2	15.7	1892.2	SF slope upper area above RZ cleared January 2003.
Clearfelling 3	3.5	909.5	SF slope lower area above RZ cleared in December 2003.
Clearfelling 4	38.8	2752.1	NF slope lower area above RZ cleared January 2004, (included the A-zone).
Total Clearfelling	65.4		

3.8 Catchment scale modelling

3.8.1 Introduction to Soil Water Assessment Tool (SWAT)

The forest hydrology group of the CSIR has identified the need for suitable hydrological models to assist in predicting the impact of land and water management alternatives. Because of the complex mosaic of different landuses in most catchments, the need for a spatially explicit model was also identified. Thus the chosen model had to be integrated with recent advances in geographic information systems (GIS) and other spatial analysis software. Many hydrological models are widely available, but few have been seamlessly integrated into the GIS environment. One such model is the Soil Water Assessment Tool (SWAT), developed at the Blackland Research Centre in Texas for the USDA Agricultural Research Service.

The SWAT model is a daily time step model and some of its key strengths lie in the ability to predict the relative impacts of changes in management practices, climate and vegetation on water quantity and quality. The aim of this aspect of the project was to conduct a verification of the SWAT model using the Two Streams Catchment data.

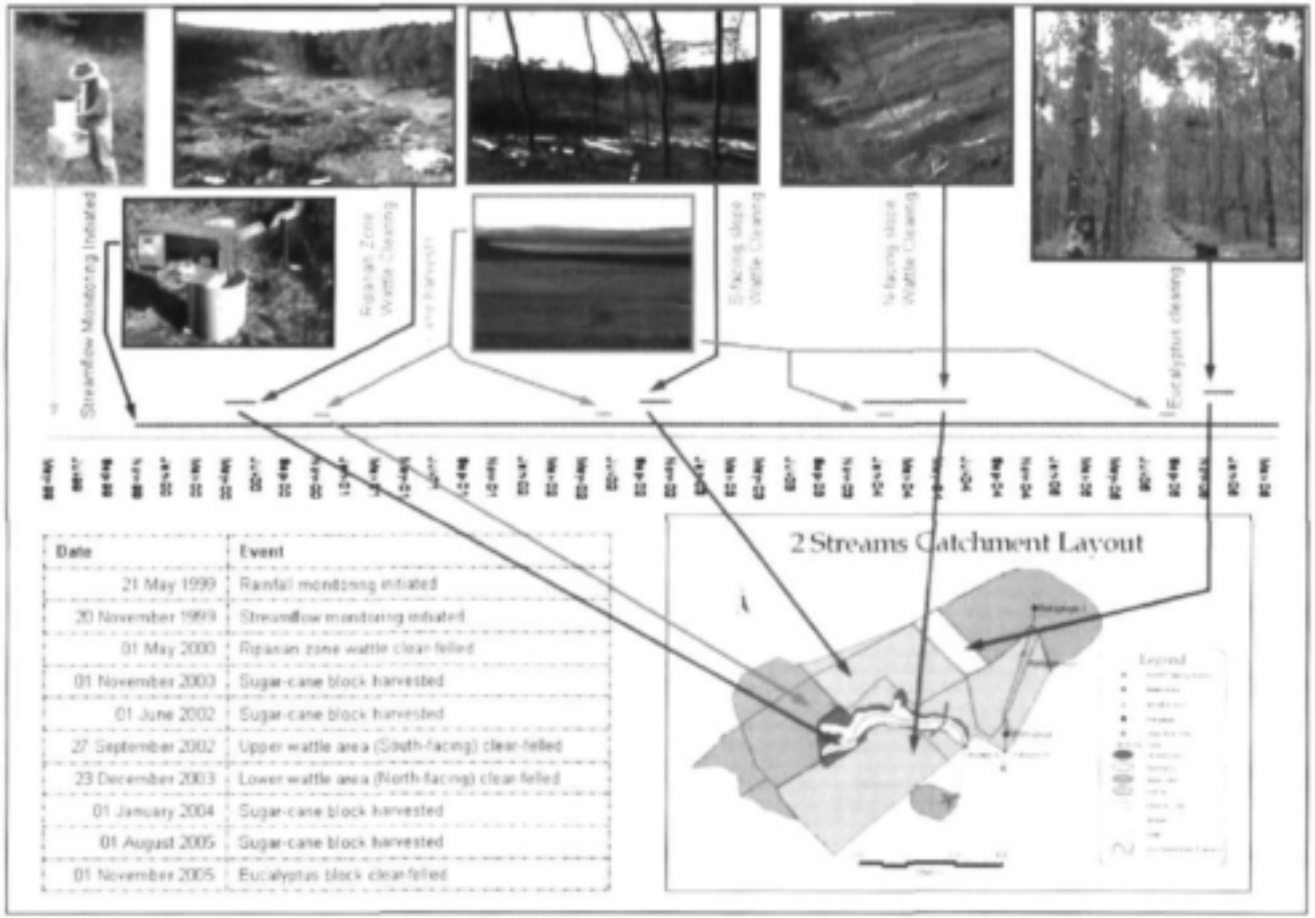

Date	Event
21 May 1999	Rainfall monitoring initiated
20 November 1999	Streamflow monitoring initiated
01 May 2000	Riparian zone wattle clear-felled
01 November 2003	Sugar-cane block harvested
01 June 2002	Sugar-cane block harvested
27 September 2002	Upper wattle area (South-facing) clear-felled
23 December 2003	Lower wattle area (North-facing) clear-felled
01 January 2004	Sugar-cane block harvested
01 August 2005	Sugar-cane block harvested
01 November 2005	Eucalyptus block clear-felled

Figure 3.4 A time line of the management operations carried out in the Two Streams catchment from 1999 to 2005.

3.8.1.1 Background to the SWAT model

Full details of the model are given in Arnold *et al.*, 1999 and Neitsch *et al.*, 2001, and therefore only a brief outline of the concepts and general structure of the SWAT model are included here. The model is a continuous daily time step model developed to simulate the long-term impacts of land and water management (e.g. reservoir sedimentation over several years) or agricultural practices (e.g. crop rotation, planting and harvesting dates and irrigation). It is physically based, uses readily available inputs and is computationally efficient to operate on large catchments within a reasonable time. SWAT allows a number of different physical processes to be simulated in a catchment, which may be grouped into the following major divisions:

- Hydrology, weather and soil temperature,
- Sedimentation,
- Crop growth,
- Nutrients and pesticides, and
- Agricultural management.

The model may simulate a catchment in lumped or distributed mode, by automatically delineating the catchment either into sub-catchments or hundreds of grid cells based on a Digital Elevation Model (DEM). The use of sub-catchments in a simulation is particularly beneficial to differentiate the impact of various landuses and soils on the hydrology of a catchment. The development of the model as an extension to Arcview has increased the flexibility of the model, with the special features of Arcview also being available to SWAT model users. Other data requirements include:

- spatial coverage for landcover and soil types,
- daily precipitation, and
- daily maximum and minimum temperature.

SWAT 2000 also has options to use measured solar radiation, wind speed, relative humidity and evaporation data. Daily rainfall and temperature data may be generated if unavailable or missing for the simulation period. There are no limitations to the number of rainfall and temperature gauges that can be used in the simulation (Neitsch *et al.*, 1999). The model includes a number of storage databases, which may be customized for an individual catchment. Included are soils, landcover/plant growth, weather stations, pesticides, tillage, fertilizer and urban datasets. A single growth model in SWAT is used for simulating all crops based on a simplification of the EPIC crop growth model (Williams *et al.*, 1984). Phonological development of the crop is based on daily heat unit accumulation, with the growing season being defined by date or accumulated heat units. The model can simulate up to 10 soil layers if sufficiently detailed information is available. SWAT 2000 is also acknowledged for the ability to model across a range of timescales i.e. hourly, daily, monthly and annual time step (Neitsch *et al.*, 2001).

3.8.1.2 Streamflow Generation by SWAT.

SWAT provides two methods for estimating surface runoff: the SCS curve number procedure (SCS, 1972) and the Green & Ampt infiltration method (1911). The latter method requires sub-daily precipitation data supplied by the user and was not used in this study and is therefore not described here.

The SCS runoff equation is an empirical model that came into common use in the 1950s. The model was developed to provide a consistent basis for estimating surface runoff volume under varying land use and soil types (Rallison and Miller, 1981).

The SCS curve number equation is (SCS, 1972):

$$Q_{surf} = \frac{(R_{day} - I_a)^2}{(R_{day} - I_a + S)} \quad (3.6)$$

where Q_{surf} is the accumulated runoff or rainfall excess (mm H2O), R_{day} is the rainfall depth for the day (mm H_2O), I_a is the initial abstractions which includes surface storage, interception and infiltration prior to runoff (mm H2O), and S is the retention parameter (mm H2O). The retention parameter varies spatially due to changes in soils, land use, management and slope and temporally due to changes in soil water content. The retention parameter is defined as:

$$S = 25.4\left(\frac{1000}{CN} - 10\right) \quad (3.7)$$

where CN is the curve number for the day. The initial abstractions, I_a, is commonly approximated as $0.2S$ and equation 4.1 becomes:

$$Q_{surf} = \frac{(R_{day} - 0.2S)^2}{(R_{day} + 0.8S)} \quad (3.8)$$

Runoff will only occur when $R_{day} > I_a$. The SCS curve number is a function of the soil's permeability, land use and antecedent soil water conditions. Curve numbers for various land covers and soil types are described in the SCS Engineering Division, 1986. These values are appropriate for a 5% slope.

Soil Hydrologic Groups

The U.S. Natural Resource Conservation Service (NRCS) classifies soils into four hydrologic groups based on infiltration characteristics of the soils. NRCS Soil Survey Staff (1996) defines a hydrologic group as a group of soils having similar runoff potential under similar storm and cover conditions. Soil properties that influence runoff potential are those that impact the minimum rate of infiltration for a bare soil after prolonged wetting and when not frozen. These properties are depth to seasonally high water table, saturated hydraulic conductivity, and depth to a very slowly permeable layer. Soil may be placed in one of four groups, A, B, C, and D, or three dual classes, A/D, B/D, and C/D.

Definitions of the classes are:

A: (Low runoff potential). The soils have a high infiltration rate even when thoroughly wetted. They chiefly consist of deep, well drained to excessively drained sands or gravels. They have a high rate of water transmission.

B: The soils have a moderate infiltration rate when thoroughly wetted. They chiefly are moderately deep to deep, moderately well-drained to well-drained soils that have moderately fine to moderately coarse textures. They have a moderate rate of water transmission.

C: The soils have a slow infiltration rate when thoroughly wetted. They chiefly have a layer that impedes downward movement of water or have moderately fine to fine texture. They have a slow rate of water transmission.

D. (High runoff potential). The soils have a very slow infiltration rate when thoroughly wetted. They chiefly consist of clay soils that have a high swelling potential, soils that have a permanent water table, soils that have a claypan or clay layer at or near the surface, and shallow +soils over nearly impervious material. They have a very slow rate of water transmission.

Dual hydrologic groups are given for certain wet soils that can be adequately drained. The first letter applies to the drained condition, the second to the undrained. Only soils that are rated D in their natural condition are assigned to dual classes.

In addition the SCS defines three antecedent moisture conditions: I—dry (wilting point), II—average moisture and III—wet (field capacity). The moisture condition II curve numbers are assumed to be appropriate for 5% slopes. Williams (1995) developed an equation to adjust the curve number to a different slope. SWAT does not adjust curve numbers for slope. If the user wishes to adjust the curve numbers for slope effects, the adjustment must be done prior to entering the curve numbers in the management input file.

3.8.2 Introduction to the ACRU model

The ACRU agrohydrological modelling system has been developed by the School of Bioresources Engineering and Environmental Hydrology (previously the **A**gricultural **C**atchments **R**esearch **U**nit). The model has its hydrological origins in a distributed catchment evapotranspiration based study carried out in the KwaZulu-Natal Drakensberg in the early 1970's (Schulze, 1975). Since 1975 the model has been continually updated by research by post graduates and collaboration with both international and national partners. There are two main user references to ACRU: *Hydrology and Agrohydrology: A Text to Accompany the ACRU 3.00*

Agrohydrological Modelling System (Schulze 1995) and *The ACRU User Manual Version 3.00* (*Smithers and Schulze, 1995*). *These manuals are available on-line at www.beeh.unp.ac.za/acru.*

3.8.2.1 Background to the ACRU model

Concepts and Structure of the *ACRU* Agrohydrological Modelling System

The *ACRU* agrohydrological model is a multipurpose, daily time step, physically-based model. It has a multi-layer soil water budgeting routine, with outputs that include streamflow, sediment yield, reservoir yield, irrigation supply and demand, as well as a daily water balance. The *ACRU* model was originally developed in the early 1980s for studies of land use change and water resource assessment, and has subsequently undergone continuous development and enhancement. It is well suited to use in southern Africa, with links to appropriate land use, soil and climate databases.

ACRU can operate in lumped mode for smaller catchments or as a distributed cell-type model for areas with more complex land uses or soils. Individually requested outputs for each sub-catchment, which may be different to those of other sub-catchments or with different levels of information, may be generated. The multi-layer soil water budgeting accounted for in the model by partitioning and redistribution of soil water is depicted in Figure 3.5 (Schulze, 1995).

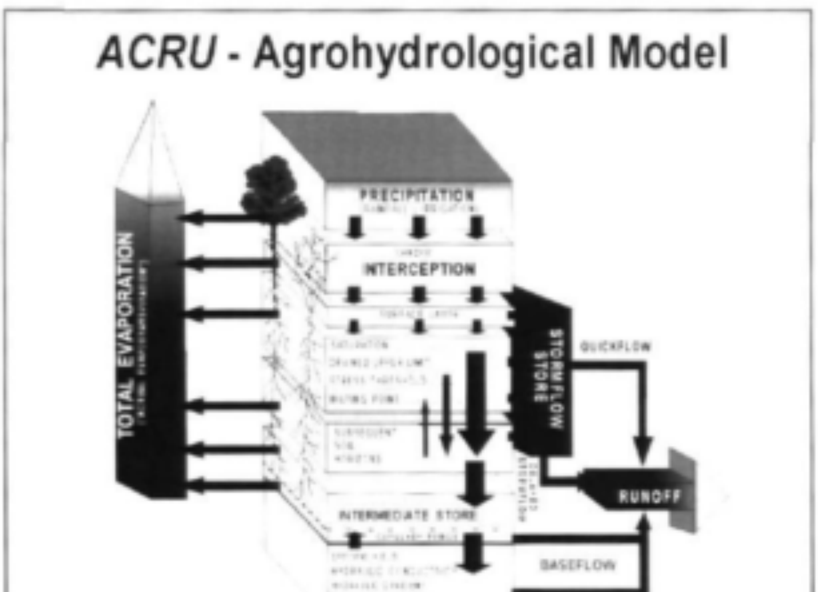

Figure 3.5 General structure of the *ACRU* agrohydrological modelling system.

The model also includes a dynamic input option to facilitate modelling the hydrological response to climate or land use management changes in a time series, be they long-term/gradual changes e.g. forest growth, urbanisation, climate trends or abrupt changes e.g. clearfelling, fire impacts or construction of a dam. *ACRU* also operates in conjunction with interactive *ACRU* Utilities, a suite of software tools to aid in the preparation of input and output information e.g. Menubuilder (to compile catchment menus for *ACRU* application), CALC_PPTCOR (to facilitate selection of appropriate rainfall stations), AUTOSOILS (to extract appropriate relevant soil characteristics) and Outputbuilder (to select the relevant output variables for graphical or statistical analysis as displayed in Figure 3.6 (Schulze, 1995). The version of the model used in this study was *ACRU* 331.

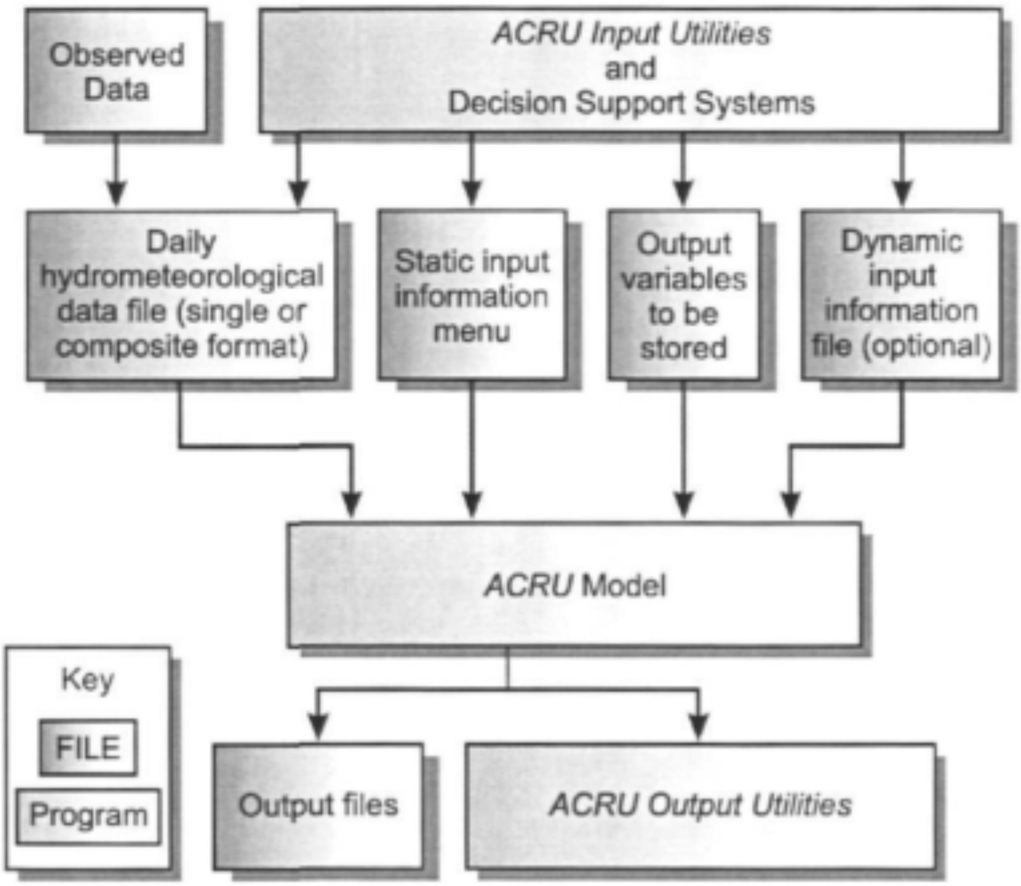

Figure 3.6 Components and structure of the *ACRU* modelling system.

3.8.2.2 *Streamflow Simulation by **ACRU***

Streamflow generated by the ACRU model comprises of baseflow and stormflow. Stormflow consists of a quickflow response which is released into the stream on the same day as the rainfall event, and delayed stormflow response or post-storm interflow. Baseflow is derived from the groundwater store which is recharged by drainage out of the lower active soil horizon when its water content exceeds the drained upper limit (Schulze, 1995).

The estimation of stormflow depth is based on the equation derived by the Soil Conservation Services (United States Department of Agriculture, 1985) and Schmidt and Schulze (1987) cited by Schulze (1995),

$$Q = \frac{\left(P_g - I_a\right)^2}{P_g - I_a + S} \quad for P_g > I_a \qquad (3.9)$$

where,

Q	=	stormflow depth (mm)
Pg	=	gross daily precipitation amount (mm)
Ia	=	initial abstractions (mm) before stormflow commences
S	=	potential maximum retention (mm).

There are several conceptual differences between the original SCS stormflow equation (used in the SWAT model) and the form in which it is used in the ACRU model noted by Schulze (1995):

- Intercepted water is abstracted separately and before the commencement of potential runoff- producing rainfall, and is not part of the initial abstractions as in the SCS model.
- The coefficient of initial abstraction (COIAM) is a parameter in the model, which may be varied monthly, and is dependent on rainfall intensity, vegetation, site and management characteristics. A default value of 0.2 is suggested.
- The potential maximum retention S, is calculated as a soil water deficit by the multi-layer soil water budgeting routines of *ACRU* as the difference between water retention at porosity and the actual soil water content just prior to the rainfall event assumed to occur at the end of the day.
- A coefficient of quickflow response (QFRESP) has been included in the model to account for any lagged response caused by for example catchment size, soils with high or low interflow potential, steep or urbanized catchments, and different vegetation types. Therefore this parameter acts as a decay function controlling the timing or distribution of stormflow over one or several days but does not control the total amount of stormflow.
- The critical soil depth (SMDDEP) for which the soil moisture deficit is calculated for stormflow generation attempts to account for different dominant streamflow producing mechanisms due to different catchment conditions. Figure 3.7 suggests values for SMDDEP according to differing climate, vegetation and soil characteristics.

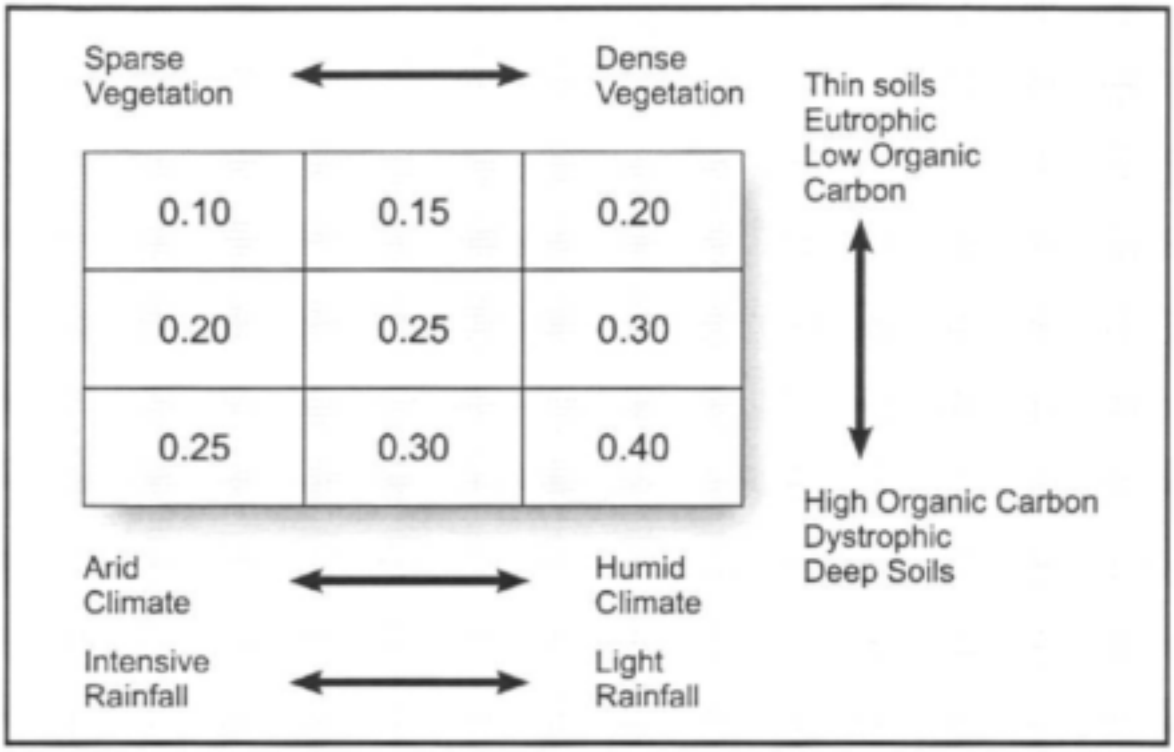

Figure 3.7 Suggested values for SMDDEP according to climatic, vegetation and soils characteristics (after Schulze, 1995)

With regard to baseflow generation the following response coefficients have been incorporated into the model:

- ABRESP, which determines the rate at which water drains from the A- to B-horizon.
- BFRESP, which similarly controls the rate of drainage from the B-horizon to the groundwater store.
- Lastly, the coefficient of baseflow response (COFRU), which determines the rate at which water in the groundwater store is released as the baseflow per day.

Evaporation takes place from previously intercepted water as well as simultaneously from the various soil horizons. It is either spilt into separate components of soil water evaporation (from the topsoil only) and plant transpiration (from all horizons in the root zone), or combined as total evaporation or actual evapotranspiration. Soil water evaporation for a day can either be occurring at maximum rate, if a minimum threshold of soil water resides in the topsoil horizon, or below the maximum rate once soil water has dropped below the threshold, in which case soil water evaporation declines very rapidly with time. Evaporation demand on the plant is estimated according to atmospheric demand through reference potential evaporation and the plant's growth stage. The roots absorb soil water in proportion to the distributions of root mass density of the respective horizons, except when conditions of low soil water content prevail. In such cases the relatively wetter soil horizons provide higher proportions of soil water to the plant in order to obviate plant stress as long as possible.

CHAPTER 4: RESULTS AND DISCUSSION

4.1 Rainfall monitoring

The Two Streams research catchment lies in the summer rainfall zone of South Africa where summers are wet and humid and the winters are dry and cold. Daily and monthly rainfall totals exhibited typically seasonal trends, with wet summer and dry winter periods (Figures 4.1 & 4.2). The long-term mean annual precipitation for the area is 853 mm (Lynch and Schulze, 2006). The annual rainfall for the first hydrological period of study (October 1999 to September 2000) was 1071 mm. This compares with 897, 1170, 659, 727 and 1139 mm for the 2000/2001 to 2004/2005 seasons respectively. The five year study period was therefore characterized by the first three years being normal to wet, while the 2002/2004 period was dry, reflecting the severe drought conditions experienced in KwaZulu-Natal in the 2003/2004 season. The daily distribution of rainfall (Figure 4.1) reflected these dry conditions and only a few rainfall events of over 30 mm were recorded. By contrast the 2004/2005 data showed that the rain events between July and December 2004 were higher than any previously measured rain events for the study period. The highest single rainfall event during this study was measured on the 19th of November 2004 when over 90 mm of rain fell.

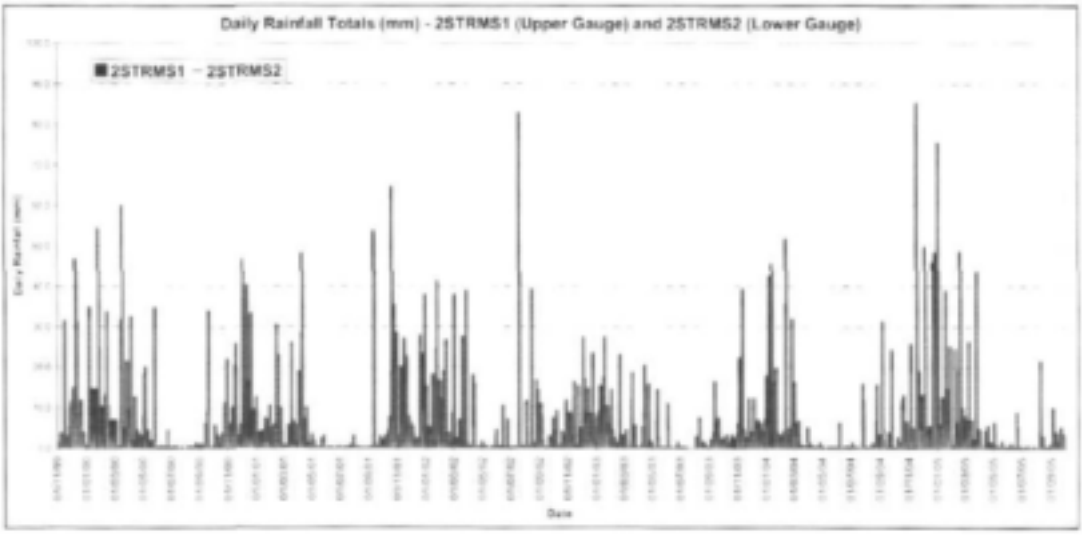

Figure 4.1 Daily rainfall totals for the two automatic rain gauges at the Two Streams study site (November 1999 to September 2005).

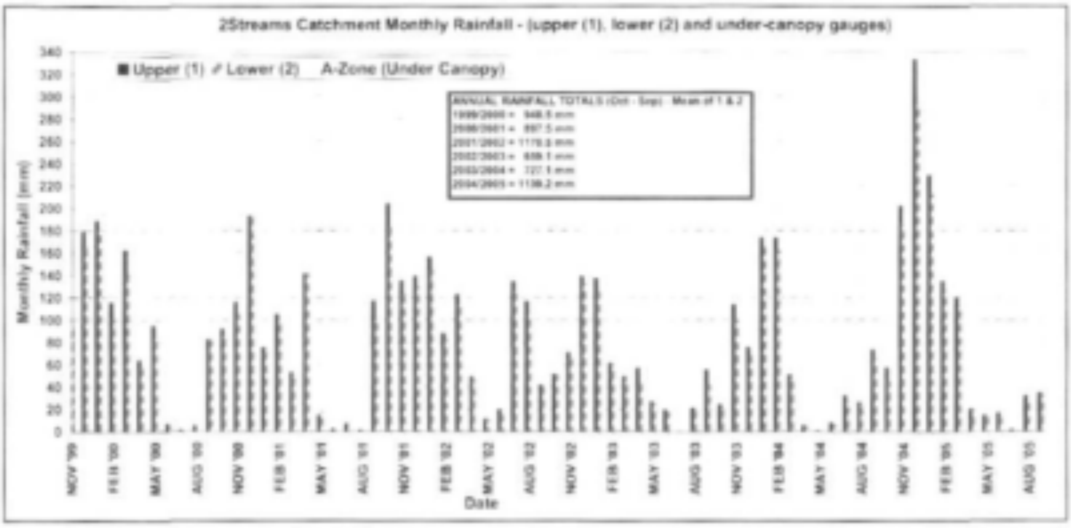

Figure 4.2 Monthly rainfall totals for the two automatic rain gauges at the Two Streams study site (October 1999 to September 2005) and beneath the wattle canopy at the A – section site (August 02 to November 2004).

To obtain an estimate of the throughfall (and hence interception) in the wattle trees, precipitation from the raingauge in the A-zone below the canopy was compared with the average of two gauges in the open (Two Streams I & II). Rainfall interception is the holding of rainfall by vegetation and subsequent evaporation to the atmosphere. Rainfall interception has been identified as an important evaporation process which may explain much of the change in streamflow ascribed to afforestation. High interception losses are explained by high wet-canopy evaporation rates, and values of 20-25% of rainfall in mature forest stands are not uncommon (Versfeld, 1985). By contrast, Dye 1993 found canopy interception loss in a four-year-old *Eucalyptus grandis* stand to be only 4% of gross rainfall. No previous records of rainfall interception by wattle in SA were available and this preliminary work was initiated to gauge the importance of the interception process in mature wattle plantations. Only a single throughfall gauge was used and no measurements of stemflow were made. These preliminary results on throughfall should therefore be treated with caution.

Between August 2002 and May 2003, 115 independent rainfall events were recorded (Figure 4.3 and 4.4). A linear regression analysis of the response of the below canopy raingauge to gross rainfall, showed a strong linear relationship, with a coefficient of determination (R^2) = 0.92 and a slope of 0.76. These data suggest therefore that gross rainfall is reduced on average by about 24% for all storms. The regression relationship for storms <5 mm showed that gross rainfall is reduced by ± 45% (R^2 =0.88).

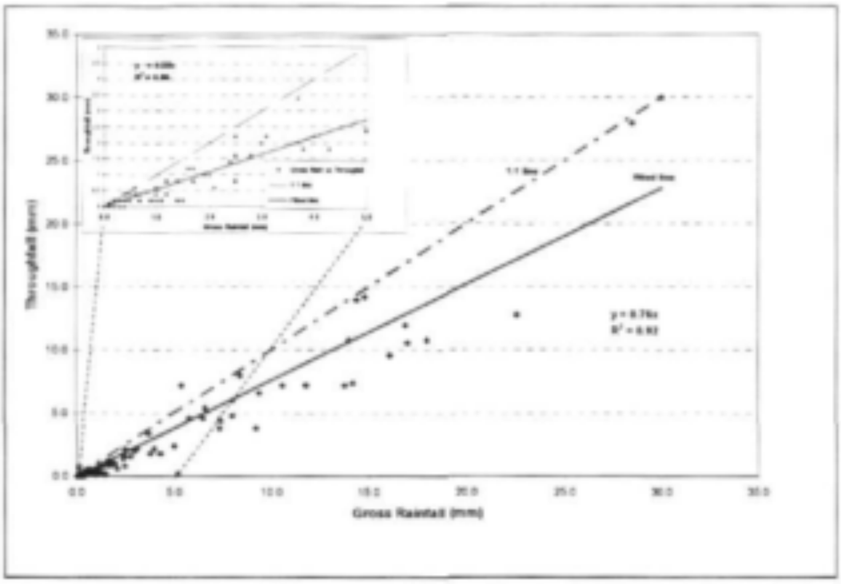

Figure 4.3 Gross rainfall against throughfall (n=115).

The relationship of gross rainfall to interception losses (Figure 4.4) showed that there was a high percentage of precipitation lost by evaporation during rainfall events < 2 mm. This percentage deceases as rainfall increases, as evidenced by the general flattening of the relationship with higher rainfall. Although these data are preliminary, the sample number was high (115), suggesting that intercepted water losses in mature wattle may be higher than expected, since interception losses in SA are generally considered to be about 4-12% of the gross rainfall (2P Dye, *pers comm.*). Stemflow is generally 1-5% of gross rainfall (Versfeld, 1985). Thus interception losses in wattle are still likely to be greater than 20% of gross rainfall when stemflow is accounted for.

[2] Dr P. Dye, CSIR, Natural Resources and the Environment.

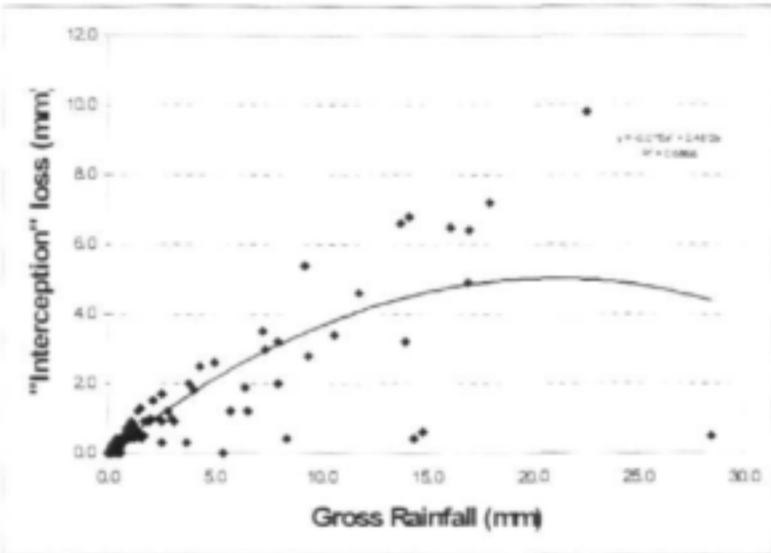

Figure 4.4 Gross rainfall against "interception" (n=115).

4.2 Streamflow gauging

Daily streamflow totals for the treated catchment (2STRMSA) together with corresponding rainfall data are illustrated in Figure 4.5, with cumulative streamflow and daily rainfall data represented in Figure 4.6. Note that streamflow totals are plotted on a log scale in order to accentuate the lower flows. The removal of the 7.5 ha of trees from the delineated riparian zone in May 2000 clearly had a positive impact on the runoff from the treated catchment. Noticeable was the fact that the stream has continued to flow throughout the five winter periods of the study, despite the droughts experienced in 2003 and 2004. This contrasts with the pre-riparian tree removal treatment when the stream only began flowing in late summer. The accumulated streamflow showed a decrease in runoff in the 2002/2003 season when compared with the previous years, a result of the low rainfall in the latter part of the 2002/2003 season. The daily streamflow in May and August 2003 reached its lowest level during the study period (Figure 4.5).

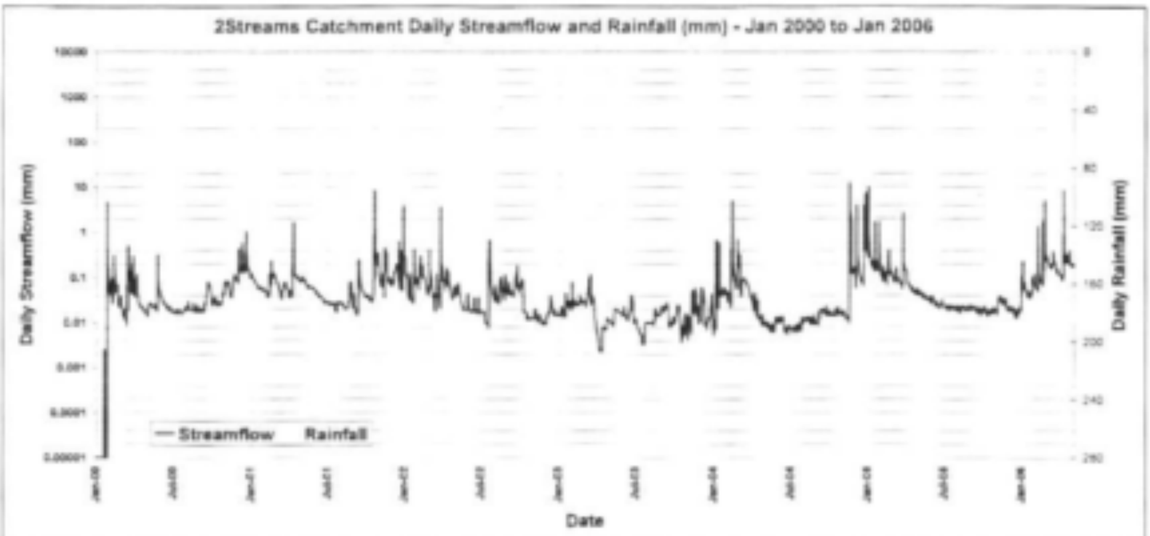

Figure 4.5 Daily streamflow totals (mm) with corresponding daily rainfall data (mm) for the treated catchment (January 2000 – July 2005).

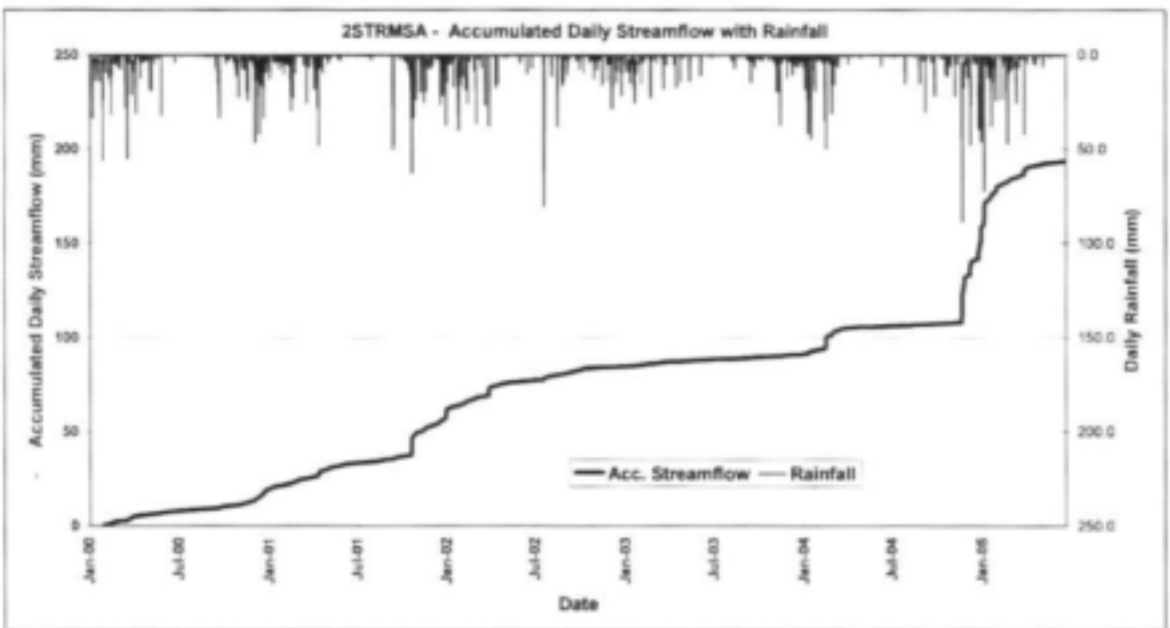

Figure 4.6 Accumulated daily streamflow totals (mm) with corresponding rainfall data for the treated catchment (January 2000 – July 2005.

The clearing of 14 ha of upslope wattle trees from the northern slope of the catchment in September 2002 did not have any noticeable impact on streamflow, demonstrating the importance of the riparian zone for streamflow generation as the clearing of 7.5 ha resulted in a significant increase in streamflow (Figure 4.7). However the clearing of the entire catchment around December 2003 / January 2004 resulted in a positive increase in the water yield from the catchment, despite the serious drought experienced in 2003/2004. The effect of the good rains in the 2004/2005 season resulted in the streamflow reaching the highest levels recorded since the start of the experiment in 2000 (Figure 4.5).

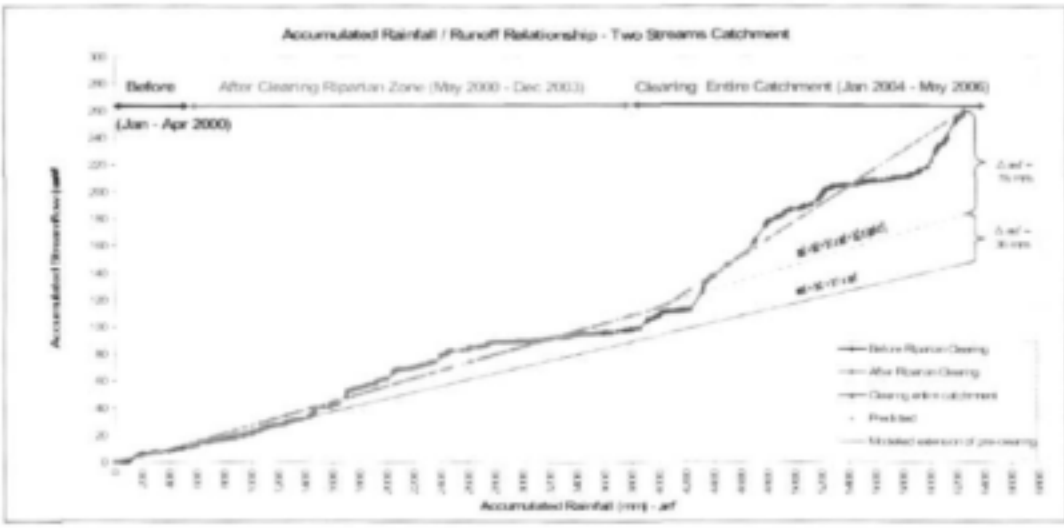

Figure 4.7 The relationship between accumulated rainfall and accumulated streamflow for the Two Streams catchment A, for the period November 1999 to May 2006 and a segmented smooth fit of accumulated stream flow (acf) on accumulated rainfall (arf).

Break point analysis was performed on the data to test the significance of these findings (Seber & Wild, 1989, Toms & Lesperance, 2003). We fitted a segmented smooth fit of accumulated stream flow (*acf*) on accumulated rainfall (*arf*). As can be seen from the graph the predicted fit is excellent (Figure 4.7).

An analysis of variance (Table 4.1) showed that the fit was significant ($p<0.0001$). The goodness of fit (R^2) was 0.995. This also indicates that 99.5% of the variation in *asf* was explained by the fit.

Table 4.1. Analysis of variance of accumulated rainfall and runoff.

Source	DF	Sum of Squares	Mean Square	F Value	Approx Pr > F
Model	5.	36408834.0	7281767	146875	<.0001
Error	2373.	117648.0	49.5778		
Uncorrected Total	2378.	36526482.0			
Parameter	**Estimate**	**Std Error**	**Approximate 95% Confidence limits**		**Label**
b0	1E-8.	0.0	1E-8.	1E-8.	
b1	0.0238	0.000931	0.0220	0.0256	
b2	0.0054	0.001070	0.0033	0.0075	
b_3	0.0362	0.000520	0.0352	0.0373	
c_1	391.7000	0.068400	391.6000	391.8000	
c_2	4052.4000	4.85E-11	4052.4000	4052.4000	
Bound2	11.6873	25.1717	-37.6440	61.0186	0 < b0

The model equation is:

$$asf = \begin{cases} b_0 + b_1 \times arf & if \ \ arf \le c_1 \\ b_0 + b_1 \times arf + b_2 \times (arf - c_1) & if \ c_1 < arf \le c_2 \\ b_0 + b_1 \times arf + b_2 \times (arf - c_1) + b_3 \times (arf - c_2) & if \ arf > c_2 \end{cases}$$

where c_1 and c_2 are the breakpoints (thresholds) ε and are assumed to be independent, addititive errors with mean zero, constant variance, and finite absolute moment of some order > 2. The values of b_2 and b_3 can be interpreted as the difference in slopes.

The breakpoints (or the change points) are c_1 and c_2. These breakpoints are obtained from the model. Restrictions that the first breakpoint, c_1, should not be less than 319.2 and that b0 > 0 and c_2 > 3000 were applied (these points corresponded with the start of the riparian and upslope clearings respectively).

To determine whether the riparian zone clearing had a significant effect on streamflow, the change of the slope from Phase 1 to Phase 2 (measured by b_2) was calculated. The approximate 95% confidence limits for the difference are found to be between 0.00333 and 0.00754. This indicates a significant change in slope from Phase 1 to Phase 2.

The effect of clearing the entire catchment was determined by calculating the significance of the change of the slope from Phase 2 to Phase 3 (i.e. b_3). The approximate 95% confidence limits for b_3 were significant (between 0.0352 and 0.0373) showing that clearing the entire upslope area of the catchment had a significant effect on streamflow.

The predicted lines for each phase change were extended to obtain an estimate of the increase in accumulated streamflow with the incremental clearings. The modelled increase in the accumulated streamflow was 36 mm and 78 mm for the riparian and upslope clearing respectively (114 mm overall). Total accumulated streamflow for the five years was 245 mm. The modelled impact of the clearing of **all** the trees was therefore a 44% increase in streamflow. This is equivalent to 75 000 cubic meters for the catchment. The relative contributions of the riparian and upslope regions to asf during the period when both areas were cleared (January 2004 to May 2006) was 16 mm and 78 mm respectively (the riparian zone therefore contributing 21% to asf). Since the riparian zone represents only 11% of the total catchment area (7.5 ha versus 65 ha, Table 3.1), the significance of the riparian zone to streamflow generation is clearly demonstrated.

A survey of tree diameters (mean of 50 trees at each site) from the riparian zone, north slope and south slope at the start of the experiment (May 1999), revealed that the average tree diameter was 239.7 mm, 156.8 mm and 155.7 mm for each site respectively. The riparian trees were therefore on average 84 mm greater in diameter than the trees on the two upslope sites. This increase is attributed to their easier access to soil water in the riparian zone. The corollary of the trees growing 34% faster in the riparian zone than on the drier upslopes, is that their transpiration rates would be much higher due to the increased exchange of CO_2 and H_2O during photosynthesis.

It should be noted that the riparian zone was quickly colonized by herbaceous vegetation (predominantly *Setaria megaphylla)* following clearing. Clearly this vegetation will transpire and have some influence on streamflow. However, the Bowen ratio evaporation data from the riparian zone (see section 4.7 for full discussion) showed that riparian zone evaporation was small during the winter and early spring when most herbaceous species were dormant.

4.3 Soil Water Monitoring

4.3.1 Soil Properties

The topsoil within the B zone has a sandy clay loam texture and is of the Hutton form (orthic A/ red apedal B). The bulk density is moderately low owing to the inclusion of plant litter that accumulates beneath the plantation canopy. This litter also leads to a moderately high organic carbon content of 5.9%. The movement of clay down the soil profile, termed clay illuviation, is a process often encountered in several of the deep well-drained red soils that are common within this region. Table 4.2 provides clear evidence of this process as the clay content at a depth of 1.5 m was approximately 10% higher than that of the topsoil. Soil bulk density also increased with depth but remains within the range normally encountered in uncompacted soils of this type.

Table 4.2 Soil physical properties at the two streams study site.

Position	Depth (m)	Sand (%)			Silt (%)			Clay (%)	Bulk Density ($g\ cm^{-3}$)	HC ($mm\ hr^{-1}$)	Organic Carbon (%)
		Coarse	Medium	Fine	Coarse	Fine	Very Fine				
B Zone North facing slope	Surface	3.8	18.1	22.6	7.2	15.2	8.6	24.6	1.14	94.2	5.9
	0.5	3.8	17.7	20.9	6.5	12.7	7.7	30.8	1.21	127.2	3.7
	1.5	5.1	14.1	19.0	6.0	10.2	8.8	37.0	1.25	132.7	0.9
Riparian zone	Surface	0.5	1.7	4.1	18.7	36.5	9.6	29.0	0.85	150.7	12.6
	0.5	3.8	9.9	18.4	15.9	23.8	18.4	10.0	1.09	172.2	7.7

Sediment that is carried in suspension from further upstream is deposited within the stream bed and along the stream verge as fine silt. This particle size class is therefore the dominant fraction of the soil in the riparian zone leading to a silty clay loam texture. Alluvial soils are often unconsolidated which accounts for its low bulk density of 0.85g cm^{-3} and high saturated hydraulic conductivity. The organic carbon, namely 12.6% in the topsoil and 7.7% in the subsoil is also extremely high owing to the slow rate of decomposition of plant residue because of prolonged periods of ponding of water.

Water retention curves for the soils sampled at the study site are shown in Figure 4.8 and their corresponding air-filled porosities in Figure 4.9. At saturation the water content is usually equal to the total porosity which in turn is related to the bulk density by the relationship $Pt = 1 - \rho b/\rho s$ (where Pt is the total porosity, ρb is the bulk density and ρs is the particle density). Slight differences can often be ascribed to the presence of unconnected pores within the soil fabric or to a particle density different from the 2.65 g cm^{-3} used in the calculation. It is interesting therefore that the saturated water content of the topsoil within the B-Zone was only 0.44 m m^{-3} despite, based on the bulk density, a calculated total porosity of 0.57 m^{-3} m^{-3}. This difference of 0.13 m^{-3} m^{-3} is probably linked to increased water repellence in the topsoil, which was especially apparent when attempting to fully saturate the soil during preparation of the cores at the time of measuring the water retention properties. Lignins, tannins and other hydrophobic organic compounds that accumulate on the plantation floor may often form a thin surface seal or coat the internal walls of water conductive pores and so decrease the thorough wetting of the soil. The influence of hydrophobic compounds would also explain why the hydraulic conductivity of this soil is lower than the subsoil which has a smaller total porosity (Table 4.2). Nevertheless the hydraulic conductivity for this soil is generally high due to its good structural stability.

In general there was good correlation between the measured data and the fitted van Genuchten (1980) model results. The water retention curves are typically "S" shaped with the first inflexion point (closer to saturation) denoting the air entry potential, which for these soils is in the order of -1kPa. This is the potential at which the largest sized pores drain, which from the capillary equation $P = 2\gamma/r^2$ (P is the pressure potential, γ is the surface tension of water, and r is the pore radius) translates into pores with a diameter of 292 μm.

As the matric potential decreases, progressively smaller sized pores are drained, the extent of which depends upon the pore size distribution of the soil. Organic matter does influence this relationship by the direct absorption of water but this applies more at high matric potentials. At lower matric potentials, typically nearer the wilting point, water retention is more texturally controlled. It is of interest that the shape of the water retention curves representing the B-Zone soil at a depth of 0.5 m and 1.5 m are similar implying a similar pore-size distribution (Figure 4.8). This is typical of material having a uniform grade as was found at the site. This can also be seen when considering their nearly superimposed air-filled porosity distribution (Figure 4.9).

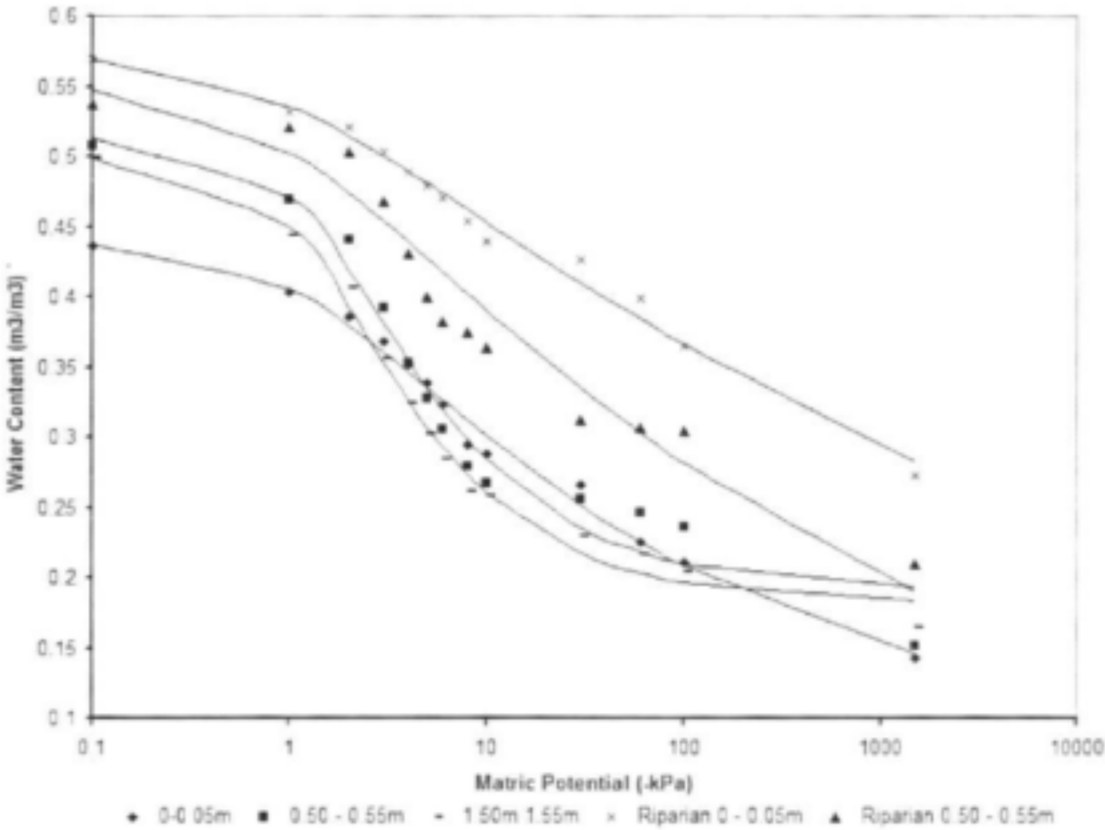

Figure 4.8 Water retention characteristic for the soils sampled from the B-zone and the riparian-zone at the research site. The numbers for each curve indicate the soil depth from which the cores were taken.

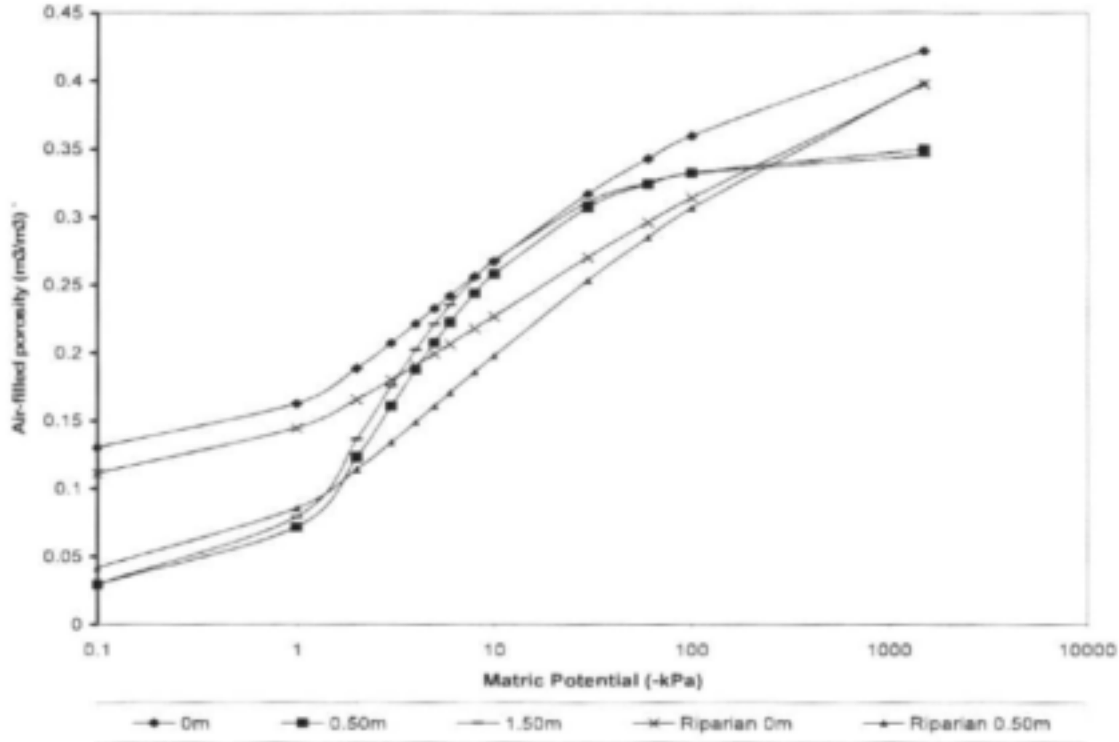

Figure 4.9 Air-filled porosity for the soils sampled from the B Zone and the riparian zone at the research site. Numbers for each curve indicate soil depth.

It is generally accepted that at field capacity (-10 kPa), where all pores > 29.2μm are drained, soils with an air filled porosity of around 12 to 15% would tend to limit root development due to inadequate aeration (Ball *et al.*, 1988). From Figure 4.9 it can be seen that none of the soils have an air-filled porosity below this critical limit. On the contrary, in all cases the critical limit is exceeded at a matric potential of only -2 kPa. The air-filled porosity of the B-Zone soil ranged in the order of 0.24 - 0.27 m^3 m^{-3} at field capacity while the riparian soil was in the order of 0.20 m^3 m^{-3}. At a matric potential of -100 kPa, when all pores > 2.92 μm are drained approximately 90% of the total pore space is air-filled, which is indicative of well-structured soil exhibiting good drainage characteristics. Readily available water contents for the B-Zone soil ranged between 0.3 and 0.7 m^3 m^{-3} while the plant available water was in the order of 0.11 to 0.14 m^3 m^{-3}. The riparian soil had slightly larger plant available water content of 0.17 m^3 m^{-3} due to the inclusion of medium sized pores in its structure.

4.3.2 Monitoring of matric potential

Since the start of this study, soil water potential has been measured every 12 minutes, initially through the tensiometer network and since October 2003 by the watermark system. This has led to the creation of an extensive dataset. In the case of the tensiometers, data processing involves converting the voltage signals from the pressure transducer to water potential by application of a calibration relationship. Although each pressure transducer was calibrated individually there was very little difference in output between these units and so a common calibration curve was adopted. An example of a typical tensiometer network response to a rainfall event is presented in Figure 4.10. The information given is extracted from tensiometer nest 2, located on the south-facing slope just above the riparian zone (Figure 2.3).

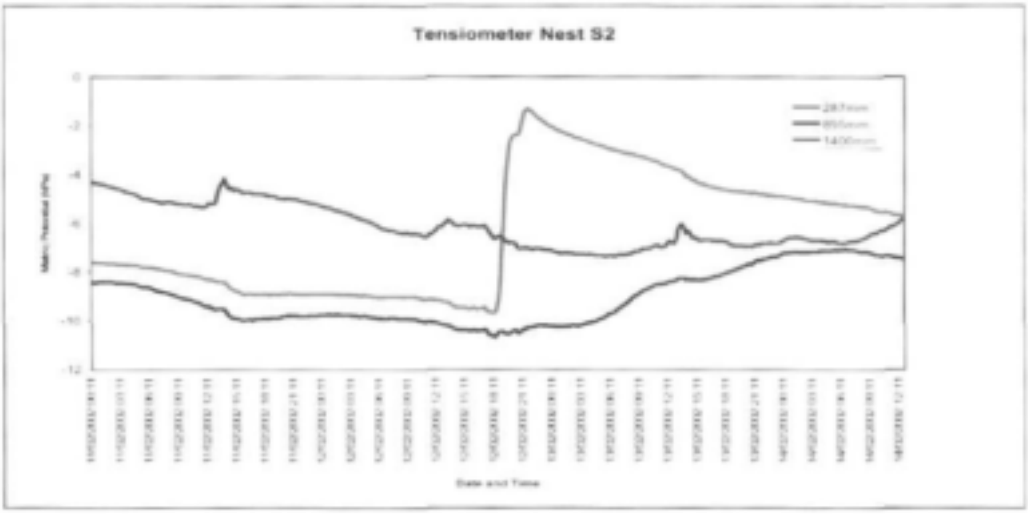

Figure 4.10 A typical response of tensiometer nest S2 (south facing slope) to a moderate rainfall event. Numbers for each curve indicate the depth of the tensiometer.

An earlier rainfall event of 19 mm on the 8th February 2002, which was followed by 0.4 mm on the 10th February 2002 that caused only the near surface to wet up, accounts for the matric potential in the tensiometer located at the 0.287 m depth being higher than that located at the 0.895 m depth. The matric potential in the deeper tensiometer (1.4 m) is considerably higher indicating far wetter conditions. Since the start of this event the soil profile has been undergoing a drying sequence denoted by a gradual decrease in matric potential for all soil depths. The rate at which this occurred appears to be very similar for the upper two tensiometers, shown by the nearly parallel response in their respective signals, which implies relatively uniform soil characteristics within this soil depth. The draining sequence for the lower tensiometer (1.4 m), however, is interrupted by two brief recharge events (13:00 on the 11th and 12:00 on the 12th) as water from the upper soil layers was received at the level of the ceramic.

On the 12th of February 2002, 26.6 mm of rain fell within the catchment mainly between 17:00 and 23:00. This translates roughly into an intensity of 4.4 mm hr^{-1}. Within an hour of the onset of rainfall, the near surface tensiometer showed a rapid increase in matric potential from –9.40 kPa at 18:00 to –1.25 kPa at 21:00, a mere 3 hours later (Figure 4.10). Thereafter, the matric potential decreased as water percolated to the deeper parts of the soil. The matric potential of the soil at a depth of 895 mm showed a more gradual response to rainfall as the matric potential increased from approximately – 11.00 KPa at the onset of rainfall to a maximum of -7.45 mm just over 24h later (Figure 4.10). The 1.4 m deep tensiometer responded more slowly to rainfall and only began to show an increase in matric potential from midday on the 13th February 2002 onwards. Even so, the matric potential of the soil at this depth reached only – 5.90 kPa at the end of this period, this indicates moderately moist but unsaturated conditions (Figure 4.10). The data generally show that the south facing slopes remain wetter for longer than north-facing slopes and those areas closer to the riparian zone are wetter than further upslope. To briefly illustrate this finding Figure 4.11 presents information for the same rainfall event extracted from the tensiometer nest located on the upper section of the north-facing slope (N6).

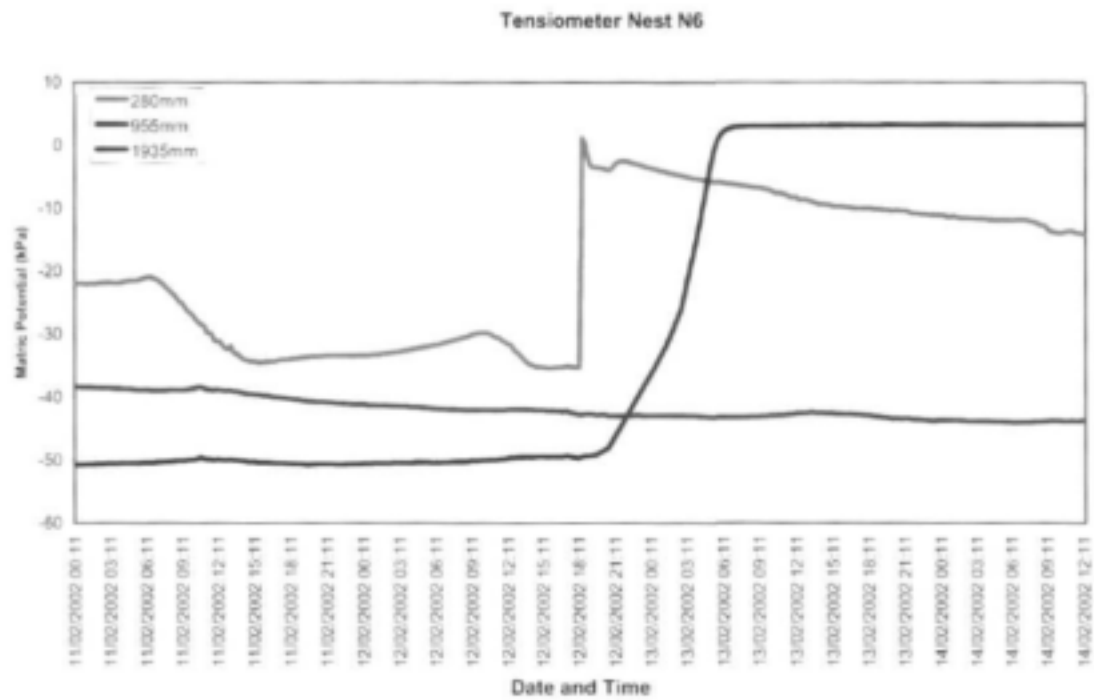

Figure 4.11 A typical response of tensiometer nest N6 located on the upper region of the north facing slope to a moderate rainfall event. Numbers for each curve indicate the depth of the tensiometer.

An important finding of this comparison of North and South facing slopes is the much lower values in matric potential that are encountered. For example, at the onset of rainfall (17:00) the 280 mm deep tensiometer at nest S2 showed a value of –9.40 kPa matric potential, which contrasts strongly against the –34.50 kPa recorded by the tensiometer located at the same soil depth further upslope (N6). Nevertheless, the overall reaction of the tensiometer network to the rain event is very similar, although there is no apparent response from the deep tensiometer (1.935 m).

To ensure functionality of the tensiometers regular replenishment of the water within the instrument is necessary in order to maintain good hydraulic contact with the surrounding soil and to eliminate any air-bubbles that may develop in the water columns. However, it was found that the tolerable limit of the instrument (-80 to -90 kPa) was frequently exceeded during the dry periods causing a break in the water column. The effects of servicing the instruments during winter, when the soils are at their driest, lasted for only a few days as water was rapidly evacuated from the tensiometer through the ceramic cup. Given that the watermark sensors have been shown to yield reliable estimates of water potential at lower matric potentials, this system was adopted and extended to the B-Zone in November 2004. Figures 4.12 and 4.13 show the water potential record for the three watermark sensor banks located within the north facing slope for the start of the 2004 and 2005 hydrological years respectively. The data, expressed in meters of water (1 m = 10 kPa), is presented in terms of the total hydraulic potential which is the sum of the matric and gravitational potentials. Strictly speaking, the total hydraulic potential should include the osmotic potential. However, the electrolyte concentration of the soil solution was considered to be uniform throughout its matrix and would thus have a negligible influence on soil water movement. For this reason the osmotic potential was not further considered for the purposes of this study.

The hydraulic potential of the soil within the B-Zone on the north facing slope shows a strong seasonal trend. Soaking rains that fell in the area at the start of the 2004/2005 hydrological year caused the soil profile to wet up thoroughly. This caused an increase in the hydraulic potential of, first, the topsoil followed progressively by the deeper layers. This abundance of rain meant that even up to a depth of 1.20 m, the hydraulic potential of the soil remained fairly high, rarely decreasing to below -4 m. This trend is similar to that reported by Goller *et al.* (2005) who conducted an isotope study tracing water paths through small catchments under a tropical montane rainforest in south Ecuador and showed that during normal wet conditions water flows mostly in a vertical direction through the soil profile to the stream network. Individual summer rainfall events on the other hand are often marked by a rapid, usually short-term, increase in hydraulic potential of the topsoil followed by a slower rate of drying. Although some drainage of water from the topsoil following the high intensity events would occur it appears likely that much of the drying phase can be attributed to evaporative demand as there was limited short-term response from the deeper sensors.

From mid-April onwards, which marks the onset of winter, a rapid decrease in hydraulic potential took place and by the end of July the soil was generally at its driest. An interesting observation from 4.12 is that during summer the subsoil was consistently found to be drier than the topsoil but over the course of winter this trend was reversed. The effect of winter rains were only sufficient to cause a slight change in the hydraulic potential of the topsoil but even this was not sustained as evaporation quickly returned the topsoil to its pre-rainfall potential.

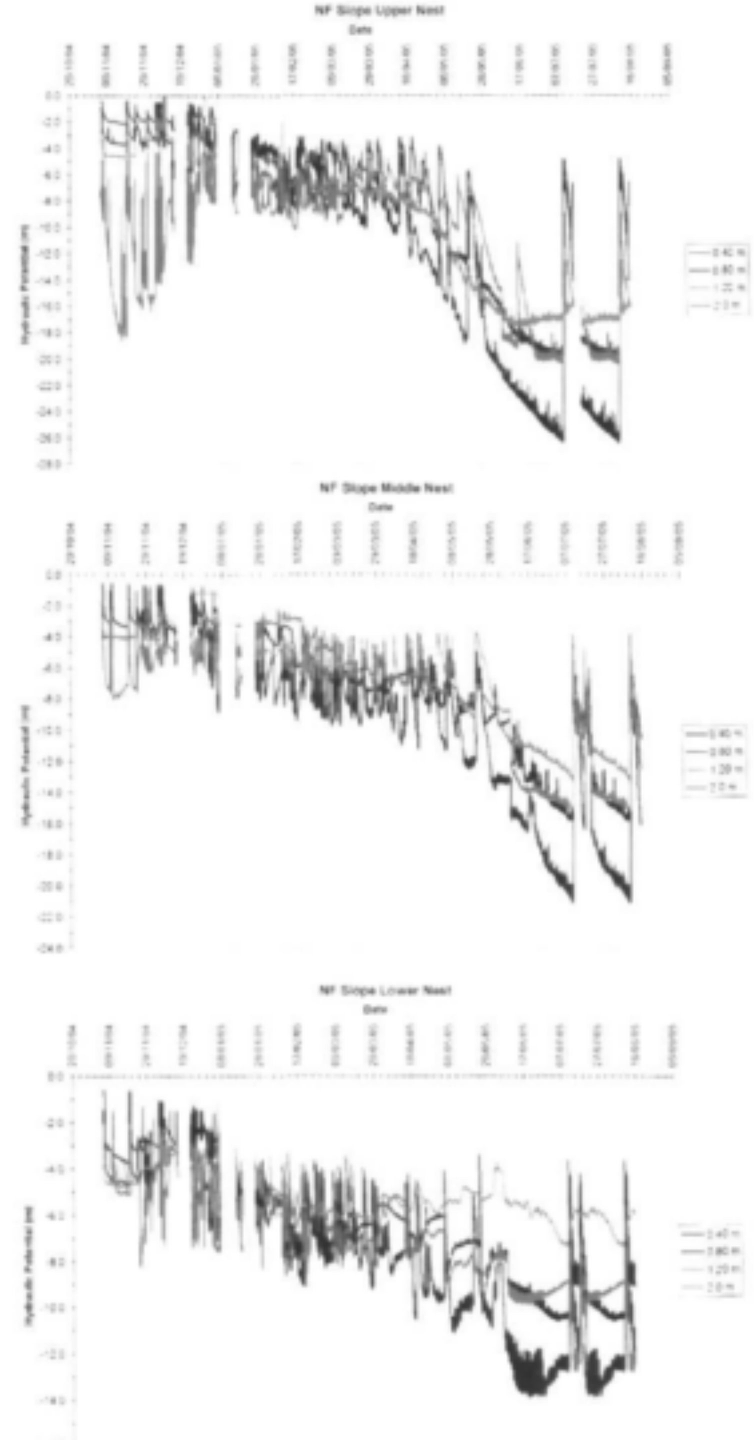

Figure 4.12 The trend in hydraulic potential for the B-Zone soil of the north-facing slope during the 2004/2005 hydrological year. Numbers for each curve indicate the depth of the sensor.

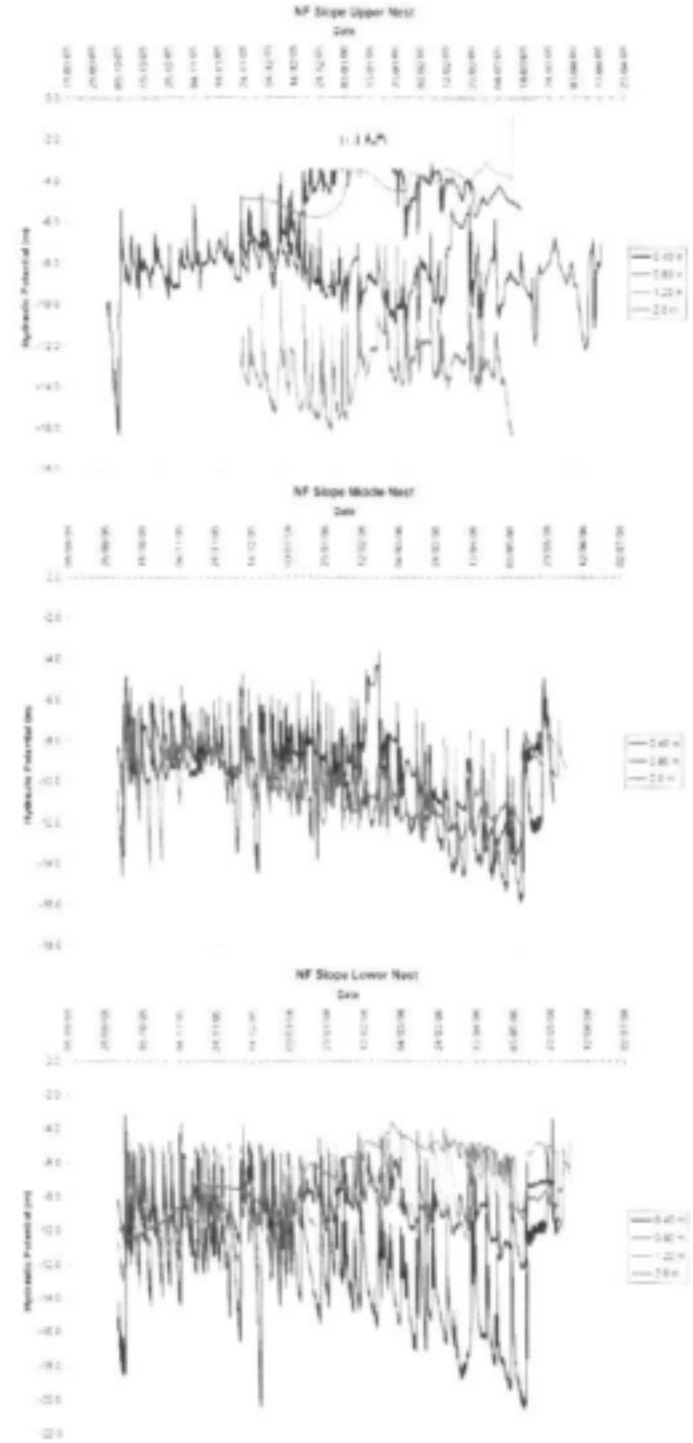

Figure 4.13 The trend in hydraulic potential for the B-Zone soil of the north-facing slope during the 2005/2006 hydrological year. Numbers for each curve indicate the depth of the sensor.

Compared with 2004, less rain fell during the summer of 2005. This had a bearing on the soil water content and thus the soil hydraulic potential. As an example, in the first three months of the 2004 hydrological year, the hydraulic potential of the topsoil ranged between -2 m to -4 m whereas in the 2005 hydrological year this had decreased to between -7 m to -10 m. Nevertheless a common trend of increasing hydraulic potential for all soil depths over the course of summer was noted. It was also interesting that the although the B-Zone remained in an unsaturated state throughout the observation period, the sensors installed within the lower part of the hillslope recorded on average higher hydraulic potentials than further upslope, i.e. the closer one gets to the riparian zone the wetter is the soil. This influence of hillslope topographic position on soil water dynamics may be better evaluated by considering the water potential of the 2.0 m deep sensors from the upper, middle and lower nests (Figure 4.14).

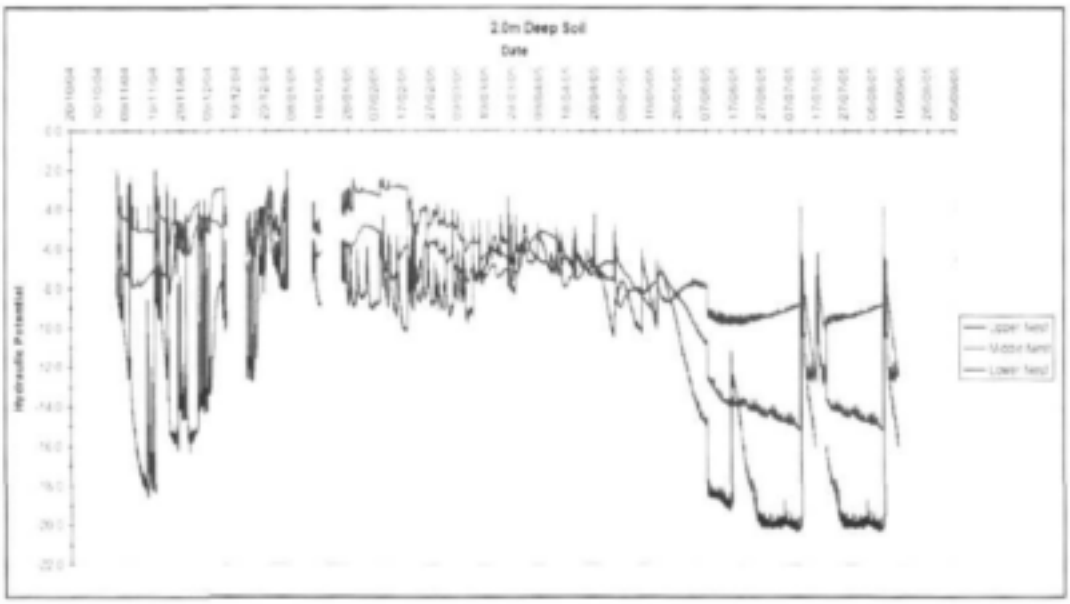

Figure 4.14 The hydraulic potential (m) of the 2.0 m deep soil within the B-Zone of the north-facing slope.

At the beginning of summer, the soil at a depth of 2.0 m had not yet been influenced by the increased rainfall mainly because of the time needed for arrival of the wetting front, but as the season progressed the hydraulic potential of the deep soil increased. From Figure 4.14 it can be seen that at the start of summer the order of increasing hydraulic potential was in a downslope direction but by mid-summer the extent of such differences were somewhat reduced, although the upper part of the slope remained the driest portion of the hillslope. The cessation of rainfall and the onset of winter caused a rapid drying of the entire soil profile with the upper part of the slope drying out at a much faster rate than the lower part of the slope. In early June the 2.0 m deep soil at the three different topographic positions had a hydraulic potential of approximately -9 m but by the end of winter the middle and lower sensors showed hydraulic potentials of -14 and -19 m respectively although the bottom of the slope was marginally drier with a hydraulic potential of just -12 m. The sustained wetness of the deep soil at the toe of the slope suggests that a portion of this water is being received from further upslope through lateral flow.

Compared to the north facing slope, a similar seasonal trend in soil water potential for the south facing slope was observed (Figures 4.15 and 4.16). However, compared with the north-facing slope the south-facing slope did not dry out to the same extent during winter, which was consistent with the tenet that south-facing slopes receive on average less radiation than north-facing slopes. As was found for the north-facing slope the deeper parts of the soil were drier (albeit to a lesser extent) than the near surface horizons, but from the onset of winter onwards this trend reversed.

Figure 4.15/...

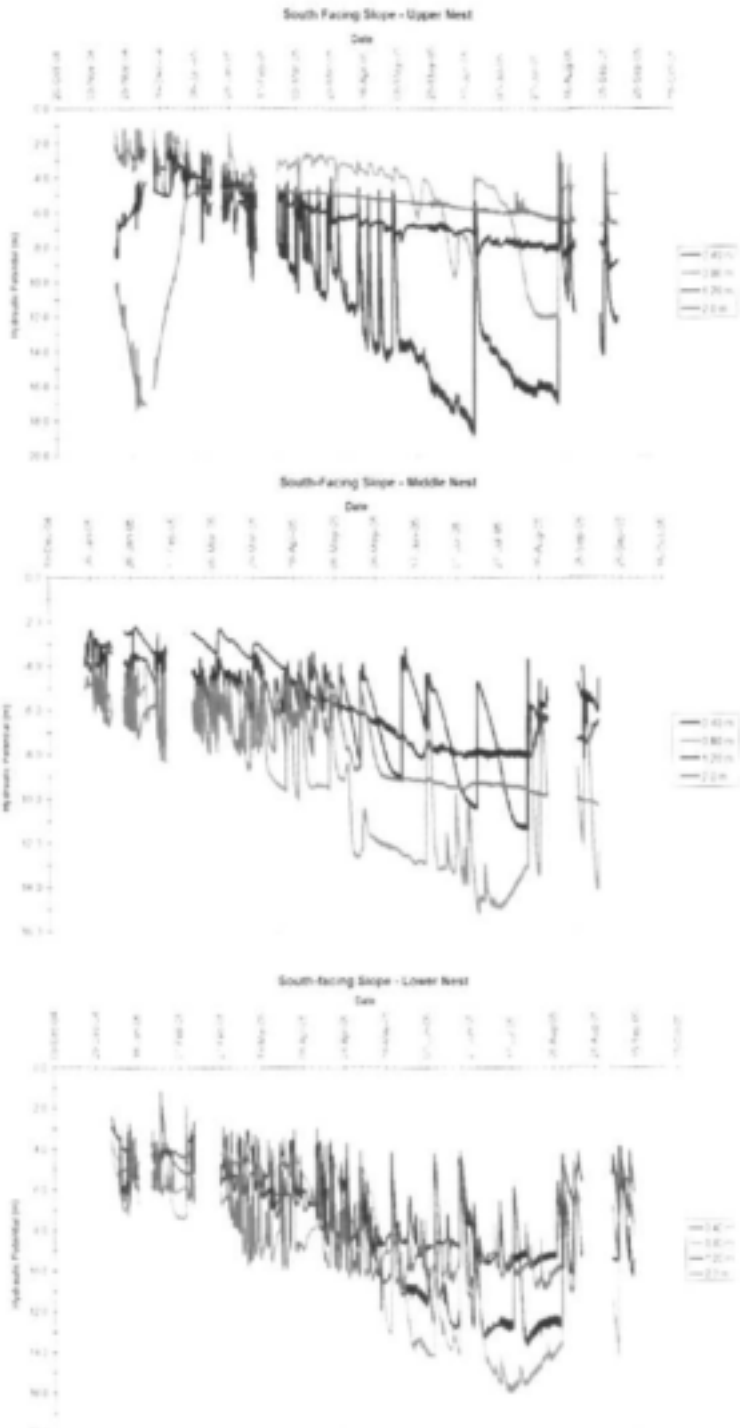

Figure 4.15 The trend in hydraulic potential for the B-Zone soil of the south-facing slope during the 2004/2005 hydrological year. Numbers for each curve indicate the depth of the sensor.

Figure 4.16 The trend in hydraulic potential for the B-Zone soil of the south-facing slope during the 2005/2006 hydrological year. Numbers for each curve indicate the depth of the sensor.

The A-Zone

An early initiative of this study was to evaluate the effects of both rainfall and land management on the soil water potential of the A-Zone. A typical tensiometer record for September 2002 extracted from nest 4, located mid-slope within the A-Zone is shown in Figure 4.17.

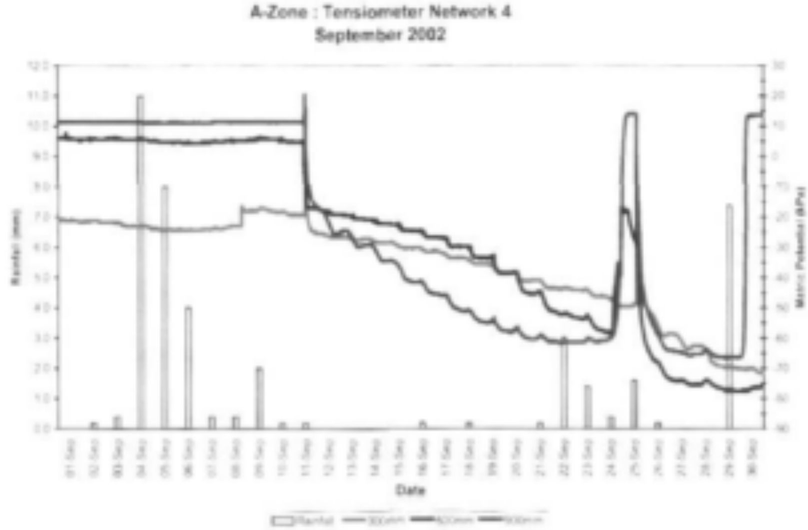

Figure 4.17 Trends in soil matric potential at a mid-slope site within the A-Zone at Two Streams catchment A. Numbers for each curve indicate the depth of the tensiometer.

Although 45 mm of rain was received in the area during the last week of August 2002 this was not enough to maintain hydraulic contact between the ceramic tensiometer cup and the surrounding soil, leading to failure of the instrument. When this occurs, the pressure transducer is sensitive to only the water retained within the column. This manifests itself in the data as nearly constant positive values as is shown in Figure 4.17 for the period 1st to the 11th September 2002. However, the deep tensiometer which continued to function over this period shows a matric potential of -30 KPa, indicating moderately wet but unsaturated conditions.

The functionality of the upper two tensiometers were restored on the 11th September when the water within the columns were replenished. From the 11th September 2002 onwards there was a slow evacuation of water from the instrument as equilibrium with the surrounding soil progressed. This was interrupted on the 24th by a second replenishment event when all of the instruments were once more serviced. Despite the 3 mm of rain that was received between the 22nd and the 24th this was largely undetected by the tensiometer network. These set of events are fairly typical of much of the record that has been collected for the A-Zone with the use of tensiometers although, in general, the frequency of failure of these instruments does suggest a much drier soil water regime than in the B-Zone where greater success with these instruments occurred. In October 2003 for reasons cited earlier, the tensiometer network was replaced by the watermark system of soil water monitoring. The installation of the watermark system resulted in the collection of a good record of soil water potential for the soils in the A-Zone.

Figure 4.18 presents the hydraulic potential record for nests A to D within the A-Zone for the 2003/2004 hydrological year respectively. Nest A is located at the foot of the slope and Nest D approximately 60 m upslope. All nests are sited along a common longitudinal transect. As was found for the other sections of the catchment, there is a strong seasonal trend in the hydraulic potential of the soil (Figure 4.18). Despite the increased wetness, the soil water potential of the topsoil fluctuated strongly because of high evaporative demands and the drainage of water to deeper layers. The presence of several large channels and pores formed by the roots of the trees could have also assisted in the rapid movement of water out of the topsoil. The deeper soil layers, however, which in general were less responsive to minor rainfall events compared with the topsoil, also showed a steady increase in hydraulic potential as summer progressed but remained fairly dry throughout this period. It was only the large rainfall events that had any meaningful influence on the hydraulic potential of the soil at this depth.

The onset of winter caused the hydraulic potential of the soil across all depths to decrease steadily. Brief episodes of rain maintained the topsoil at nest D within the -15 m to -18 m range but this effect was absent at nest A at the toe of the slope. Since the end of the rainfall period (19^{th} March) the topsoil at nest A has dried out at a higher rate than for the deeper soils and by mid June this had reached a minimum of -30 m. Much of this effect can be attributed to the loss of water from the soil by evaporative demand. A brief episode of rain at the end of August caused an increase in the hydraulic potential of the topsoil although this had less of an effect for the deeper layers. In general the hydraulic potential record for the soil at the A-Zone suggests much drier soil conditions than further down the slope.

By the end of March which coincides with the onset of winter, a rapid drying out of the soil occurred. The rate at which this took place was clearly fastest for the topsoil for reasons cited earlier and by early June the soil has reached its probable lower limit in hydraulic potential. Interestingly the topsoil remained the driest part of the soil profile throughout the winter and although minor rainfall events did cause a slight increase in hydraulic potential, this was insufficient to cause any meaningful change in the seasonal average. The deeper parts of the soil remained much wetter throughout the winter with an average hydraulic potential of -40 kPa. The rate at which this soil depth dried out was also slower. The influence of topographic position on soil water status can be seen by comparing the topsoil hydraulic potential across the different sensor nests. In nest A, B and C the hydraulic potential for the topsoil at the end of the 2004 winter (early October) did not drop lower than – 15 m whereas the topsoil at nest D, further up the slope, dried to approximately -30 m. As stated earlier the 2004/2005 hydrological year was wetter than the 2003/2004 period and the effect of this is reflected in the record of the soil hydraulic potential of the A-Zone (Figure 4.19). Early soaking rains at the beginning of summer (October) caused a rapid increase in the hydraulic potential of the soil and by the end of November the entire soil profile to a depth of 1.20 m had increased its hydraulic potential within the -3 to -5 m range. This situation persisted until the end of March when cessation of rainfall marked the beginning of a drying phase. Numerous recharge events during the course of summer maintained a high soil water content that compensated for losses by evaporation and drainage. Figures 4.20 and 4.21 provide two examples, approximately a year apart, of the soil's reaction to a high intensity event.

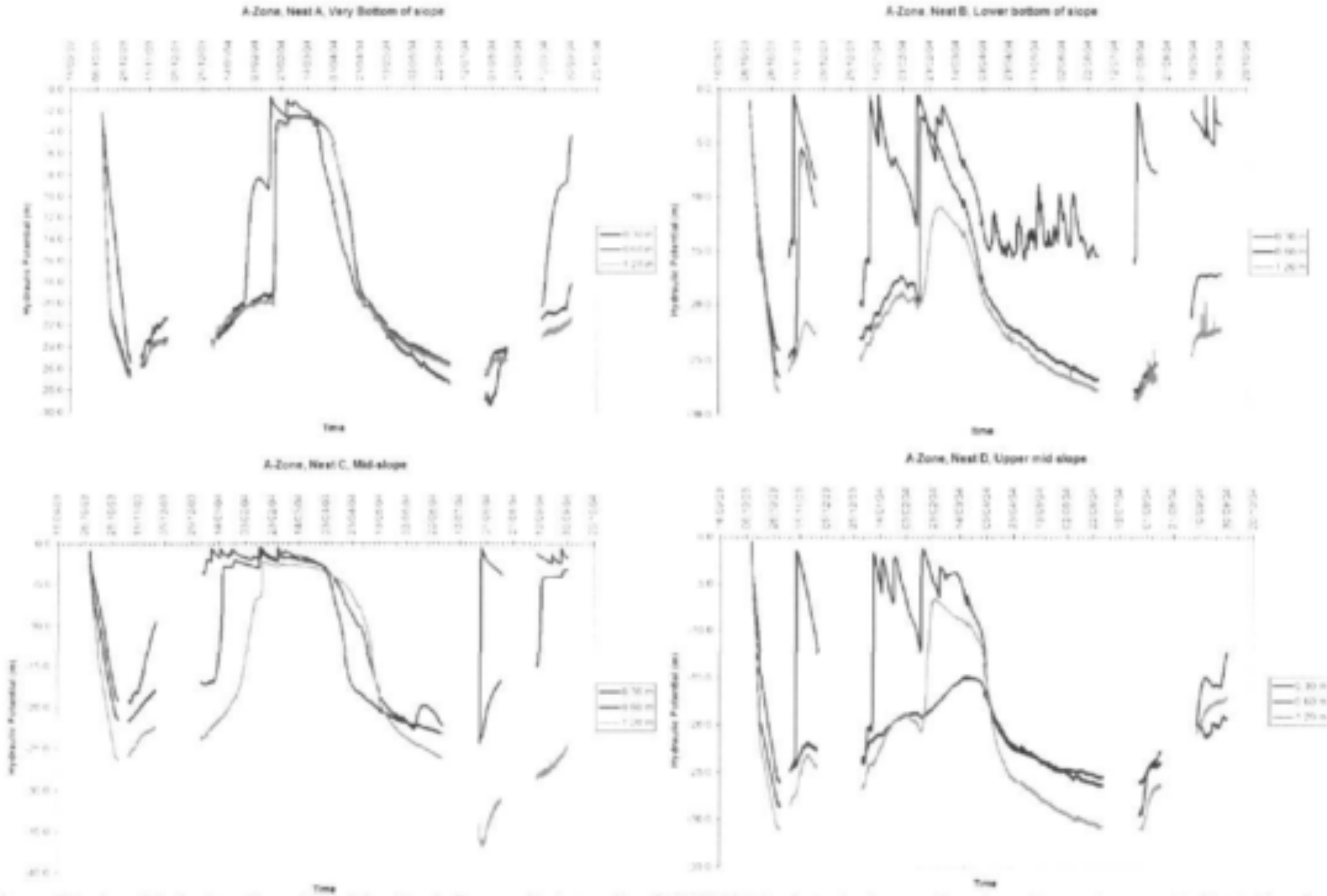

Figure 4.18 The trend in hydraulic potential for the A-Zone soil during the 2003/2004 hydrological year. Numbers for each curve indicate the depth of the sensor.

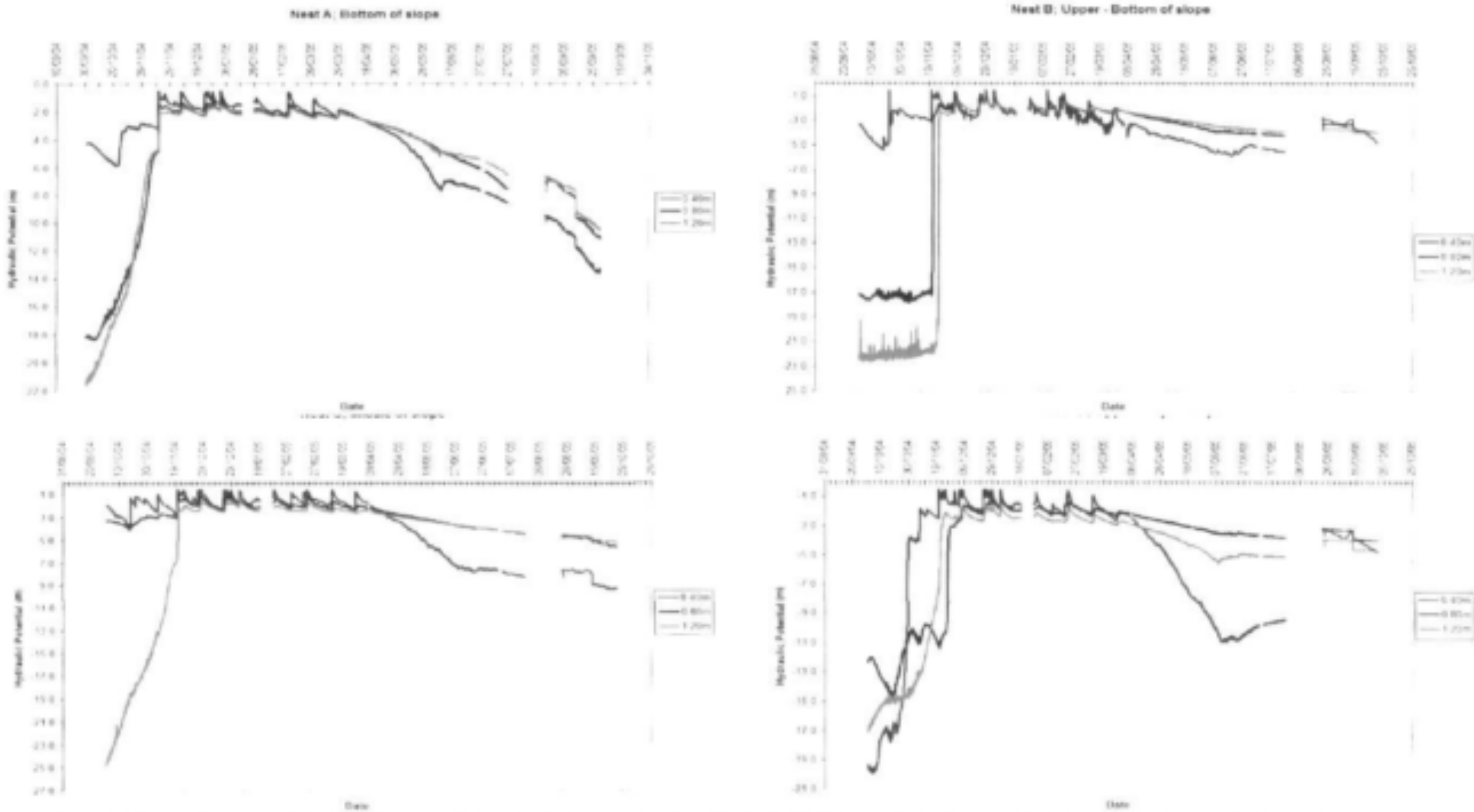

Figure 4.19 The trend in hydraulic potential for the A-Zone soil during the 2004/2005 hydrological year. Numbers for each curve indicate the depth of the sensor.

Three days of intense rain totaling 112 mm which fell between the 12 and the 14th February 2004 increased the hydraulic potential of the topsoil at nest 1 from -9 m on the 12th February to a maximum of – 1 m on the 15th (Figure 4.20).

Figure 4.20 The response in hydraulic potential at nest 1 to 112 mm rainfall between the 12th and 14th February 2004. Numbers for each curve indicate the depth of the sensor.

The arrival of the wetting front from this event was detected by the 0.8 m deep sensor two days after cessation of rainfall (16th February). It took a further three days for the complete passing of this front in which time the hydraulic potential increased from -19 m (16th February) to a maximum of -3.3 m on the 19th February. Similarly the hydraulic potential for the 1.2 m deep soil changed from – 20 m on the 18th February as the wetting front reached this depth to a maximum of -4.2 m on the 20th February. The 1.2 m deep sensor at nest B, located below the mid-slope position, shows a more gradual response in the rate at which the hydraulic potential increased reaching a maximum of just over -11 m towards the end of February. This is probably due to the lag that occurs as water is received from higher up the soil profile.

An example of an additional recharge event, almost a year later is shown in Figure 4.21, which shows the soil's reaction to 48.4 mm rainfall that occurred on the 18th February 2005. In the preceding week, the hydraulic potential of the 0.40 m, 0.80 m and 1.20 m deep soil averaged approximately -2, -2.2 and -2.3 m respectively. The onset of rainfall during the early hours of the 20th February increased the hydraulic potential of the topsoil from an initial value of -2.3 m to a maximum of -0.6 m by noon of the 21st. The passage of the wetting front was detected by the 0.80 m deep sensor in the early hours of the morning of the 22nd and by the 1.2 m deep sensor by noon of the same day. The recession or drying part of the curve is interesting as it shows that even though the topsoil wets rapidly, it also dries rapidly. Whereas the 0.80 m and 1.20 m deep sensors show a similar rate of decrease in hydraulic potential, the 0.30 m sensor shows a marginally higher rate owing mainly to evaporative demands and drainage.

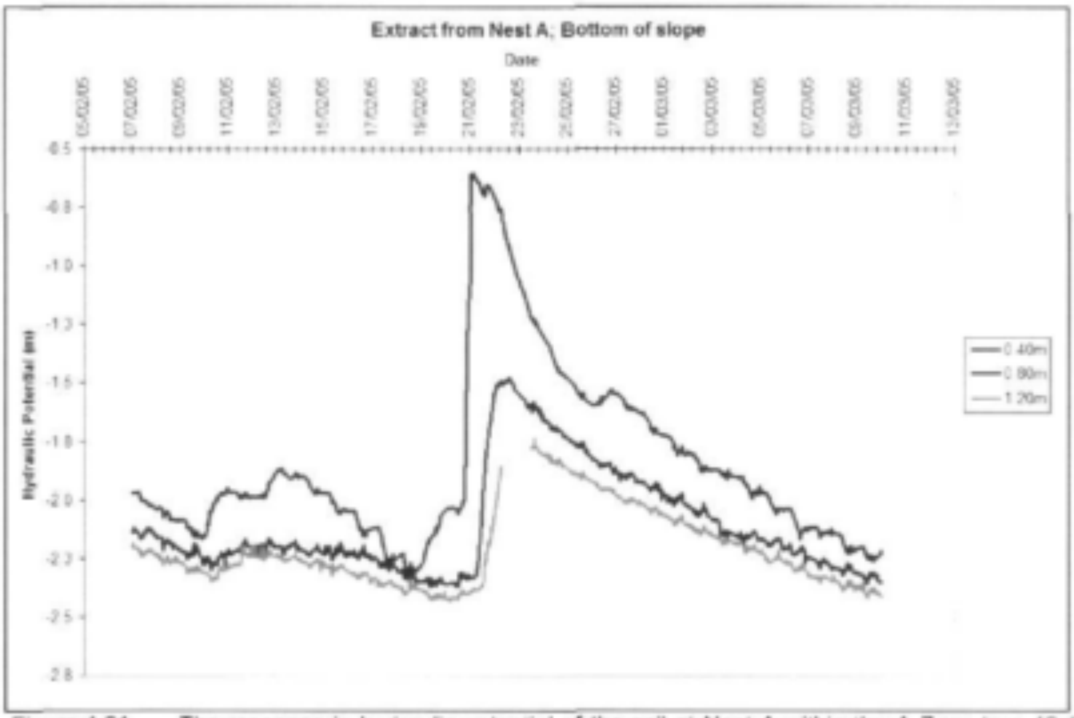

Figure 4.21 The response in hydraulic potential of the soil at Nest A within the A-Zone to a 48.4 mm rainfall event on the 18th February 2005. Numbers for each curve indicate the depth of the sensor.

The removal of the trees by the end of July 2004 appeared also to have had a positive influence on the soil water status of the A-Zone. If one considers the record in soil water potential for the period prior to removal of the trees against that obtained after the catchment was clear-felled (Figures 4.18 and 4.19) then it can be seen after clearfelling, the soil hydraulic potential on average was higher. For example during the winter of 2004 the soil water potential in nest A, located at the toe of the slope, at a depth of 0.80 and 1.20 m reached a minimum of -28 m in early August whereas in the following winter (2005) the minimum hydraulic potential was substantially higher at around -10 m. Although differences in rainfall between the 2004 and 2005 hydrological year could have had a bearing on this finding, and a few more years of monitoring will be needed to assess the long-term effects of clearfelling on soil water content, the data does suggest that the removal of the trees from the A-Zone has in general decreased the hydraulic potential of the soil profile.

Riparian Zone

An early activity in this study was the removal of the trees from the riparian zone. Since then re-establishment of the trees has been prevented in this part of the catchment although colonisation of the native vegetation occurred to some extent. The effect of this approach on soil water potential of the riparian zone is shown in Figure 4.22 for the latter part of the 2004 summer and the winter of 2005.

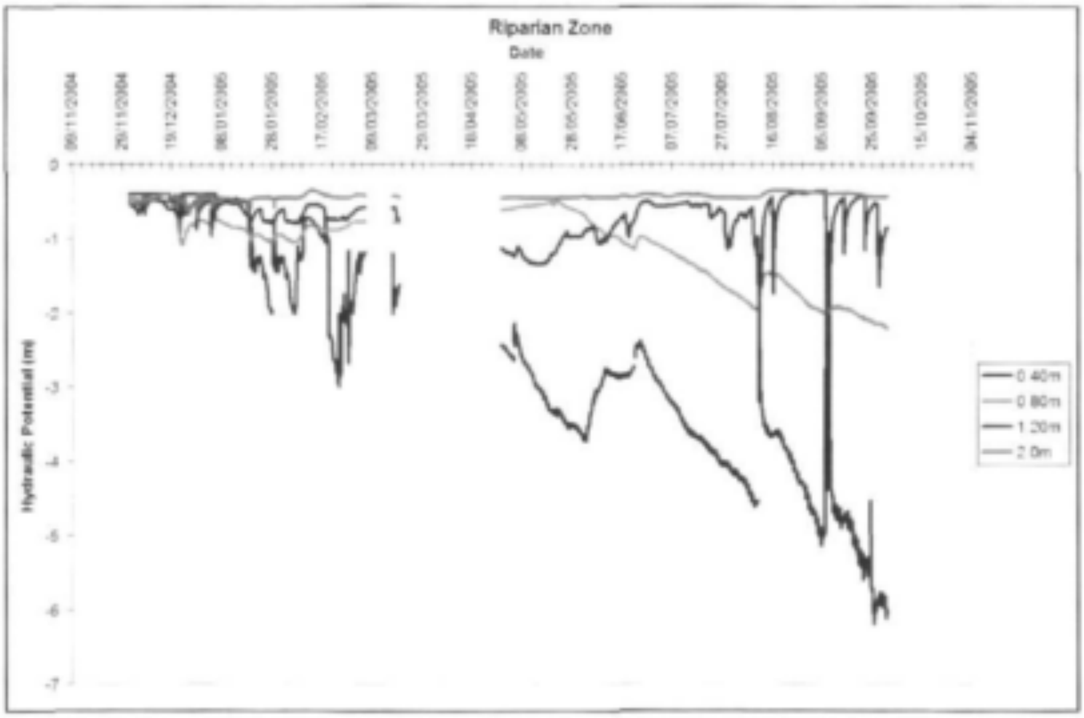

Figure 4.22 The hydraulic potential of the riparian zone soil for the period November 2004 to September 2005. Numbers for each curve indicate the depth of the sensor.

Compared to elsewhere in the catchment (B section mid-slope and up-slope and A-Zone) the soil within the B-section riparian zone was much wetter. On average the 1.20 m deep soil remained close to saturation whereas the 2.0 m deep soil was permanently saturated even during winter. Seasonal fluctuations in water potential were more accentuated for the upper part of the soil (0 - 0.80 m) as it is this part of the soil environment that would be subject to the greatest evaporative demands. Even so the water potential of the topsoil only reached a minimum of -6 m during mid-winter. The rate at which the water potential of the topsoil decreased following the onset of winter was also much lower than the B and A-zone portions of the catchment. These findings therefore corroborate quantitatively the generally accepted view that riparian zones are an integral component of the catchment responsible for the regulation of streamflow and that these systems need to be protected to ensure adequate water supply.

4.3.3 Monitoring of volumetric water content (neutron probe).

4.3.3.1 B Zone

The total profile water content in the riparian strip showed a dramatic increase following the removal of the trees in May 2000. At this time the total profile water content increased from < 200 mm to more than 600 mm (Figure 4.23). These high water contents in the riparian zone were maintained throughout the rest of the monitoring period (November 2004). Both the mid-slope and upslope sites showed similar trends with the total profile water content ranging from lows of < 150 mm at the end of the dry winter (August) to summer highs > 400 mm in December. The removal of the upslope trees in 2003 was not easily discernable from the data. These data show the importance of keeping the riparian zone cleared of trees to maintain the perennial state of the stream.

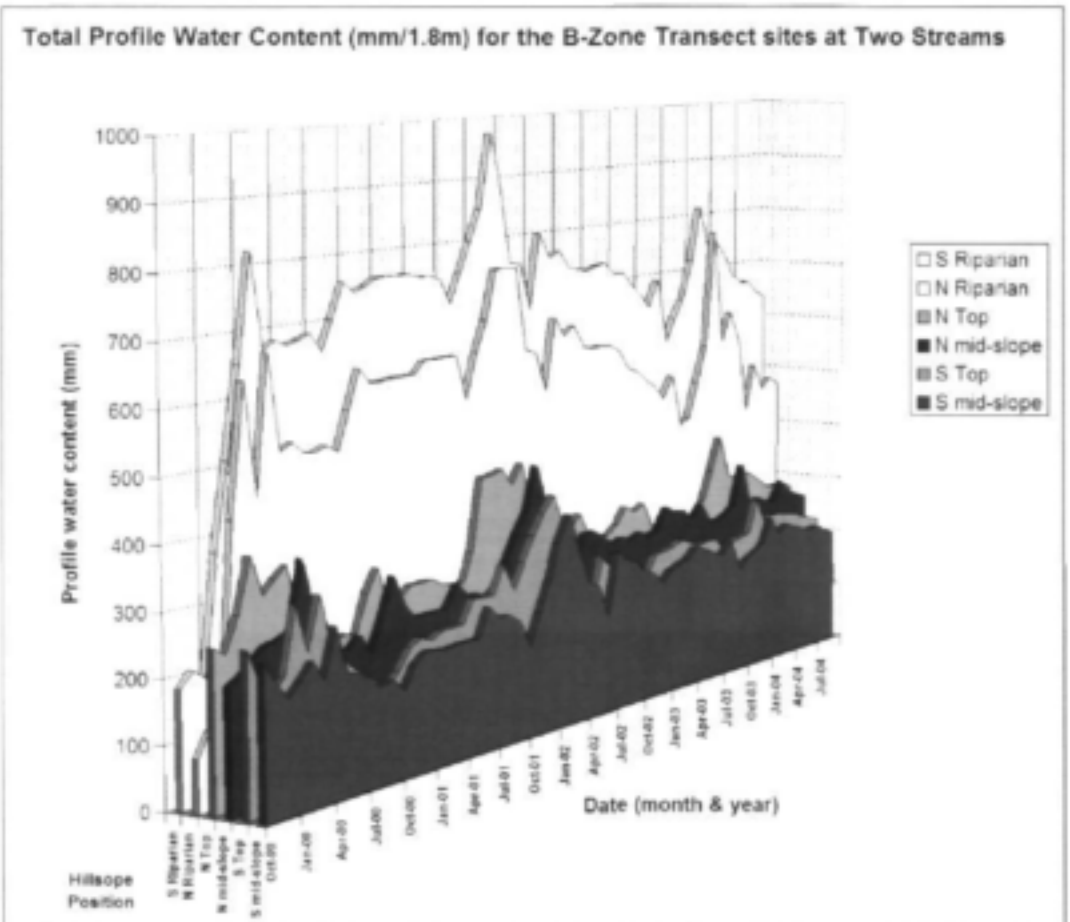

Figure 4.23 Total Profile water content (mm/1.80 m) for the B-zone transect for the period October 1999 to August 2004.

4.3.3.2 A-zone

The total profile water content over 4.5 m at the A-zone was monitored from four sites from November 2002 to June 2004. The sites were situated at various hillslope positions (Figure 2.5) with sites A2 and A3 close to the drainage line and A4 and A5 approximately 50 m away. The total profile water content over 4.5 m is also contrasted with the water content over 1.8 m (Figure 4.24) for comparison with the B zone data (Figure 4.23). The water contents in the drainage line (A2 & A3) were much higher (1200 -1400 mm) than at the sites (A3 & A4) further from the drainage line (600-800 mm), despite the fact that there was never any surface water visible. These data suggest that these drainage lines play an important role in the subsurface flow in the catchment. Summer peaks were clearly visible in 2002/2003 and 2003/2004, reaching values of 1500 and 1275 mm respectively. These maximum values represent the soil water storage at field capacity (i.e. 0.30 m^3 m^{-3}). Since the PWP is < 0.15 m^3 m^{-3} (Figure 4.24) it shows that more than 600 – 700 mm of water is available for plant water use in the upper 4.5 m of the soil profile at the end of the summer rainfall period. Clearly further studies of the root distribution of these trees are required for understanding the depths to which the *Acacia mearnsii* trees are capable of extracting water. A comparison of the A and B zone total profile water content over 1.8 m showed that the water content was generally 200 to 300 mm higher in the B zone riparian area than in the A-zone drainage line, again confirming the importance of B zone river sections in streamflow generation. However the A-zone upslope sites were surprisingly wetter than the B zone upslope sites. We ascribe this to the concave shape of the A-zone when compared with the more convex shape of the B zone slopes.

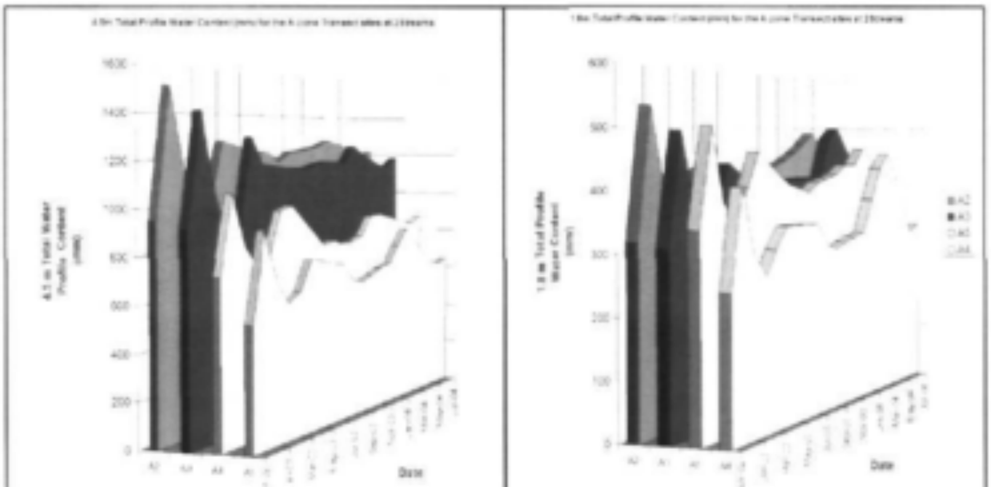

Figure 4.24 Trends in soil water content at the A-zone site (December 2002 to August 2003).

4.4 Ground Water Monitoring

Fluctuations in water table depth with time for the various boreholes, as well as flow rates from the deep aquifer are illustrated in Figure 4.25. Ground water levels in the upslope sites showed little seasonal variation over the three year monitoring period. However, the water table in the riparian zone rose from 350 mm in July 2000 to 245 mm below the surface at the end of the 2003 dry season, a significant increase of 105 mm, despite the low rainfall in the latter part of the 2003 monitoring period. This rise is interpreted as a direct result of the removal of the trees from the riparian zone. Interestingly the flow from the deep aquifer has showed a steady decline over the same period. This decline in flow rate may be from a larger regional aquifer, making interpretation of the results difficult. This decline in flow rate decreased during 2004 when the entire catchment was cleared.

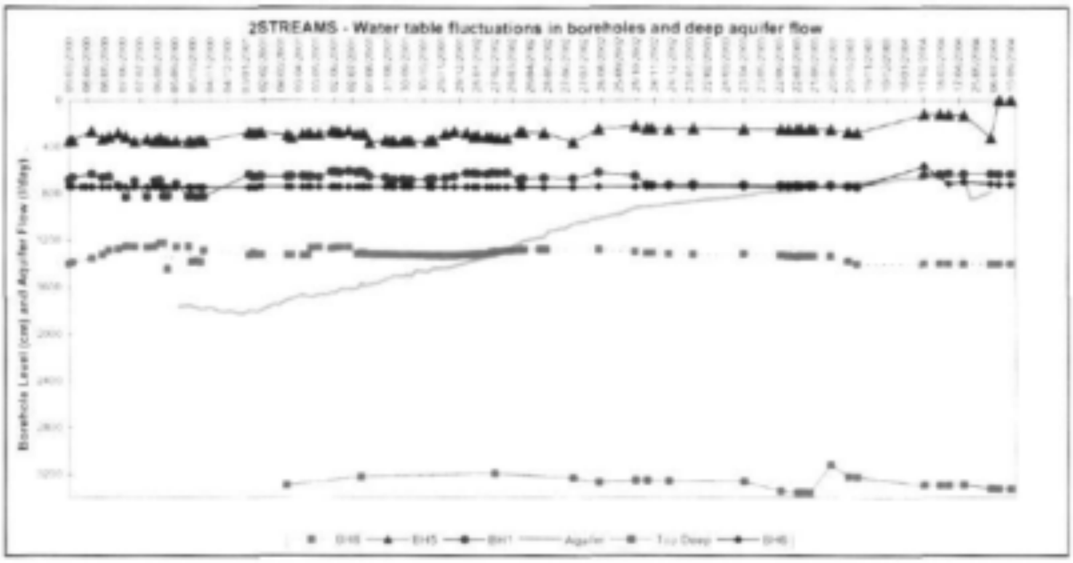

Figure 4.25 Ground water levels at various hillslope positions in the two stream A-catchment.

4.5 Surface runoff

The surface and sub-surface runoff from the A-zone was monitored using a runoff plot. Total surface and sub-surface runoff during the 2002 year was only 2034 and 376 l respectively. Clearly there is very little runoff from this portion of the catchment. An example of a rainfall-runoff event is shown in Figure 4.26. During this event 13.4 mm of rainfall was recorded, producing only 75 l of surface runoff. Six similar events were monitored, all showing similar trends, with the timing of the runoff and rainfall being closely linked.

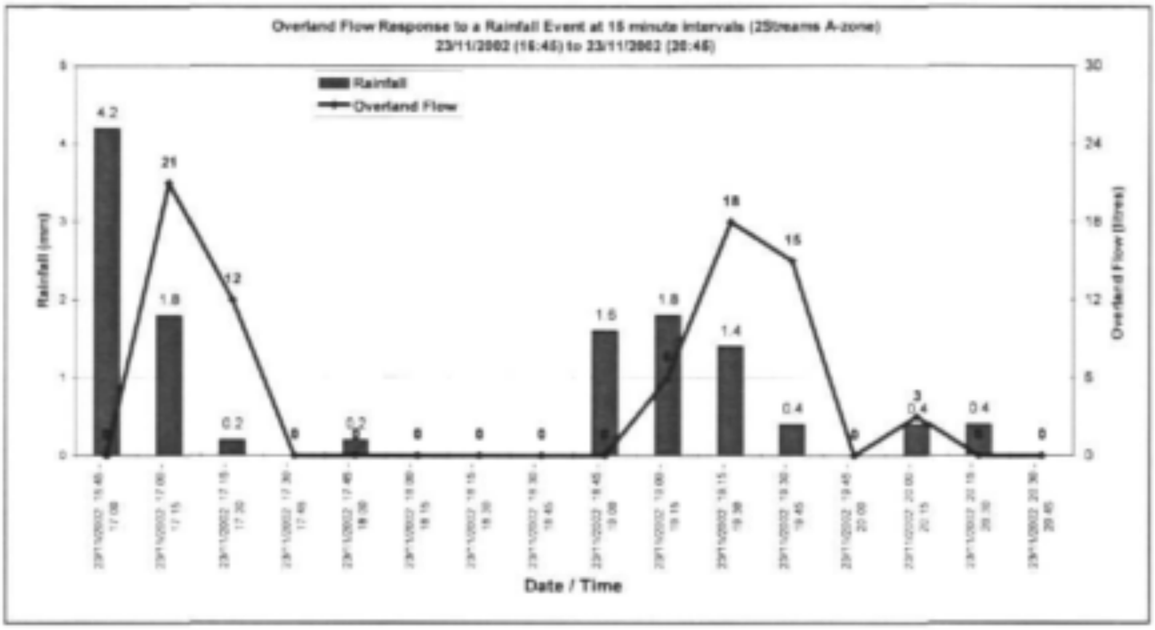

Figure 4.26 A surface runoff and rainfall event in the A-Zone during November 2002.

4.6 Sap flow studies in the wattle trees

Water balance studies in other South African research catchments have shown that the loss of water from vegetation (evapotranspiration) is commonly in the range of 45 to 80% of precipitation. Consequently, it is very important to quantify the rate of ET in order to correctly assess the storage and movement of soil and groundwater towards the stream. Sap flow measurements were concentrated in two mid-slope areas of the catchment, representing north and south-facing slopes, respectively.

Past experience has shown that wattle sap flow is highly correlated to the local air humidity, and this relationship is very useful in detecting periods of bad data and patching gaps with modelled sap flows (Dye and Olbrich, 1992). Figure 4.27 shows the relationship between mean daily humidity (vapour pressure deficit, VPD) and total daily sap flow recorded in three sample trees representing the range of tree size on the south-facing slope of the catchment. The measurements span the period from 9 – 30 January 2002, which is close to mid-summer and therefore represents the highest rates of sap flow expected in the course of the year. Daily sap flow is closely related to mean daytime VPD, indicating that the trees regulate their leaf transpiration rates to avoid excessive water loss under dry atmospheric conditions. Sap flow is proportional to tree diameter, since larger trees have greater leaf area and better exposure to sun and wind. Very similar patterns have been reported in two other tree sap flow studies in South Africa (Dye, 1996; Dye *et al.*, 2000).

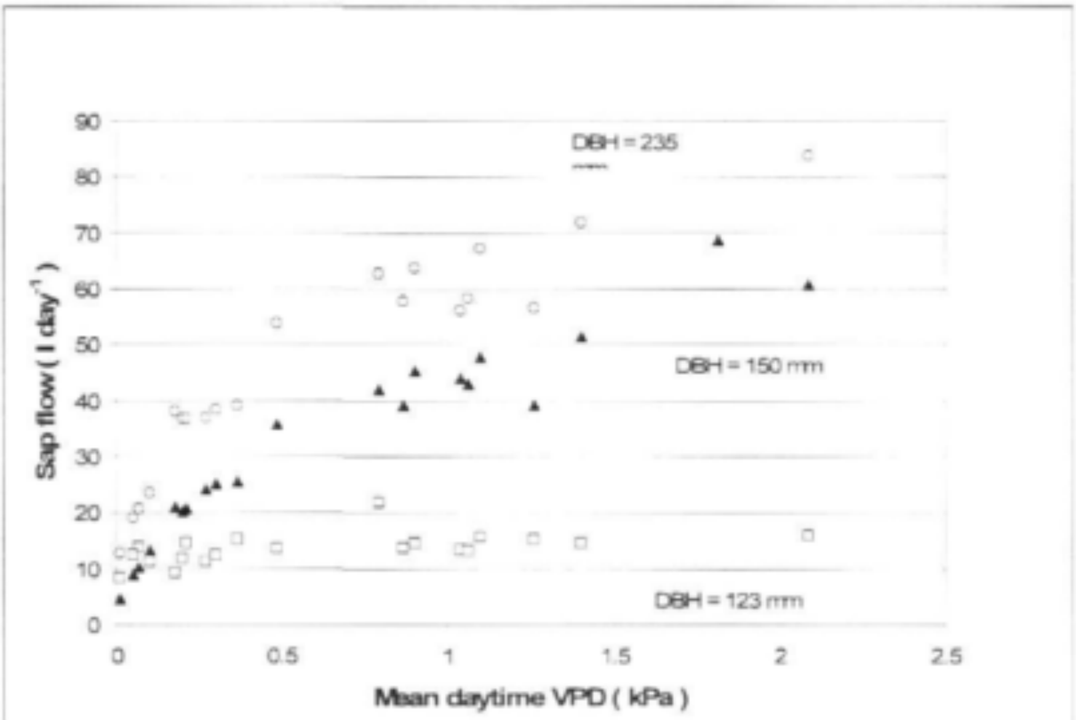

Figure 4.27 The relationship between mean daytime VPD (kPa) versus tree sapflow (l day^{-1}).

Figure 4.28 shows the estimated plot ET over the same period. A mean daily sap flow for the whole compartment of trees was calculated for each day by averaging the sample tree daily flows, after adjusting these according to the proportions of each size class in the surrounding compartment. This mean daily sap flow (l tree^{-1}) was then multiplied by the number of trees per hectare (1116) and divided by the total land area (10000 m^2) to yield daily ET in units of mm equivalent depth of water. This varies from 1 to 6.5 mm day^{-1} in response to changes in daily air humidity. The maximum compares favourably to numerous other reported rates of maximum daily ET, which commonly vary from 5-7 mm day^{-1} (Dye and Bosch, 1996).

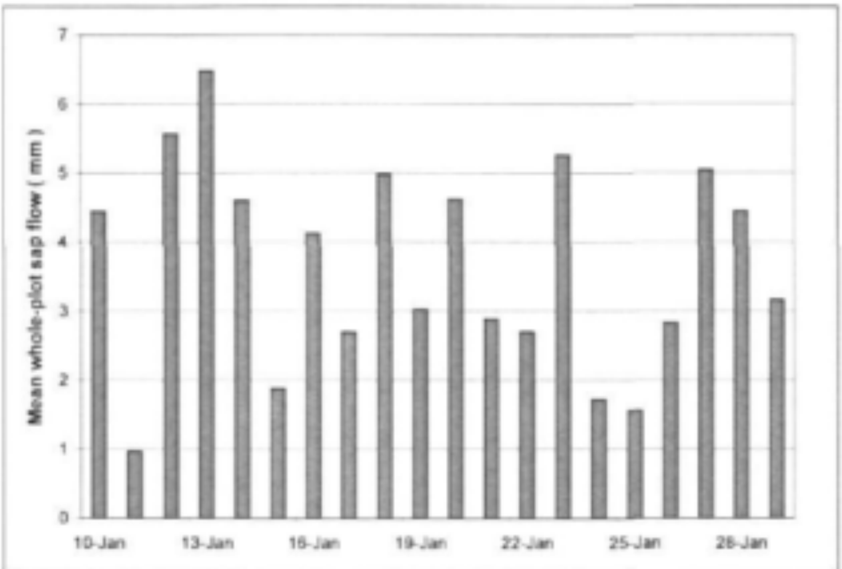

Figure 4.28 Daily ET (mm) estimated for the period 10-29 January 2001 for the south-facing *Acacia mearnsii* in the research catchment.

Measurements of sap flow were discontinued in the original north and south facing slopes, due to scheduled clearfelling. In June 2003, a fresh sample of four trees was selected within the "A-zone" site on the north-facing slope of the catchment to provide information on tree transpiration rates. These sample trees were chosen to represent four size classes of trees spanning the entire range of tree size recorded in the general vicinity. Heat pulse probes were implanted in each sample tree, and hourly heat pulse velocities recorded thereafter until 12 October 2003. Previous experience has shown that longer periods of sap flow measurement are not possible, since wounding responses in the tree severely disrupt the flow of water in the sapwood adjacent to the probes. The sample trees were felled to measure the necessary sapwood characteristics in the area where the probes were implanted. Data for the period 21 August to 2 October 2003 showed that the tree transpiration on hot days was generally about 3.5 mm day^{-1}, dropping to < 0.5 mm on cool cloudy days (Figure 4.29). These data are consistent with expected spring transpiration rates and do not differ markedly from the riparian zone grassland rates recoded in spring (Figure 4.30).

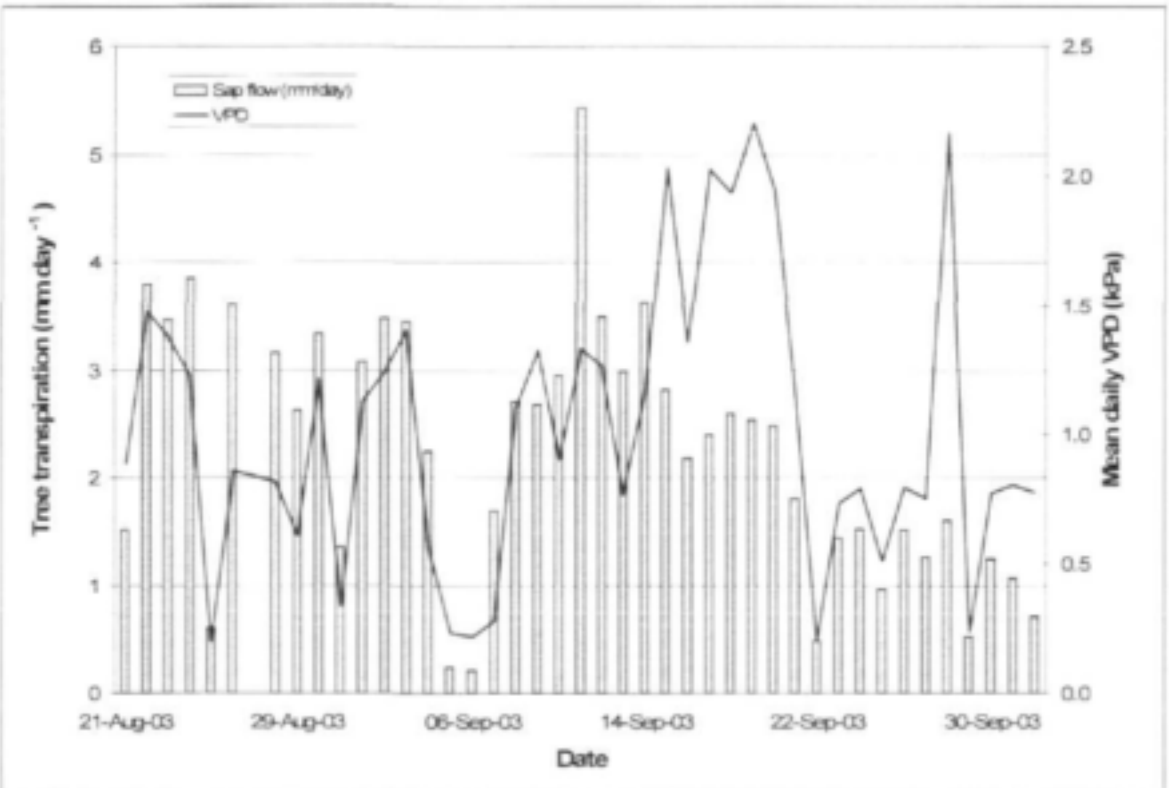

Figure 4.29 Sap flow measured in the A-Zone (August to September 2003).

4.7 Grassland evaporation in the cleared riparian strip.

Evaporation of the recolonised natural grassland in the cleared riparian strip was monitored using the Bowen ratio energy balance technique. Data were analysed for the period December 2000 to September 2005 (Figure 4.30). The grassland evaporation ranged between 3 and 7.5 mm day^{-1} during this period showing the large contribution of the grassland to water use within the catchment during the summer period (Figure 4.30). Clear trends of low evaporation in the dry winter period followed by peak rates in mid summer are shown by these data. These data illustrate the very high water use (summer maxima >7 mm day^{-1}) of the predominantly dense Setaria megaphylla vegetation in the riparian strip.

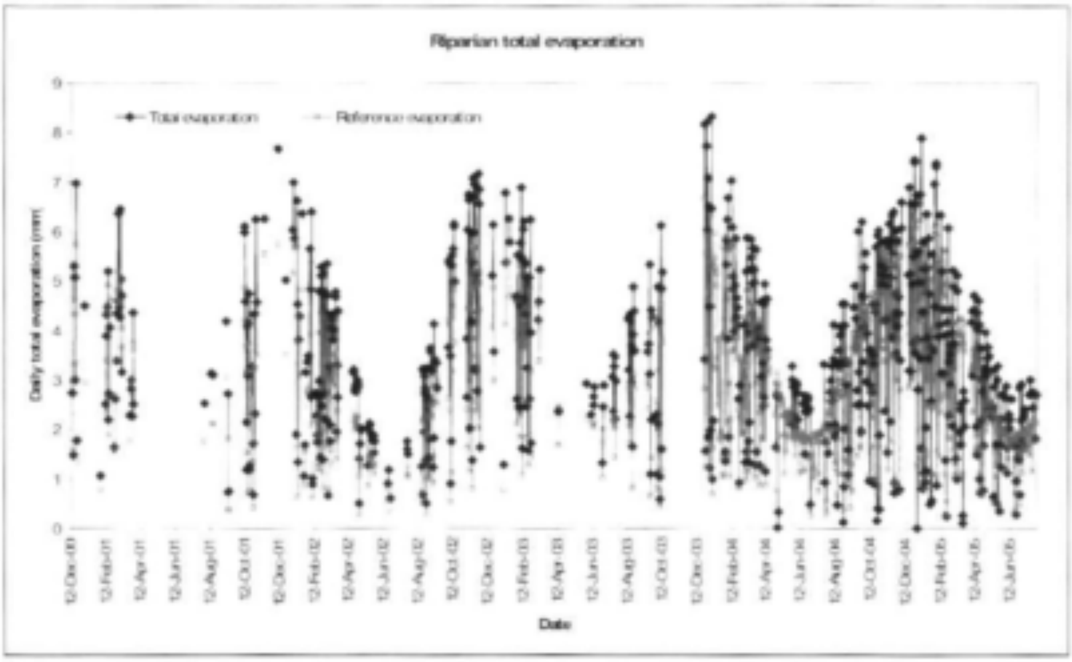

Figure 4.30 Daily evaporation in the grassland site from December 2000 – September 2005.

The Penman Monteith reference evaporation showed very similar trends to the Bowen ratio evaporation. Bowen ratio estimates were about 20% greater than the Penman Monteith evaporation (Figure 4.31), with an R^2 of 0.73 and coefficient of x=0.807. This is not unexpected as the Penman Monteith evaporation represents a well watered short grass surface and the riparian zone a well watered tall grass canopy.

The FAO 56 Penman Monteith evaporation (Figure 4.32) showed typical trends expected for the summer rainfall area of South Africa, with maximum values between 6 and 8 mm in summer and minimum values < 2 mm in winter. Annual values varied markedly with the minimum annual potential evaporation of 1050 mm in the 1999/2000 hydrological year and the maximum of 1436 mm being recorded in the 2002/2003 hydrological year. A regression of rainfall and the potential evaporation showed no significant relationship (data not shown). This is most likely because the calculation of the potential evaporation is dependent on numerous interdependent parameters (e.g. temperature, humidity and net radiation).

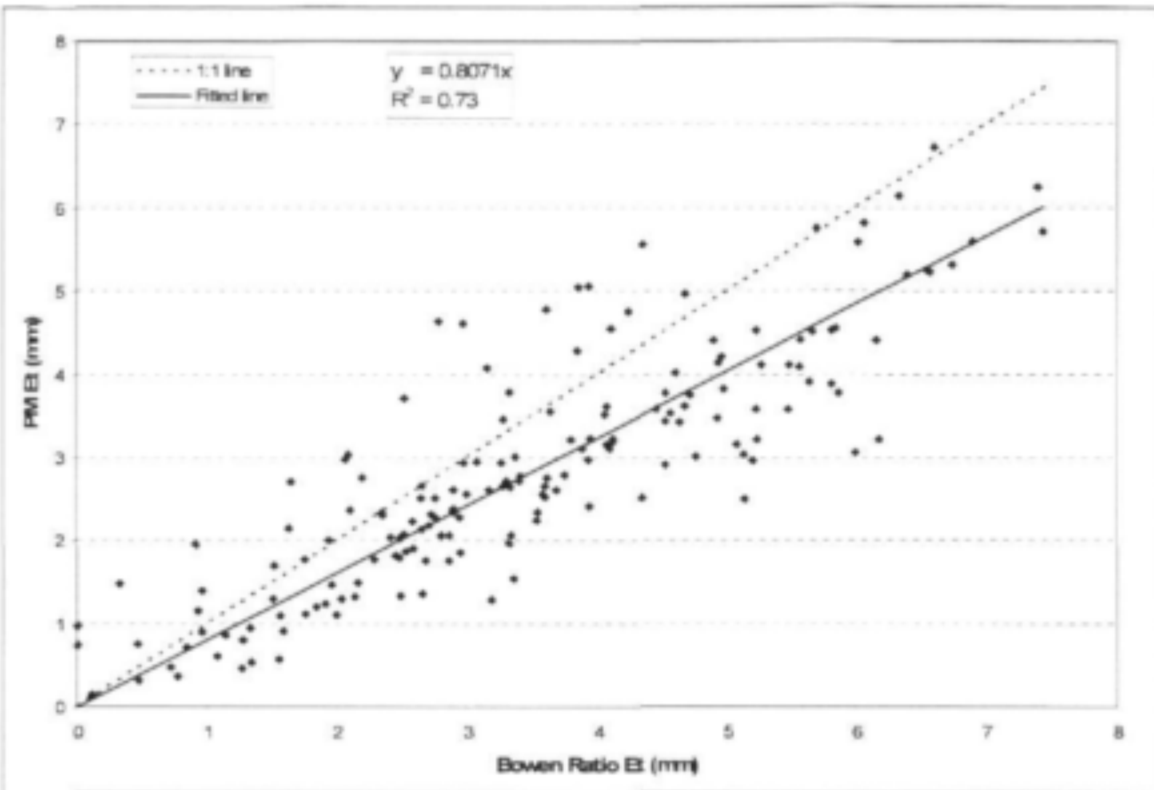

Figure 4.31 The relationship between the Bowen ratio and the Penman Monteith daily evaporation.

Actual evaporation (Bowen ratio estimates) from 1997 to 2000 from a black wattle compartment less than 1 km from the Two Streams catchment (Jarmain and Everson, 2002) varied between 1048 and 1364 mm. A range very similar to the FAO 56 potential evaporation measured in this study. The total annual rainfall recorded in the 2002 study was 874, 616, 1016 and 860 mm yr^{-1} during 97/98, 98/99, 99/00 and 00/01 respectively. The long-term average rainfall for Two streams is 853 mm yr^{-1}. This raises the question of how these trees can consistently transpire more water than the annual rainfall. This is an area of research which needs further investigation as similar results have been found for other studies (Jarmain, Govender and Everson, 2004) and have raised the question of the validity of these Bowen ratio derived total evaporation estimates.

The FAO 56 (based on daily averages) and the Penman-Monteith estimates of the reference evaporation derived from hourly data showed similar trends (Figure 4.33). However the FAO 56 estimates were consistently higher than the Penman-Monteith estimates. This overestimation in the estimates is shown in Figure 4.34 where a regression analysis (R^2= 0.83) showed that the fitted line had a coefficient of x = 1.19 (i.e. a 19% difference). We ascribe this difference mainly to the way the VPD is calculated. The FAO 56 uses the following technique to estimate the average VPD:

$$\text{VPD\_average} = \frac{(e_s T_{max}) + e_s(T_{min})}{2} - \frac{e_s(T_{min}) \times RH_{max} + e_s(T_{max}) \times) RH_{min}}{2} \quad (4.1)$$

This estimate of VPD_average is different from what the logger would calculate the daily average VPD to be for the Penman-Monteith estimate (MJ Savage, *pers comm.*). The logger calculates the VPD every 10 seconds and then averages that over 60 minutes. It is these VPD values that should then be used to estimate ET_0. So this problem with the VPD averaging will always occur if the VPD is calculated from RH averages as prescribed by the FAO 56 method. RH is an index and therefore it should not be averaged or weighted. The equations are non-linear so averaging compounds the problem. These data highlight the differences that may be obtained in estimating ET_0 using different algorithms. However considering that the input data were not the always from the same weather station (some of the FAO 56 data were obtained from a weather station situated in Wartburg) the agreement found is acceptable.

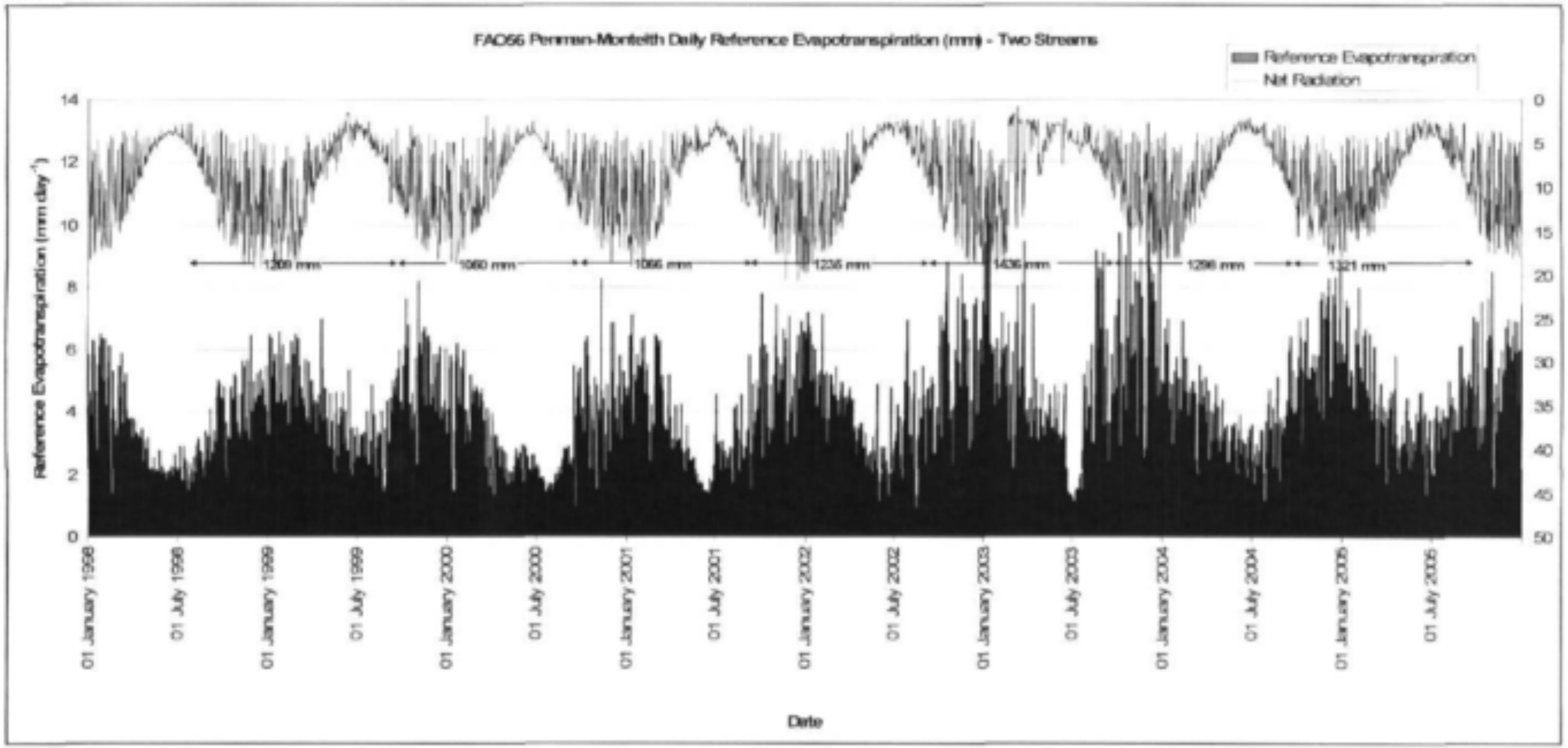

Figure 4.32 Daily FAO 56 Reference evaporation (mm) and net radiation (MJ day^{-1}) for the period January 1998 to December 2005. Annual totals are from 1 October to 30 September.

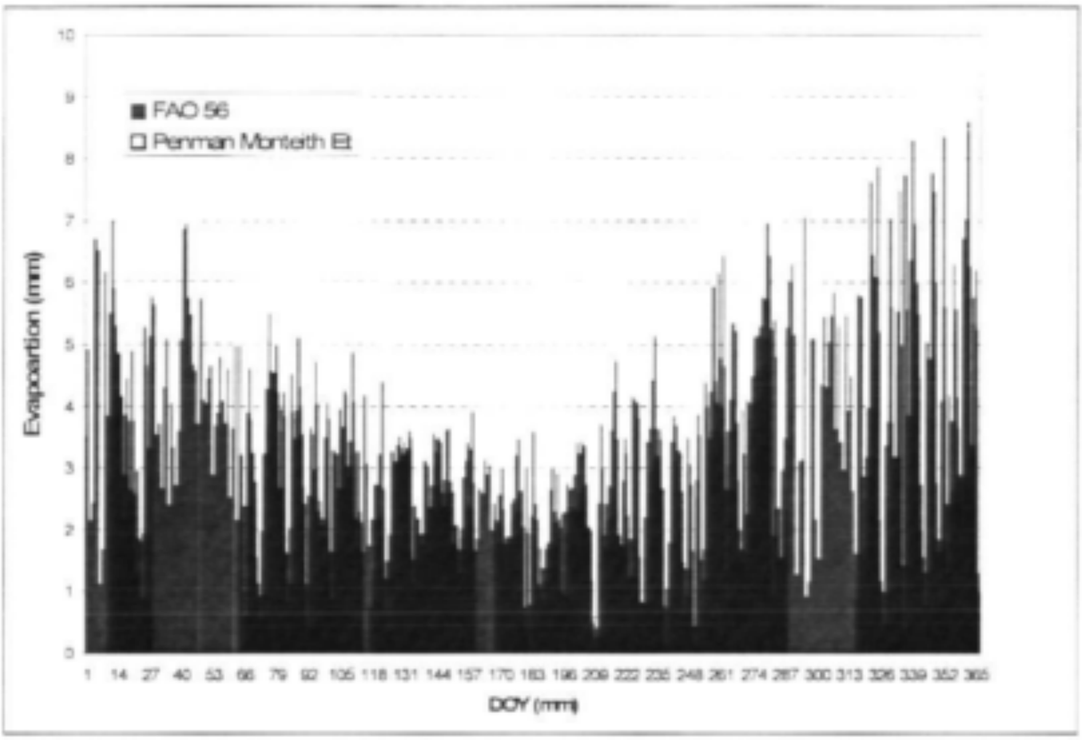

Figure 4.33 Daily estimates of the FAO 56 and Penman-Monteith evaporation (mm) for 2004.

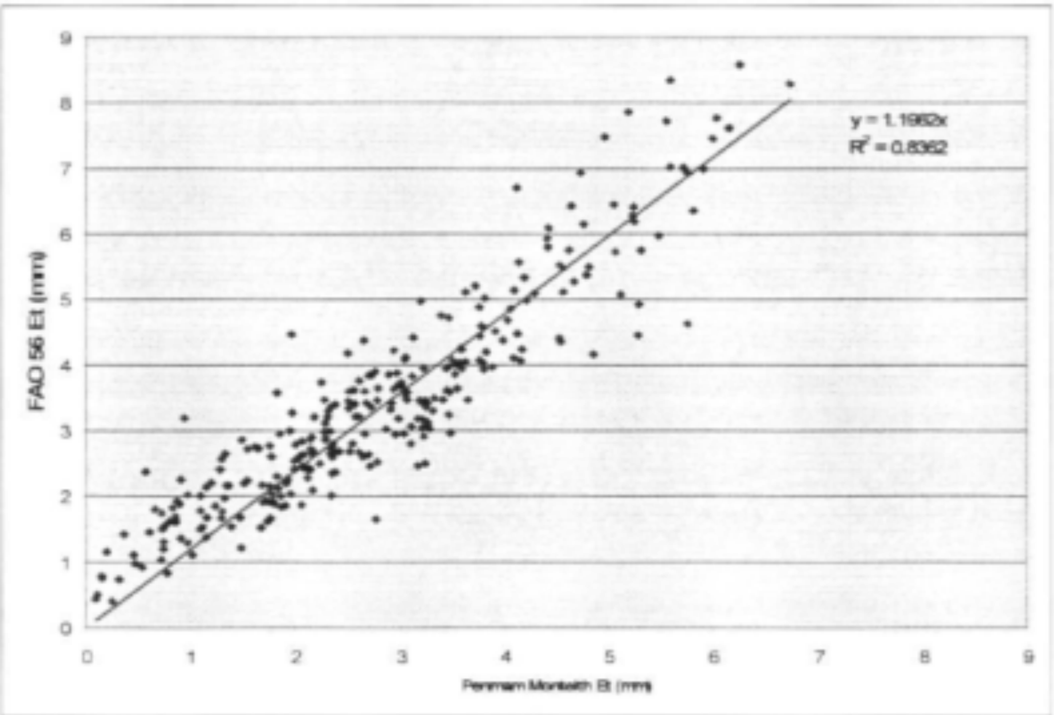

Figure 4.34 A linear regression of the FAO 56 and Penman-Monteith evaporation estimates (mm).

4.8 *Catchment scale modelling (SWAT)*

4.8.1 Data Sources

Digital Elevation Models (DEMs) of a fine resolution are not freely available in South Africa. Therefore 1:5000 scale contour maps for the study sites were digitized and used to create DEMs in ArcInfo. DEMs having a 10 m resolution were produced. Soil type data were obtained from the ISCW database and Mondi soils maps. Landuse layers were obtained from the GPS data collected during the mapping exercise.

Long-term daily rainfall and temperature data from 1950-2000 were used in the model simulations. The data were obtained from the daily rainfall and temperature databases developed by the University of KwaZulu-Natal's, School of Bioresources Engineering and Environmental Hydrology.

4.8.2 Model Configuration

Because of the small size of the catchment only one hydrological response unit (HRU) based on the predominant soils and landuse data was delineated by the model. The model was setup to utilize SWAT's landcover classes listed in the landcover database, but modified to represent South African conditions. Sugar cane, wattle, veld and eucalyptus vegetation types were configured for the SWAT growth model.

Potential Evapotranspiration (ET) was estimated using the Penman Monteith formulation (Monteith, 1965). Where the Penman-Monteith method required solar radiation, air temperature, windspeed and relative humidity as inputs, the data were simulated using a weather generator file, created from the Seven Oaks automatic weather station daily data. Measured daily temperature data were used, while monthly averages of solar radiation, windspeed and relative humidity values were retrieved from the weather generator file.

The model was configured to test three different scenarios: 1. Complete afforestation with *Acacia mearnsii* (including trees in the riparian zone) 2. Riparian zone unplanted with *Acacia mearnsii* trees and 3. Natural veld (Baseline condition).

4.8.3 Results

Annual rainfall for the fifty year period showed a clear cyclical trend in the rainfall pattern with three peaks occurring in about 1961, 1976 and 1997 (Figure 4.35). The high rainfall of 1987 (1438 mm) is also prominent in the data. Simulated streamflow followed the cyclical rainfall pattern, with values generally less than 20 mm in dry years (e.g. 1970-72) and between 100-250 mm in wet years. Predicted streamflow in 1999 was only 4 mm (Figure 4.35), and coincides with observations from this project of no visible streamflow at this time (see Figure 4.5 in January 2000).

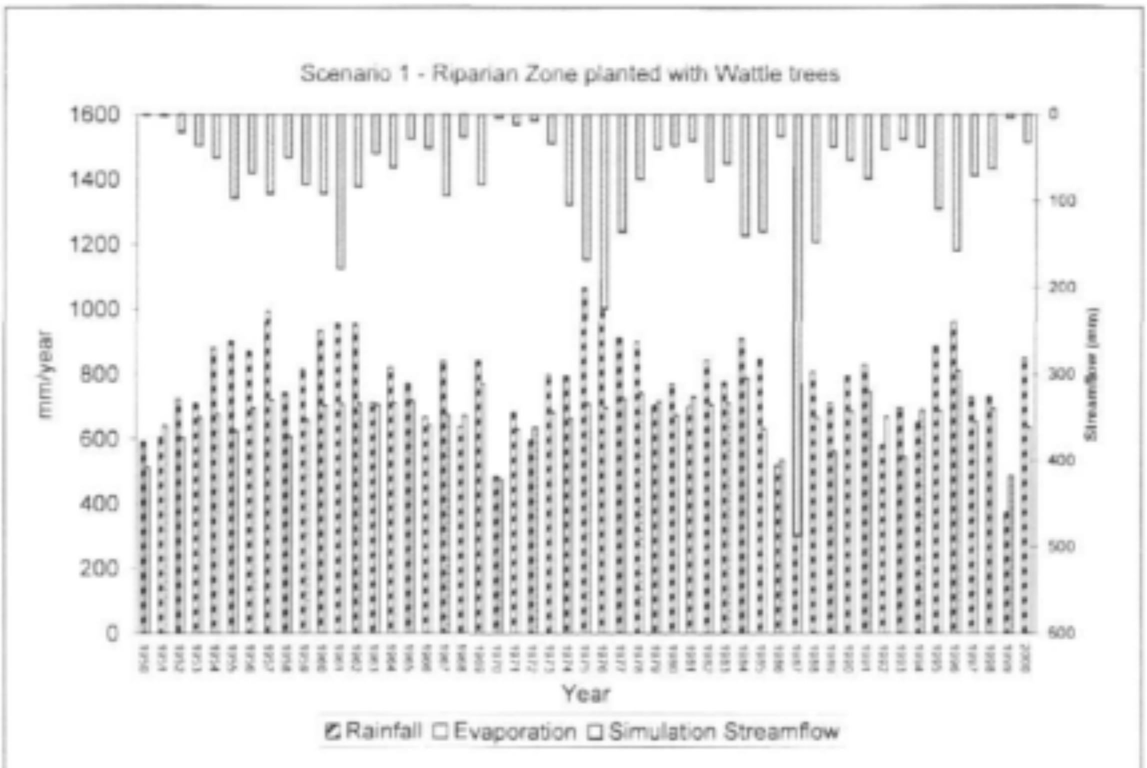

Figure 4.35 Streamflow, rainfall and evaporation for a fifty year period for the Two Streams Catchment A using the SWAT model.

Recorded streamflow in 2000 was 20 mm compared with 32 mm predicted by the SWAT model. From these data we concluded that the model was predicting annual streamflow with reasonable accuracy. Annual evaporation for the Wattle trees varied between 600 mm in dry years to over 800 mm in wet years for the completely afforested catchment. Evaporation only exceeded rainfall in the very dry years of the simulation (e.g. 1999). Annual streamflow for the three different scenarios and the accumulated totals (Figures 4.36 and 4.37) showed that the streamflow was reduced by the wattle trees when compared with the natural veld scenario.

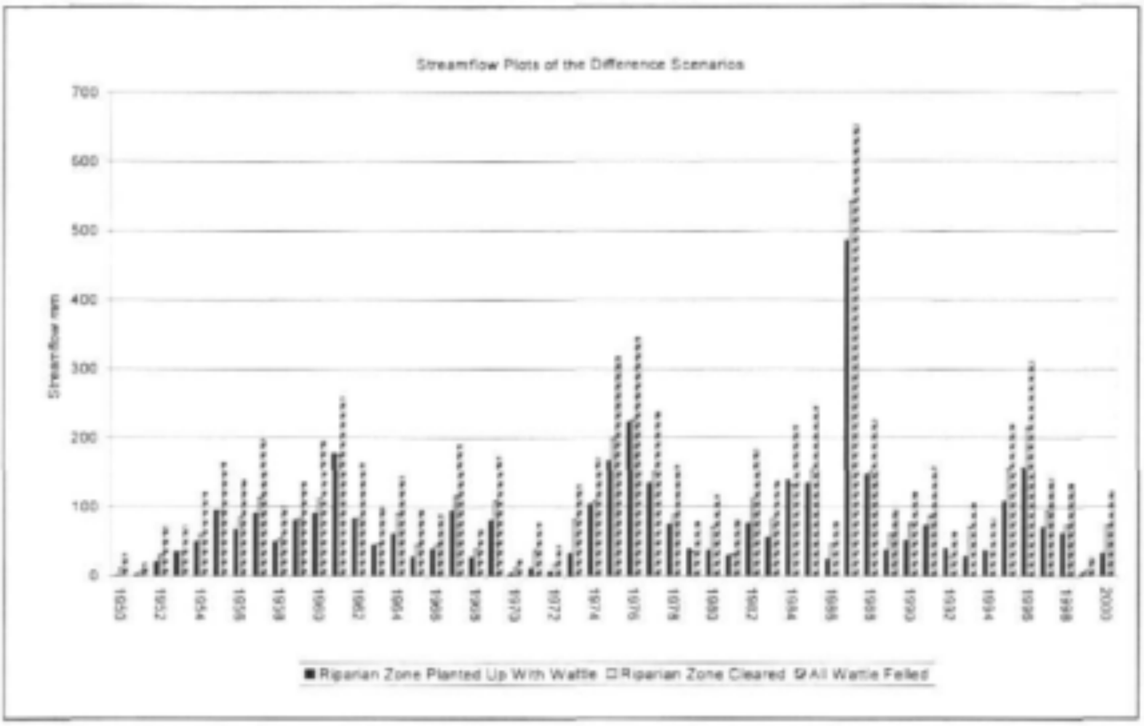

Figure 4.36 Annual predicted streamflow for the three different scenarios.

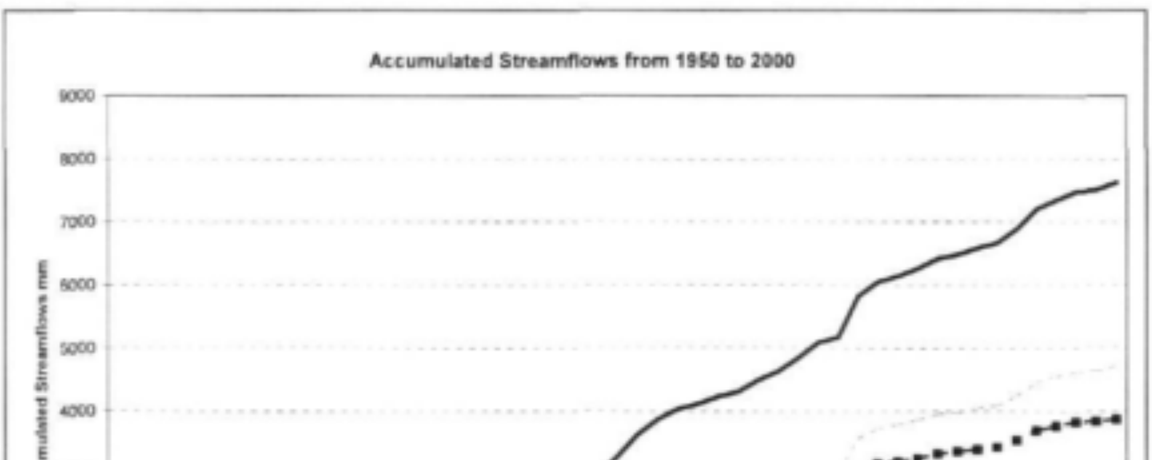

Figure 4.37 Accumulated streamflow for the three different scenarios using the SWAT model

No riparian trees (referred to as riparian zone cleared in the simulations), resulted in an increase in streamflow when compared with the streamflow from the total afforestation scenario (Figure 4.37). A plot of these data (accumulated streamflow vs accumulated rainfall) showed the same trends (Figure 4.38).

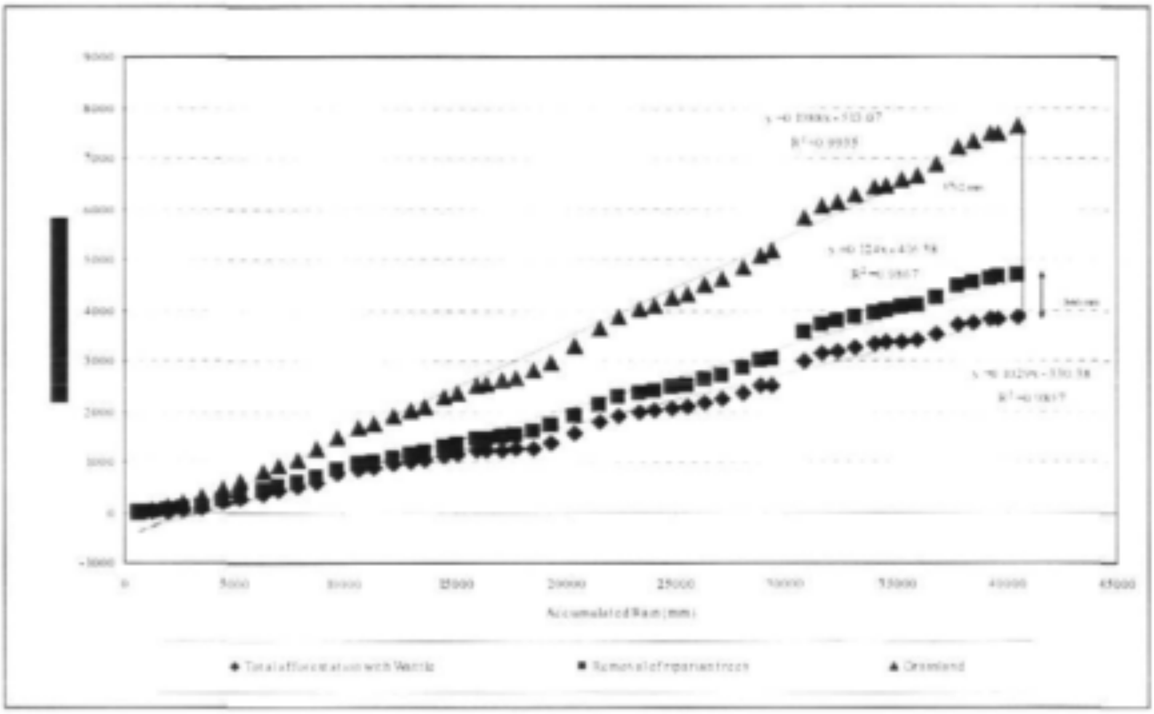

Figure 4.38 Single mass plots for simulations of three land cover scenarios for the period 1950-2000.

The total increase in predicted streamflow caused by the removal of the riparian trees over the fifty year period was 846 mm (approximately 17 mm annum^{-1} or 20% of MAR). This compares with the 35 mm increase actually measured over the three year period following the post riparian clearing operation (i.e. 12 mm annum^{-1} or 40% of MAR). Modelled and measured predictions were therefore in close agreement. The difference between the total afforestation and natural veld over the 50 year simulation was 3762 mm or about 75 mm annum^{-1}.

4.9 Catchment scale modelling (ACRU)

4.9.1 Data Sources

Long-term daily rainfall and temperature data from 1950-2000 were used in the model simulations. The same rainfall and temperature data files were used to run the ACRU simulation as were used for SWAT.

4.9.2 Model Configuration

The ACRU model was configured to test the same three scenarios as for the SWAT model: 1. Complete afforestation with *Acacia mearnsii* (including trees in the riparian zone) 2. Riparian zone with natural vegetation (i.e. no trees) and 3. Natural veld (Baseline condition). Originally the simulations were run in "lumped" mode but on advice from the ACRU modelling group the model was setup to simulate the riparian zone explicitly using the IVLEI-3 option in distributed mode.

4.9.2.1 Two Streams input data

Rainfall and streamflow data

Two raingauges were used to determine the rainfall data for the simulation. The majority of the data was derived from the Mistley raingauge based at the Mondi Forest offices on the estate, with subsequent data obtained from the CSIR's electronic tipping-bucket raingauge (2STRMS2) installed later in the study catchment.

Additional climatic data for Seven Oaks

Average monthly totals of A-pan equivalent evaporation data as well as monthly means of daily maximum and minimum temperatures were extracted from the Agrohydrological and Climatological Atlas (Schulze, 1997). These data are summarised in Table 4.3.

Table 4.3 Monthly climatic data for Seven Oaks

Month/ Variable	Jan	Feb	Mar	Apr	May	Jun	Jul	Aug	Sep	Oct	Nov	Dec
T-Max (°C)	21	20	19	18	17	15	13	17	21	22	23	22
T-Min (°C)	13	14	13	11	8	6	6	8	10	12	14	13
A-pan (mm)	190	170	150	125	105	95	105	125	145	150	160	180

The data used to parameterise the ACRU model using the ACRU menu builder are included in Appendix 1.

4.9.3 Results

The cyclical trends in annual rainfall for the fifty-one year period were identical to that for the SWAT modelling exercise since the same climate database was used for both catchment models. The ACRU streamflow for total afforestation with *A. mearnsii* followed the cyclical rainfall pattern, with annual values generally less than 5 mm in dry years (e.g. 1970-72) and > 10 mm for the catchment in wet years (e.g. 1974-78) (Figure 4.39). Evaporation (soil and plant) varied from less than 400 mm annum^{-1} in dry years (e.g. 1950) to > 1000 mm in very wet years (e.g. 1978) (Figure 4.39). The intercepted portion of evaporation (modelled separately by ACRU and determined by the difference between the gross and effective rainfall) was high, averaging 192 mm for the 51 year simulation period. This was 24% of the average rainfall of 787 mm annum^{-1}

recorded during the modelled period and similar to the results measured in the pilot interception study (section 4.1). For the natural grassland (baseline) scenario, evaporation averaged 583 mm annum^{-1} and interception 146 mm annum^{-1}. The model therefore predicted a mean annual increase in total evaporation of 250 mm from the trees, resulting in a decrease in streamflow from 40.4 to 20.5 mm annum^{-1}.

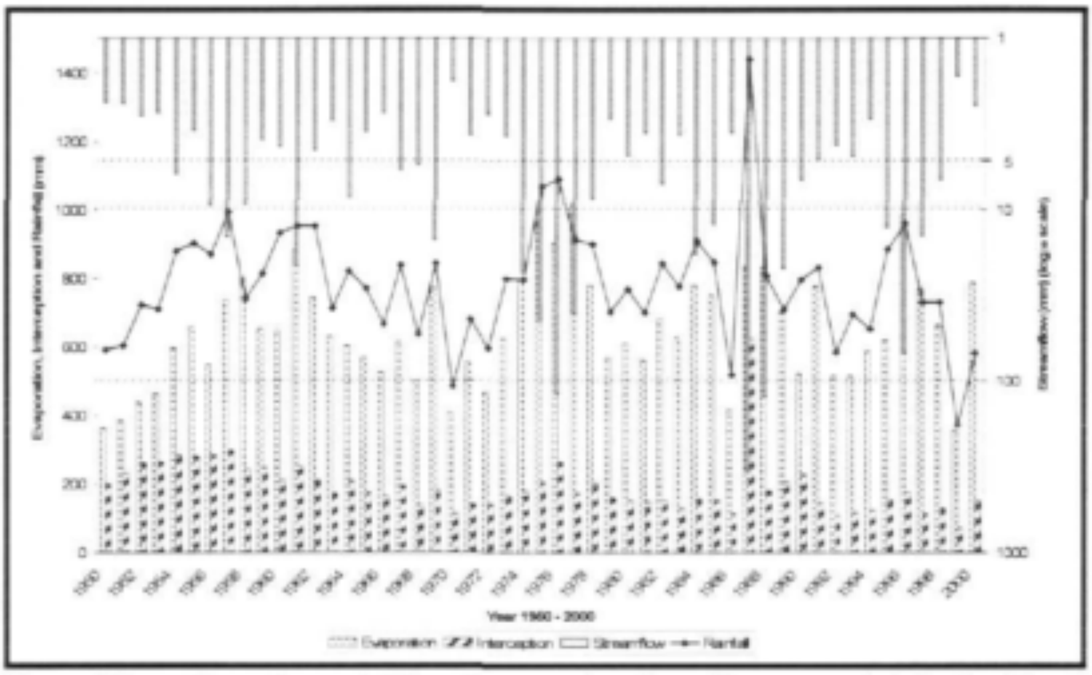

Figure 4.39 Streamflow, rainfall and evaporation for a fifty year period for the Two Streams Catchment A predicted using the ACRU model.

The impact of changing the landuse from grass to trees on the catchment water balance is shown by plotting the deviations between the annual rainfall and the sum of the total annual evaporation and streamflow for the natural grassland and *Acacia mearnsii* scenarios (Figure 4.40). The grassland and wattle residual water balances showed completely different trends, with the grassland residual water balance being generally positive while in the *Acacia mearnsii* scenario the annual residuals were mostly negative. The accumulated impact over the 51 year period was a positive gain of 814 mm for the grassland and a loss of -3772 mm when planted with *Acacia mearnsii*. These modelled losses due to trees are a direct result of the increased transpiration and interception losses and allude to a situation where the wattle trees are obtaining additional soil water from deeper horizons, since the total evaporation exceeded the rainfall. This excess of evaporation over rainfall has also been shown by direct measurements of evaporation using the Bowen ratio technique (Jarmain and Everson, 2002) and requires further research in order to understand the long-term sustainability of afforestation in South Africa.

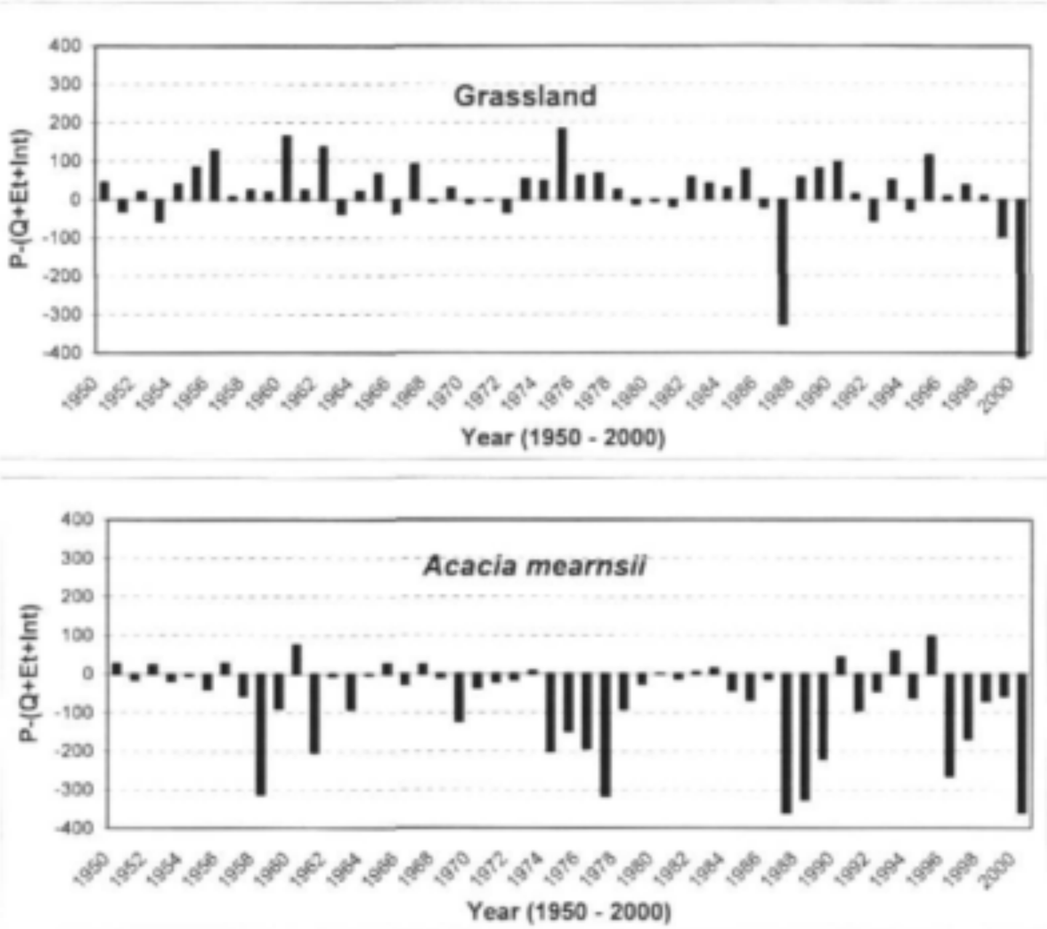

Figure 4.40 The residual of the annual water balance ($P - [Q + E_t$ + Interception]) for a fifty one year period for the Two Streams Catchment, predicted using the ACRU model for the grassland and *Acacia mearnsii* scenarios.

Differences in annual total evaporation between the three different land cover scenarios (Figure 4.41) showed that the highest evaporation rates were in the *Acacia mearnsii* scenario, the lowest in the grassland, and the wattle with riparian grassland being intermediate between the former two scenarios. What is striking about these data is the strong relationship (R^2 =0.76) between the annual rainfall and the total evaporation (Figure 4.41). This situation is consistent with drier climates, where evaporation increases with rainfall, while there is no strong relationship with streamflow and rainfall (In this instance the R^2 for the relationship between P and Q for the wattle scenario was only 0.41). This difference in behaviour can be explained by the relative magnitude of precipitation and potential evapotranspiration (E_{pot}). When P is much greater than E_{pot}, the evaporative demand can be totally satisfied and the remaining water becomes streamflow. In contrast, when rainfall is lower than E_{pot} then the water supply in wetter years is still not enough to satisfy all transpiration and potential evaporation. As a result, streamflow is more dependent on rainfall distribution in time than on annual volume (Pinol *et al.*, 1991).

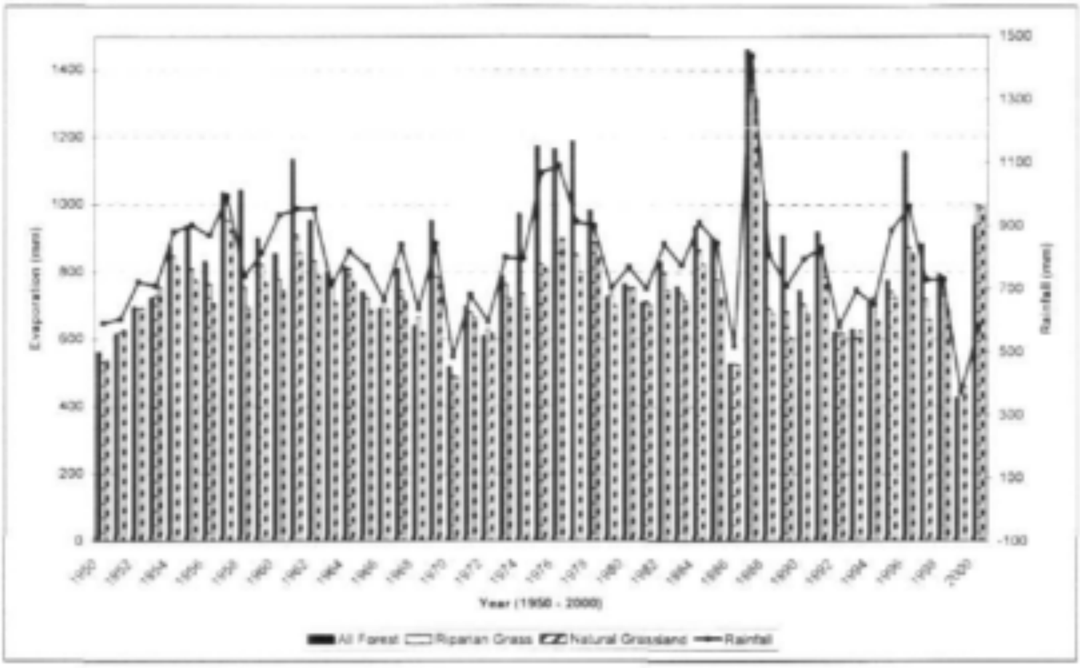

Figure 4.41 The annual rainfall and annual total evaporation for a fifty one year period for the Two Streams Catchment, predicted using the ACRU model for the grassland, *Acacia mearnsii* , and riparian grassed scenarios. Note the strong relationship between annual E_T and P.

The accumulated totals for 51 years of data for the three modelled scenarios (Figure 4.42) showed that the streamflow was reduced by a total of 1066 mm due to the wattle trees when compared with the natural veld scenario ($\bar{x}$ = 21 mm yr^{-1}). The difference between the total afforestation and riparian zone removal scenarios was 287 mm after 51 years of simulation ($\bar{x}$ = 5.6 mm yr^{-1}).

To allow direct comparison of the predicted and measured streamflow the ACRU model was configured using the actual input-data collected in this study from 1999 to 2006. Total accumulated streamflow predicted for the grassland, wattle with riparian as grass and total afforestation with wattle was 355, 185 and 142 mm respectively (Figure 4.43). This compares with the total of 307 mm of actual streamflow when the different management practices were applied to the catchment over the seven year study period. Thus the modelled reduction in streamflow from the natural grassland condition was 43 mm and 213 mm for the riparian cleared and totally afforested scenarios respectively. This translates into mean annual reductions of 6.1 and 30.4 mm yr^{-1} respectively. A single mass plot of accumulated rainfall versus the accumulated streamflow (Figure 4.44) illustrates the observed catchment response to the various management practices from January 2000 to May 2007. A hypothetical line of no change (i.e. total afforestation), determined by a regression of the pretreatment data, showed average reductions in streamflow of 4 mm yr^{-1} and 50.3 mm yr^{-1} following actual riparian clearing and total removal of the trees respectively. The modelled values are considered realistic if one considers that in the ACRU simulations we did not use the dynamic files option (mature trees were assumed for the entire simulation). Secondly, in the real situation the catchment was allowed to lay fallow for 24 months before planting. Thus modelled evaporation would be higher than

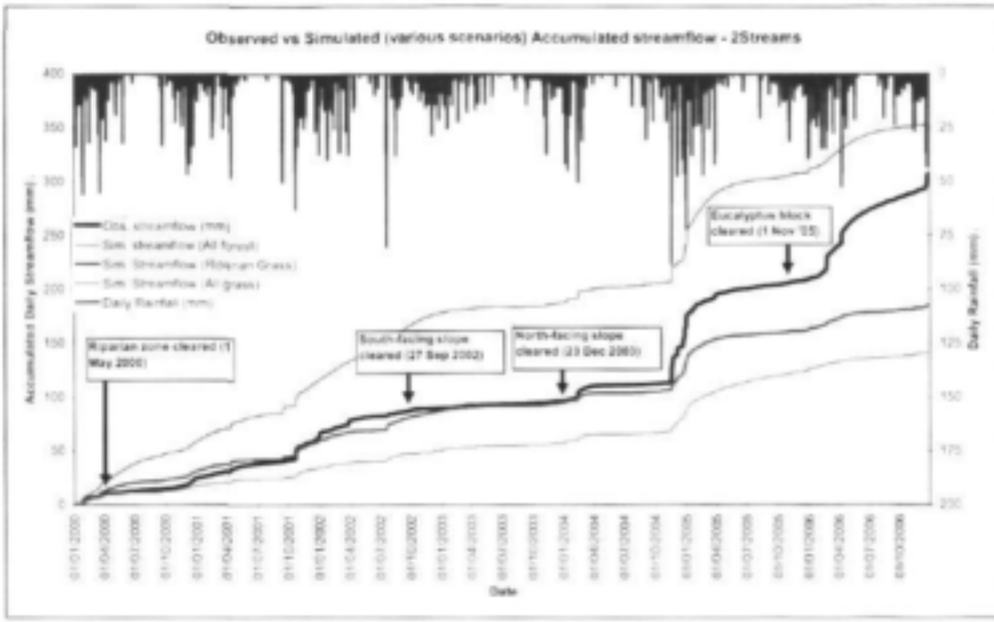

Figure 4.42 ACRU accumulated stream flows for the three different scenarios from 1950 to 2000.

expected (reducing streamflow), while actual evaporation would be lower than expected (increasing streamflow). Also note that the effects of sugarcane harvesting (Jul 2002, Feb 2004 and Sep 2005) as well as the clearfelling of the eucalyptus block (Dec 2005) may have increased streamflow independently (and led to an under-simulation of streamflow). The ACRU model results were therefore considered good when one considers the small scale of the catchment and the acceptable error related to these hydrological models.

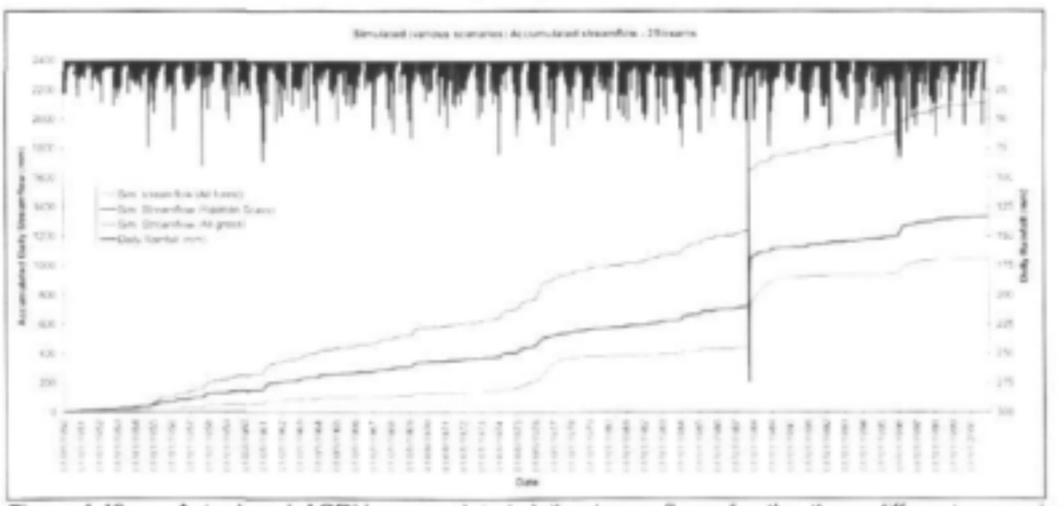

Figure 4.43 Actual and ACRU accumulated daily stream flows for the three different scenarios from 2000 to 2006.

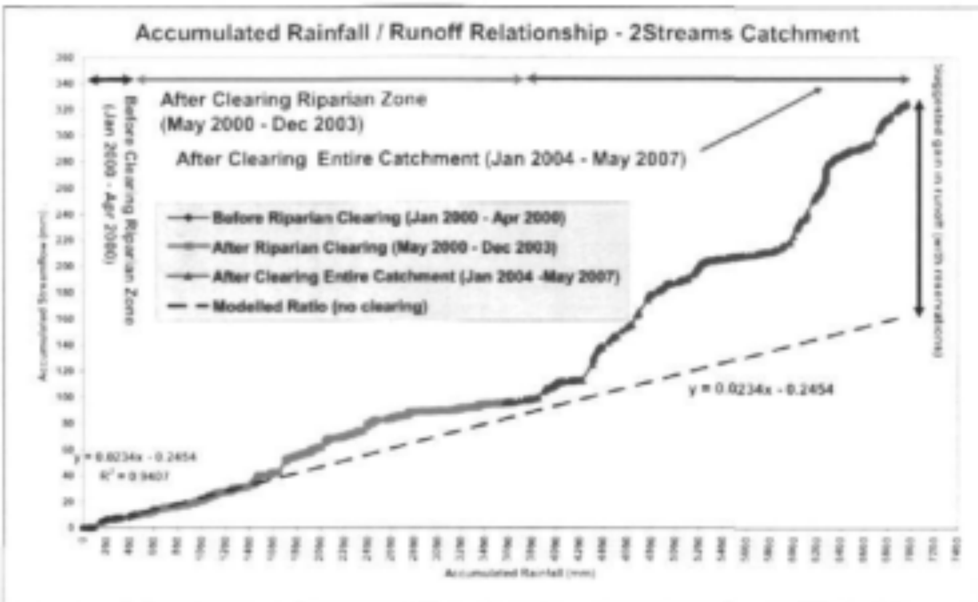

Figure 4.44 The relationship between accumulated rainfall and accumulated streamflow for the Two Streams catchment A, for the period November 1999 to May 2007.

CHAPTER 5: FINAL DISCUSSION AND CONCLUSIONS

In the previous chapter we have presented actual and modelled data on the various hydrological components of the Two Streams catchment. Measuring the water use of the vegetation in the catchment can also be done by monitoring the difference between the annual precipitation and measured streamflow (Bosch, 1979). While these studies enable broad estimates of water loss, they do not distinguish for losses by interception and evaporation from the soil.

Water balance is a deterministic relation between the water balance components which are random variables in time and space, with usually unknown probability distributions. The independent input variable is rainfall, which is transformed in the hydrological system into the dependent output variables evaporation, streamflow and change in soil storage. These hydrological processes are dynamically coupled through the physical processes of energy and water supply, transformation (latent and sensible heat), and transport (streamflow) at a land-atmosphere interface (Dyck, 1983). A useful test of the reliability of the data collected in a study such as this is to perform a catchment water balance.

To allow mathematical prediction of the various hydrological variables, some simplifications are necessary. The most practical method is the use of the deterministic approach of applying the macroscopic version of the continuity equation. The various continuous water movement processes of the hydrological cycle are lumped over finite time intervals and areas and related by the water balance equation. The volumetric water balance per unit area may be expressed as:

$$P - E_a - SS = Q \qquad (5.1)$$

Where P = precipitation; E_a= actual evaporation; SS = soil storage; and Q = streamflow (Eagleson, 1978). All terms except P depend upon soil moisture level and distribution which is generally not measured, the problem being overcome by assuming the system to be stationary in the mean. If the integration interval is a full year and expected values are substituted, the change of storage is negligible and the average annual water balance equation is as follows:

$$\overline{P} + \overline{E_a} = \overline{Q} \qquad mm\ year^{1} \qquad (5.2)$$

Reliable data for annual *P* and *Q* were measured in the Two Streams catchment from the 1999/2000 to 2005/2006 hydrological years. Total evaporation data were not available in all years and therefore E_a could be obtained by subtraction, using the annual water balance equation (equation 5.2). This assumes that deep losses of water are negligible and that the soil water content is identical at the beginning and at the end of the hydrological year (1 October and 30 September respectively). With respect to the first assumption, the Two Streams catchment is underlain by a fractured rock layer and it is possible that deep water losses occurred. The second assumption was tested using data on the total profile water content. Because the evaporation record was incomplete, we used the FAO 56 reference evaporation (Allen *et al.*, 1998), for comparison with the water balance determined E_a. Although we investigated the possibility of determining a crop coefficient for the wattle trees, we were unable to find a satisfactory relationship between the actual tree and the reference evaporation to do this. This is an area that requires further research.

The variable annual precipitation during the study period (688 mm to 1170 mm – Table 5.1) provided an opportunity for contrasting the water balance of wet, dry and average hydrological years. Daily precipitation in the six year study period showed the characteristic pattern found in the summer rainfall regions, with the summer months being wet and the winters very dry (Figure 4.1). There was a high frequency of dry days during the period June through to August. During the dry period, the vegetation in the riparian zone was largely dormant and evaporation was minimal. Our data indicated that evaporation in the riparian zone was approximately 1-2 mm day^{-1} during the winter months. However, wattle tree transpiration during August was generally above 3 mm day^{-1}. It is these seasonal differences in evaporation between the dormant grassland and evergreen exotic trees which result in streamflow reductions, as summer evaporation values for the trees and grasses were similar.

Annual streamflow for the study period averaged only 33.5 mm annum^{-1}, with highs of 46.1 and 91.8 mm in the high rainfall years (2001/02 and 2004/05 respectively) (Table 5.1). In the driest year (2002/2003 – MAP of 659.1 mm) the stream discharge was only 6.7 mm. Steamflow was only a small fraction of the annual rainfall, with the average rainfall:runoff ratio (Rr) = 3.4% (Table 5.1). The average change in soil storage was 25 mm and varied from -52.5 mm in the driest year to +104.5 mm in the 1999/2000 hydrological year (Table 5.1). Therefore the change in soil storage (SS) was generally only a small percentage of the annual rainfall.

The annual evaporation estimated by subtraction in the water balance equation, varied widely from 700.7 mm in 2003/2004 to 1120.7 mm in 2001/2002 and averaged 884.7 mm over the six years of measurement. The average annual FAO 56 reference evaporation was 1234 mm annum^{-1} (Table 5.1). The evaporation was a very high percentage of the annual rainfall (mean = 94.5%). In the 2002/2003 year this percentage was 106.9%, indicating that the evaporation exceeded rainfall. Actual Bowen ratio estimates of evaporation from the riparian zone and from previous studies (see section 4.6 & 4.7) indicated that evaporation would generally be in excess of 1000 mm. Although this was the case in the high rainfall years, it is not consistent with the low evaporation rates estimated using the water balance equation in the dry years (± 700 mm). This "additional" water is either being obtained from deeper soil layers or there is a problem with the actual evaporation estimates. These anomalous findings of excess evaporation over rainfall require further study, as they have been observed in other evaporation studies (Jarmain, Govender and Everson,2004). In addition, in this study we also showed that interception losses in *Acacia mearnsii* are likely to be greater than 20% of gross rainfall. Thus the effective rainfall may be less than the gross rainfall figures used to estimate evaporation in Table 5.1. This would result in even lower evaporation estimates using the water balance technique. Clearly this is an area for future research.

The low response ratios (Rr in Table 5.1) are similar to others reported in the drier and more arid areas where response ratios between 0.07 and 0.25 are common (Lewis, 1968, Burch *et al.*, 1987 and Pinõl et al. (1991). The data contrast markedly with the Rr of 0.43 measured in a similar study at Cathedral Peak (Everson et al., 1998). In other colder climates of the world, Likens *et al.* (1977) calculated a response ratio of 0. 61 for the Hubbard Brook catchments in New Hampshire (USA) and in Greece, Nakos & Vouzaras (1988), estimated a response ratio of 0.51.

Table 5.1 Components of the water balance equation measured in the Two Streams catchment (1999/2000 to 2004/2006). P = precipitation; Ea= estimated evaporation; SS = soil storage; Q = measured streamflow.

Year	P	-	Q	-	SS	=	Ea	% of P	Rr
1999/2000	1071.0	-	15.2	-	(+104.5)	=	951.3	88.8	0.014
2000/2001	897.0	-	26.6	-	(+77.3)	=	793.1	88.4	0.030
2001/2002	1170.9	-	46.1	-	(+4.2)	=	1120.7	95.7	0.039
2002/2003	659.1	-	6.7	-	(-52.5)	=	704.9	106.9	0.010
2003/2004	727.1	-	17.8	-	(+8.5)	=	700.7	96.4	0.024
2004/2005	1139.2	-	91.8	-	(+9.5)	=	1037.9	91.1	0.080
Mean	**944.0**	-	**34.0**	-	**25.3**	-	**884.7**	**94.5**	**0.033**

The Two Streams evaporation data were checked to determine if the estimates correspond to global trends. Zhang *et al.* (1999) analyzed catchment data from over 250 different gauged catchments from around the world, and derived two trend lines linking mean annual precipitation to mean annual evaporation from grassland and forest cover, respectively. These trend lines, together with the Two Streams and Cathedral Peak estimates are shown in Figure 5.1. According to these trends a catchment receiving a mean annual rainfall of 944 mm (i.e. as measured at Two Streams) would result in a mean annual evaporation loss of 808 mm, while the Cathedral Peak Grassland catchment (mean annual rainfall 1200 mm) would have an annual evaporation loss of 680 mm. The actual evaporation estimated for the forest and grassland from the two South African catchments was 884.7 mm and 666 mm, respectively. The South African data therefore are similar to those predicted by Zhang *et al.* and lend credibility to our estimates.

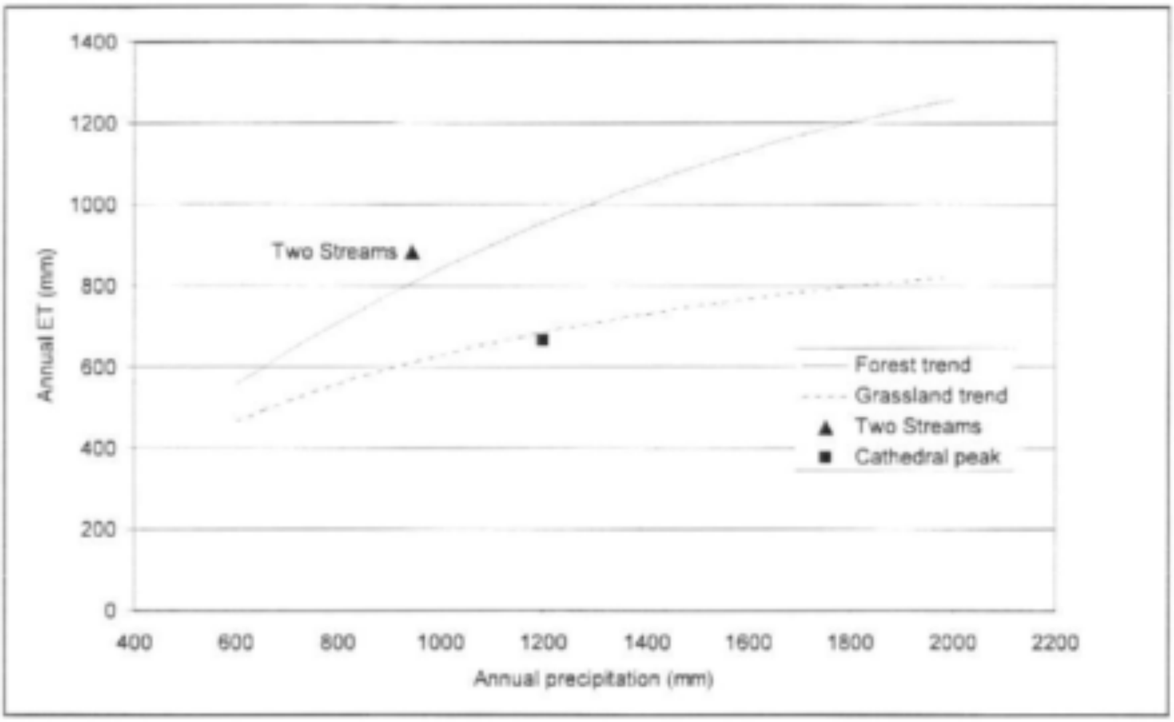

Figure 5.1 Global trends in mean annual evaporation from catchments dominated by forests and grasslands as calculated by Zhang *et al.* (1999) from a global review of catchment data from over 250 catchment studies. Data from Two Streams (forest) and Cathedral Peak (grassland) are superimposed on the data.

In a similar study Bosch and Hewlett (1982) reviewed 94 catchment experiments world wide to investigate the effect of vegetation changes on water yield. These authors concluded that coniferous and eucalypt cover types have the greatest influence on water yield, followed by deciduous and mixed hardwoods and finally scrub or grasslands. *Acacia mearnsii* was not studied in any of the catchments reviewed but the data gathered was used to develop general guidelines. Data from catchment experiments in South Africa extend over a period of at least 50 years and have shown that afforestation with alien trees decreases streamflow (Van Der Zel and Kruger, 1975; Van Wyk, 1977, 1987; Bosch and von Gadow, 1990). However, there are only a few studies that have been undertaken to investigate the effect of clearing of indigenous and invasive vegetation in riparian zones. Those that have been undertaken have all shown increases in streamflow (Nanni, 1972; Dye and Poulter, 1995a; Scott and Lesch, 1995, 1996). Dye and Poulter (1995b) found clearing 2.5 hectares of trees accounted for a 120% increase in streamflow, equivalent to 1.2 mm day^{-1} over the cut area. Dye and Poulter (1995b) concluded that invasive exotic trees should be removed from riparian zones to increase streamflow from afforested catchments. These short term studies only considered the immediate impact of tree clearing. It is also important to measure the subsequent re-colonisation of the site by indigenous vegetation to obtain the true difference. No previous studies have looked at the removal of pure stands of *Acacia mearnsii* from the riparian zone and none have looked at the subsequent effect of clearing the upslope areas on catchment water yield and hillslope processes. In addition, the previous studies were all short term (< 1 yr) as opposed to the six years of data collected in this study. For these reasons it is recommended that these studies on the hydrological impacts of *Acacia mearnsii* be extended to the next rotation.

The impact of the clearing of all the trees in this study was a 44% increase in streamflow. This was equivalent to 17.5 mm for the catchment. The relative contribution of the riparian zone compared to the upslope region during the period when both areas were cleared (January 2004 to May 2006) was 16 mm and 78 mm respectively (the riparian zone therefore contributing 21% to annual streamflow). Since the riparian zone represented only 11% of the total catchment area (7.5 ha versus 65 ha, Table 3.1), the significance of the riparian zone to streamflow generation was clearly demonstrated. Scott and Lesch (1995) analysed three paired catchments (two in Mpumalanga and one in the south Western Cape Province) in order to show that the water use of riparian vegetation was higher than that in other parts of a catchment. These experiments led the authors to conclude that trees in the riparian zone are liberal users of water when compared to vegetation in the surrounding catchment as was found in this study.

The data collected in this study have demonstrated the impact of both riparian and upland wattle on the streamflow of a small catchment in the KwaZulu-Natal midlands. Both the ACRU and SWAT models have been successfully validated using the Two Streams catchment data sets. The ACRU and SWAT models showed streamflow reductions of 50 mm and 75 mm annum^{-1} respectively when compared with natural grassland. The modelled data were therefore in good agreement with the measured data.

A final, but crucial, benefit of this study has been to extend the range of catchment afforestation experiments into the drier rainfall regions of South Africa (MAP = 853 mm). The vast majority of long-term South African catchment experiments in the past were established in regions where the MAP exceeded 1100 mm. However, as land with afforestation potential becomes increasingly difficult to locate, and as clonal varieties of commonly planted exotic tree genera are developed for greater drought tolerance, forestry is moving into more marginal (drier) regions. The value of having a long-term catchment afforestation experiment representative of the drier end of the forestry zone can not be over-emphasised.

CHAPTER 6: REFERENCES

Allen, R.G., Pereira, L.S., Raes, D. and Smith, M., 2004. Crop evapotranspiration: Guidelines for computing crop water requirements. FAO Irrigation and Drainage Paper 56. pp 300.

Arnold, J.G., Williams, J.R., Srinivasen, R. and King, K.W. 1999. SWAT: Soil and Water Assessment Tool-Model Documentation. USDA, Agricultural Research Service, Texas, USA.

Ball, B.C. O' Sullivan, M.F. and Hunter, R. 1988. Gas diffusion, fluid flow and derived pore continuity indices in relation to vehicle traffic and tillage. *Journal of Soil Science*, 39, 327-339.

Bosch, J.M. 1979. Treatment effects on annual and dry period streamflow at Cathedral Peak.

Bosch, J.M. and Hewlett, J.D. 1982. A review of catchment experiments to determine the effect of vegetation changes on water yield and evapotranspiration. *Journal of Hydrology*, 55, 3-23.

Bosch, J.M. and von Gadow, K. 1990. Regulating afforestation for water conservation in South Africa. South African Forestry Journal, 153, 41-54 Commonwealth Forestry Review, 75: 31-38.

Burch, G.J., Bath, R.K., Moore, I.D. and O'Loughlin, E.M. 1987. Comparative hydrological behaviour of forested and cleared catchments in Southeastern Australia. *J.Hydrol.* 90, 19-42.

Camp, K.G.T. 1997. The bioresources of KwaZulu-Natal. Cedara report N/A/95/32. KwaZulu-Natal Department of Agriculture, Pietermaritzburg.

DWAF, undated. A practical field procedure for identification and delineation of wetlands and riparian areas. Department of Water and Affairs and Forestry, Republic of South Africa.

Dyck, S. 1983. Overview on the present status of the concepts of water balance models. In New Approaches in Water Balance Computations Proceedings of the Hamburg Workshop, August 1983 . IAHS Publ. no. 148, pp 3-19.

Dye, P.J. and Olbrich, B.W. 1992. Estimating transpiration from 6-year-old *Eucalyptus grandis* trees: development of a canopy conductance model and comparison with independent sap flux measurements. Plant, Cell and Environment, 16: 45-53.

Dye, P.J., Soko, S. and Poulter, A.G. 1993. Progress report: development of a model to predict potential transpiration rates from different age classes of *Pinus patula*.

Dye, P.J. 1996. Climate, forest and streamflow relationships in South African afforested catchments.

Dye, P.J. and Poulter, A.G. 1995b. A field demonstration of the effect of streamflow of clearing invasive pine and wattle trees from a riparian zone. *South African Forestry Journal*, 173, 37-30

Dye, P.J. and Poulter, A.G. 1995a. Clearing invasive trees in riparian zones increases streamflow. Environmental Protection and Management, May 1995, 13-15.

Dye, P.J., Poulter, A.G., Soko, S. and Maphanga, D. 1997. The determination of the relationship between transpiration rate and declining available water for *Eucalyptus grandis*. Water Research Commission Report No. 441/1/97. 101 pp.

Dye, P.J. and Bosch, J.M. 1999. Water, wetlands and catchments. In: South African Forestry Handbook 2000. Vol 2, 567-573. Southern African Institute of Forestry, Pretoria.

Dye, P.J. 2000. Water use efficiency in South African Eucalyptus plantations: a review. *Southern African Forestry Journal*, No 189: 17-26

Dye, P.J., Moses, G., Vilakazi, P., Ndlela, R. and Royappen, M. 2001. Comparative water use of wattle thickets and indigenous plant communities at riparian sites in the Western Cape and KwaZulu-Natal. *Water SA*, 27: 529-538.

Eagleson, P.S. 1978. Climate, soil and vegetation. *Wat. Resour. Res.* 14 5 , 705-776.

Everson, C.S., Molefe, G.L. and Everson, T.M. 1998. Monitoring and modelling Components of the Water Balance in a Grassland Catchment in the Summer Rainfall Area of South Africa. Water Research Commission Report No. 493/1/98. 137pp.

Goller, R., Wilcke, W., Leng, M.J., Tobschall, H.J., Wagner, K., Valarezo, C. and Zech, W. 2005 Tracing water paths through small catchments under a tropical montane rain forest in south Ecuador by an oxygen isotope approach. *Journal of Hydrology*. 308: 67-80.

Green, W.H. and G.A. Ampt. 1911. Studies on soil physics, 1. The flow of air and water through soils. Journal of Agricultural Sciences 4:11-24.

Gush, M.B., Scott, D.F., Jewitt, G.P.W., Schulze, R.E., Lumsden, T.G., Hallowes, L.A. and Görgens, A.H.M., 2002. Estimation of streamflow reductions resulting from commercial afforestation in South Africa. Water Research Commission Report No. TT 173/02.

Jarmain & Everson 2002. Comparative evaporation measurements above commercial forestry and sugarcane canopies in the KwaZulu-Natal Midlands. Final Report: DWAF

Jarmain, C., Govender M. and Everson C.S. 2004. Improving the basis for predicting total evaporation from natural veld types in South Africa. A focus on moist upland grassland, valley thicket and coastal bushveld/d. WRC Report No. 1219/1/04.

Klute, A. and Dirksen, C. 1986. Hydraulic conductivity and diffusivity: laboratory methods. Pp 687 – 770. In Klute ed . Methods of soil analysis. Part 1. Physical and Mineralogical Methods. 2nd edition. Am. Soc. Agron. Soil Sci. Soc. Am. Madison, Wisconsin, U.S.A.

Lewis, D.C. 1968. Annual hydrologic response to watershed conversion from oak woodland to annual grassland. *Wat. Resour. Res.* 4, 59-72.

Likens, G.E., Bornmann, F.H., Pierce, R.S., Eaton, J.S. and Johnson, N.M. 1977. Biogeochemistry of a forested ecosystem. Springer Verlag, New York, USA.

Lynch, S. D. and Schulze, R. E. 2006. Rainfall Databases. In: Schulze, R. E. Ed . 2006. South African Atlas of Climatology and Agrohydrology. Water Research Commission, Pretoria, RSA, WRC Report 1489/1/06, Section 2.2.

Marshall, D.C. 1958. Measurement of sap flow in conifers by heat transport. Plant Physiology, 33:385-396.

Monteith, J.L. 1965. Evaporation and the environment. In: The state and movement of water in living organisms. 19th Symposia of the Society for Experimental Biology. Cambridge Univ. Press, London, U.K.

Nakos, G and Vouzaras, A. 1988. Budgets of selected cations and anions in two forested experimental watersheds in central Greece. *For. Ecol. Manag.* 24, 85-95.

Nänni, U.W. 1972. Water use by riparian vegetation at Cathedral Peak, South African Forestry Journal, 80, 1-10

National Water Act of 1998. National Water Act, RSA Government Gazette No. 36 of 1998: 26 August 1998, No 19182. Cape Town, South Africa.

Natural Resources Conservation Service Soil Survey Staff. 1996. National soil survey handbook, title 430-VI. U.S. Government Printing Office, Washington, D.C.

Neitsch, S.L., Arnold, J.G., Kiniry, J.R. and William, J.R. 2001. Soil and Water Assessment Tool: Version 2001 – Theoretical Documentation. Agricultural Research Service. Texas, USA.

Neitsch, S.L., Arnold, J.G. and William, J.R. 1999. Soil and Water Assessment Tool User's Manual, Version 99.2. Agricultural Research Service. Texas, USA.

Olbrich, B.W. 1994. The application of the heat pulse velocity technique to the study of transpiration from *Eucalyptus grandis*. Unpublished Ph.D. Thesis, University of Natal, Durban, South Africa.

Pinõl, J., LLedó, M.J. and Escarré, A. 1991. Hydrological balance of two Mediterranean forested catchments Prades, northeast Spain . *Hydrol. Sci.* J. 36, 95-107.

Rallison, R.E. and Miller, N. 1981. Past, present and future SCS runoff procedure. p. 353-364. In V.P. Singh ed. . Rainfall runoff relationship. Water Resources Publication, Littleton, CO. *S. Afr. For. J.* 108: 29-38.

Schulze, R.E., 1975. Catchment evapotranspiration in the Natal Drakensberg. Unpublished PhD Thesis, University of Natal, Pietermaritzburg. pp 244.

Schulze, R.E. 1995. Hydrology and Agrohydrology. A text to accompany the ACRU 3.00 Agrohydrological modelling system. SA Water Research Commission. Report No. TT 69/95

Schulze, R.E. 1997. South African Atlas of Agrohydrology and -Climatology. Water Research Commission, Pretoria, Report TT 82/96, pp 276.

Scott, D.F. and Lesch, W. 1995. The water yield gains obtained from clearfelling riparian zone vegetation. Paper presented at the SANCIAHS 7th National Hydrology Symposium, Grahamstown.

Scott, D.F. and Lesch, W. 1996. The effects of riparian clearing and clearfelling of an indigenous forest on streamflow, stormflow and water quality. *South African Forestry Journal*, 175, 1-13.

Seber, G.A.F and Wild, C.J. 1989. Nonlinear regression. John Wiley and sons, New York. Toms J.D. and M.L Lesperance 2003 . Piecewise Regression: A tool for identifying ecological Thresholds. *Ecology* 84 8, 2034-2041.

Smith, C.W. 1995. Assessing The Compaction Susceptibility Of South African Forestry Soils. Unpublished PhD thesis, University of Natal, Pietermaritzburg.

Smithers, J.C. and Schulze, R.E. 1995. ACRU 3.0 User Manual. Water Research Commission, Report.

Soil Conservation Service Engineering Division. 1986. Urban hydrology for small watersheds. U.S. Department of Agriculture, Technical Release 55.

Soil Conservation Service. 1972. Section 4: Hydrology, In National Engineering Handbook. SCS.

Swanson, R.H. and Whitfield, D.W.A. 1981. A numerical analysis of heat pulse velocity theory and practice. *Journal of Experimental Botany*, 32, 221-239.

Swanson, R.H. 1983. Numerical and experimental analysis of implanted-probe heat pulse theory. PhD Thesis, University of Albert, Canada, pp 1-235.

Toms J.D. and M.L Lesperance 2003. Piecewise Regression: A tool for identifying ecological Thresholds. Ecology 84 8, 2034-2041.

United States Department of Agriculture. 1985. National Engineering Handbook, Section 4, Hydrology. USDA Soil Conservation Service, Washington DC, USA.

Versfeld, D.B. 1985. Rainfall interception in Protea Neriifolia, measurement and prediction. MSc Thesis, University of Stellenbosch.

Van den Berg, M., Klampt, E., van Reeuwijk, L.P. and Sombroek, W.G. 1997. Pedotransfer functions for the estimation of moisture retention characteristics of ferrasols and related soils. *Geoderma*. 78, 161-180.

Van Genuchten, M. Th. 1980. A closed-form equation for predicting the hydraulic conductivity of unsaturated soils. *Soil Sci. Soc. Am. J.* 44, 892-898.

Van Genuchten, M. Th., Leij, F.J and Yates, S.R. 1991. The RETC code for quantifying the hydraulic functions of unsaturated soils. Report EPA/600/2-91/0651. U.S. Environmental Protection Agency, ADA, Oklahoma.

Van Der Zel, D.W. and Kruger, F.J. 1975. . Results of the multiple catchment experiments at the Jonkershoek Research Station, South Africa. *Forestry in South Africa*, 16, 13-18

Van Wyk, D.B 1977. Die invloed van bebossing met Pinus radiate op die totale jaarlikse afvoer van die Jonkershoek strome. M.Sc. Thesis, Univ. Stellenbosch, Unpublished .

Van Wyk, D.B. 1987. Some effects of afforestation on streamflow in the western Cape Province, *South Africa. Water SA*, 13, 1, 31-36.

Williams, J.R., Jones, C.A. and Dyke, P.T. 1984. A modelling approach to determining the relationship between erosion and soil productivity. Trans. ASAE Vol. 21, 129-144.

Williams, J.R. 1995. Chapter 25: The EPIC model. p. 909-1000. In V.P. Singh ed . Computer models of watershed hydrology. Water Resources Publications, Highlands Ranch, CO.

Woodborne, S., Robertson, I. and February, E. 2003. The use of isotope δ13C techniques to define the riparian zone in commercially afforested catchments. Water Research Commission Report No. 1218/1/03. 58pp. ISBN No: 1-77005-097-3.

Zhang, L., Dawes, W.R. and Walker, G.R. 1999. Predicting the effect of vegetation changes on catchment average water balance. CSIRO Technical Report 99/12, CRC for Catchment Hydrology, CSIRO, Canberra, Australia.

Appendix 1.

Values utilised in respect of input variables for respective verification simulations for the ACRU model.

Note: The convention (1,2) in the variable column is used when values in cell 1 and cell 2 are identical.

Variable	All Forest	All Grass	Riparian Grass
ICELL	1(distributed)	1 (distributed)	1 (distributed)
ISUBNO	2	2	2
MINSUB	1	1	1
MAXSUB	2	2	2
LOOPBK	0 (no)	0 (no)	0 (no)
IROUTE	0 (none)	0 (none)	0 (none)
DELT	1440.0	1440.0	1440.0
ICELLN 1	1	1	1
ICELLN 2	2	2	2
IDSTRM 1	2	2	2
IDSTRM 2	2	2	2
IRAINF 1	Cmp2S5000	Cmp2S5000	Cmp2S5000
IRAINF 2	Cmp2S5000	Cmp2S5000	Cmp2S5000
FORMAT			
1	3	3	3
2	3	3	3
PPTCOR			
1	0	0	0
2	0	0	0
MAP 1	964	964	964
MAP 2	964	964	964
CORPPT			
1	Jan-Dec 1.00	Jan-Dec 1.00	Jan-Dec 1.00
2	Jan-Dec 1.00	Jan-Dec 1.00	Jan-Dec 1.00
IOBSTQ (1,2)	0 (none)	0 (none)	0 (none)
IOBSPK (1,2)	0 (none)	0 (none)	0 (none)
IOBOVR (1,2)	0 (none)	0 (none)	0 (none)
ISTRMF	(n/a)	(n/a)	(n/a)

Variable	All Forest	All Grass	Riparian Grass
DNAMIC			
1	0 (none)	0 (none)	0 (none)
2	0 (none)	0 (none)	0 (none)
IDYNFL			
1	2s1.fil	2s1.fil	2s1.fil
2	2s1.fil	2s1.fil	2s1.fil
HEAD			
1	02s1-ALLFOREST	02s1-ALLGRASS	02s1-RIPGRASS
2	02s1-ALLFOREST RIPARIAN	02s1-ALLGRASS	02s1-RIPGRASS RIPARIAN
CLAREA			
1	.65	.65	.65
2	.08	.08	.08
ELEV			
1	1000.0	1000.0	1000.0
2	1000.0	1000.0	1000.0
ALAT(1,2)	29.20	29.20	29.20
ALONG(1,2)	30.65	30.65	30.65
IHEMI(1,2)	2 (south)	2 (south)	2 (south)
IQUAD(1,2)	1 (east)	1 (east)	1 (east)
IYSTRT(1,2)	1950	1950	1950
IYREND(1,2)	2000	2000	2000
TMAX(i) (1,2)	J=26.2, F=26.6, M=26.6, A=24.8, M=22.8, J=21.0, J=20.3, A=21.1, S=22.4, O=23.4, N=24.3, D=25.5	J=26.2, F=26.6, M=26.6, A=24.8, M=22.8, J=21.0, J=20.3, A=21.1, S=22.4, O=23.4, N=24.3, D=25.5	J=26.2, F=26.6, M=26.6, A=24.8, M=22.8, J=21.0, J=20.3, A=21.1, S=22.4, O=23.4, N=24.3, D=25.5
TMIN(i) (1,2)	J=16.1, F=16.3, M=15.4, A=13.4, M=10.4, J=8.3 J=7.9, A=8.8, S=10.1, O=12.0, N=13.3, D=14.8	J=16.1, F=16.3, M=15.4, A=13.4, M=10.4, J=8.3 J=7.9, A=8.8, S=10.1, O=12.0, N=13.3, D=14.8	J=16.1, F=16.3, M=15.4, A=13.4, M=10.4, J=8.3 J=7.9, A=8.8, S=10.1, O=12.0, N=13.3, D=14.8

Variable	All Forest	All Grass	Riparian Grass
EQPET (1,2)	109	109	109
IEIF(1,2)	0 (n0)	0 (no)	0 (no)
ILRF(1,2)	0 (no)	0 (no)	0 (no)
IWDF(1,2)	0 (no)	0 (no)	1 (yes)
IRHF(1,2)	0 (no)	0 (no)	0 (no)
ISNF(1,2)	0 (no)	0 (no)	0 (no)
IRDF(1,2)	0 (no)	0 (no)	0 (no)
IPNF(1,2)	0 (no)	0 (no)	0 (no)
E(i) (1,2)	J=176.0, F=153.0, M=146.0, A=124.0, M=108.0, J=95.0, J=105.0, A=132.0, S=148.0, O=160.0, N=159.0, D=177.0	J=176.0, F=153.0, M=146.0, A=124.0, M=108.0, J=95.0, J=105.0, A=132.0, S=148.0, O=160.0, N=159.0, D=177.0	J=176.0, F=153.0, M=146.0, A=124.0, M=108.0, J=95.0, J=105.0, A=132.0, S=148.0, O=160.0, N=159.0, D=177.0
TELEV(1,2)	1040.0	1040.0	1040.0
LRREG(1,2)	0	0	0
TMAXLR(1,2)	7.00	7.00	7.00
TMINLR(1,2)	5.50	5.50	5.50
WNDSPD(1,2)	2.1	2.1	2.1
LINWIN(1,2)	2	2	2
WIND(i) (1,2)	J=183.0, F=159.0, M=151.0, A=140.3, M=149.2, J=156.2, J=180.0, A=198.7, S=227.4, O=215.9, N=223.4, D=202.1	J=183.0, F=159.0, M=151.0, A=140.3, M=149.2, J=156.2, J=180.0, A=198.7, S=227.4, O=215.9, N=223.4, D=202.1	J=183.0, F=159.0, M=151.0, A=140.3, M=149.2, J=156.2, J=180.0, A=198.7, S=227.4, O=215.9, N=223.4, D=202.1

Variable	All Forest	All Grass	Riparian Grass
RH(i) (1,2)	J=80.4, F=80.2, M=78.4, A=78.4, M=64.5, J=62.3, J=63.4, A=63.5, S=66.9, O=72.7, N=76.4, D=77.5	J=80.4, F=80.2, M=78.4, A=78.4, M=64.5, J=62.3, J=63.4, A=63.5, S=66.9, O=72.7, N=76.4, D=77.5	J=80.4, F=80.2, M=78.4, A=78.4, M=64.5, J=62.3, J=63.4, A=63.5, S=66.9, O=72.7, N=76.4, D=77.5
ALBEDO(1,2) ICONS ISWAVE	(0.07) (n/a) (n/a)	(0.07) (n/a) (n/a)	(0.07) (n/a) (n/a)
ASSH(i) (1,2)	(2.0) J-D	(2.0) J-D	(2.0) J-D
ACONS(i) (1,2)	J=0.22, F=0.23, M=0.25, A=0.25, M=0.34, J=0.30, J=0.34, A=0.27, S=0.29, O=0.22, N=0.20, D=0.21	J=0.22, F=0.23, M=0.25, A=0.25, M=0.34, J=0.30, J=0.34, A=0.27, S=0.29, O=0.22, N=0.20, D=0.21	J=0.22, F=0.23, M=0.25, A=0.25, M=0.34, J=0.30, J=0.34, A=0.27, S=0.29, O=0.22, N=0.20, D=0.21
BCONS(i) (1,2)	J=0.71, F=0.67, M=0.54, A=0.49, M=0.36, J=0.40, J=0.36, A=0.45, S=0.45, O=0.58, N=0.76, D=0.76	J=0.71, F=0.67, M=0.54, A=0.49, M=0.36, J=0.40, J=0.36, A=0.45, S=0.45, O=0.58, N=0.76, D=0.76	J=0.71, F=0.67, M=0.54, A=0.49, M=0.36, J=0.40, J=0.36, A=0.45, S=0.45, O=0.58, N=0.76, D=0.76
RADMET(1,2)	J=19.5, F=18.3, M=16.3, A=13.7, M=12.4, J=11.5, J=12.5, A=13.9, S=15.6, O=16.7, N=17.3, D=18.9	J=19.5, F=18.3, M=16.3, A=13.7, M=12.4, J=11.5, J=12.5, A=13.9, S=15.6, O=16.7, N=17.3, D=18.9	J=19.5, F=18.3, M=16.3, A=13.7, M=12.4, J=11.5, J=12.5, A=13.9, S=15.6, O=16.7, N=17.3, D=18.9
SAPANC(1,2)	1	1	1
SARAT(i) (1,2)	J=1.26, F=1.25, M=1.26, A=1.27, M=1.30, J=1.34, J=1.36, A=1.37, S=1.35, O=1.32, N=1.28, D=1.27	J=1.26, F=1.25, M=1.26, A=1.27, M=1.30, J=1.34, J=1.36, A=1.37, S=1.35, O=1.32, N=1.28, D=1.27	J=1.26, F=1.25, M=1.26, A=1.27, M=1.30, J=1.34, J=1.36, A=1.37, S=1.35, O=1.32, N=1.28, D=1.27
PANCOR(1,2)	0 (no)	0 (no)	0 (no)
CORPAN(1,2)	1.00(J-D)	1.00(J-D)	1.00(J-D)
PEDINF(1,2)	1	1	1
ITEXT 1 2	 10 2	 10 2	 10 2
IRDIST(1,2)	1	1	1

Variable	All Forest	All Grass	Riparian Grass
PEDDEP(1,2)	2	2	2
DEPAHO(1,2) DEPBHO(1,2) WP1 1 2 WP2 1 2 FC1 1 2 FC2 1 2 PO1 1 2 PO2 1 2 ABRESP 1 2 BFRESP 1 2	.34 .87 .143 .272 .165 .288 .268 .420 .257 .364 .579 .590 .535 .594 0.36 0.10 0.36 0.10	.34 .62 .143 .272 .165 .227 .268 .420 .257 .364 .579 .590 .535 .594 0.36 0.10 0.36 0.10	.34 .87 .143 .272 .165 .227 .268 .420 .257 .364 .579 .590 .535 .594 0.36 0.10 0.36 0.10
ICRACK(1,2)	0	0	0
SMAINI 1 2 SMBINI 1 2	 .20 .40 0.30 0.50	 .50 .60 0.60 0.70	 .20 .40 0.30 0.50
SWLOPT(1,2)	0	0	0

Variable	All Forest	All Grass	Riparian Grass
SWLAM(i)(1,2)	1=0.018 2=0.050 3=0.100 4=0.150 5=0.200 6=0.300	1=0.018 2=0.050 3=0.100 4=0.150 5=0.200 6=0.300	1=0.018 2=0.050 3=0.100 4=0.150 5=0.200 6=0.300
SWLBM(i)(1,2)	1=0.018 2=0.050 3=0.100 4=0.150 5=0.200 6=0.300	1=0.018 2=0.050 3=0.100 4=0.150 5=0.200 6=0.300	1=0.018 2=0.050 3=0.100 4=0.150 5=0.200 6=0.300
LCOVER(1,2)	1,1	1,0	0,0
CROPNO 1 2	 6030303 6030303	 2030104 2030104	 6030303 2030104
INTLOS(1,2)	1	1	1
LAIND(1,2)	1,1	0,0	1,0
CAY(i) 1 2	 J=.90, F=.90, M=.90, A=.88, M=.85, J=.86, J=.89, A=.90, S=.92, O=.92, N=.90, D=.90 J=.90, F=.90, M=.90, A=.88, M=.85, J=.86, J=.89, A=.90, S=.92, O=.92, N=.90, D=.90	 J=.75, F=.75, M=.75, A=.65, M=.40, J=.20, J=0.20, A=.20, S=.30, O=.60, N=.65, D=.70 J=.75, F=.75, M=.75, A=.65, M=.40, J=.20, J=0.20, A=.20, S=.30, O=.60, N=.65, D=.70	 J=.90, F=.90, M=.90, A=.88, M=.85, J=.86, J=.89, A=.90, S=.92, O=.92, N=.90, D=.90 J=.75, F=.75, M=.75, A=.65, M=.40, J=.20, J=0.20, A=.20, S=.30, O=.60, N=.65, D=.70

Variable	All Forest	All Grass	Riparian Grass
ELAIM(i)			
1	J=2.62, F=2.61, M=2.60, A=2.45, M=2.24, J=2.11, J=2.04, A=2.09, S=2.20, O=2.38, N=2.48, D=2.46	J=2.62, F=2.61, M=2.60, A=2.45, M=2.24, J=2.11, J=2.04, A=2.09, S=2.20, O=2.38, N=2.48, D=2.46	J=2.62, F=2.61, M=2.60, A=2.45, M=2.24, J=2.11, J=2.04, A=2.09, S=2.20, O=2.38, N=2.48, D=2.46
2	J=3.40, F=3.39, M=3.38, A=3.31, M=3.25, J=3.16, J=2.96, A=2.92, S=2.97, O=3.09, N=3.22, D=3.30	J=3.40, F=3.39, M=3.38, A=3.31, M=3.25, J=3.16, J=2.96, A=2.92, S=2.97, O=3.09, N=3.22, D=3.30	J=3.40, F=3.39, M=3.38, A=3.31, M=3.25, J=3.16, J=2.96, A=2.92, S=2.97, O=3.09, N=3.22, D=3.30
VEGINT(i)			
1	J=1.76, F=1.76, M=1.76, A=1.73, M=1.70, J=1.68, J=1.67, A=1.68, S=1.70, O=1.72, N=1.74, D=1.76	J=1.50, F=1.50, M=1.50, A=1.50, M=1.50, J=1.50, J=1.50, A=1.50, S=1.50, O=1.50, N=1.50, D=1.50	J=1.76, F=1.76, M=1.76, A=1.73, M=1.70, J=1.68, J=1.67, A=1.68, S=1.70, O=1.72, N=1.74, D=1.76
2	J=2.07, F=2.07, M=2.07, A=2.06, M=2.05, J=2.04, J=2.01, A=2.00, S=2.01, O=2.03, N=2.05, D=2.06	J=1.50, F=1.50, M=1.50, A=1.50, M=1.50, J=1.50, J=1.50, A=1.50, S=1.50, O=1.50, N=1.50, D=1.50	J=1.50, F=1.50, M=1.50, A=1.50, M=1.50, J=1.50, J=1.50, A=1.50, S=1.50, O=1.50, N=1.50, D=1.50
ROOTA(i)			
1	J=.70 ,F=.70, M=.70, A=.70, M=.70, J=.79, J=.70, A=.70, S=.70, O=.70, N=.70, D=.79	J=.90, F=.90, M=.9, A=.94, M=.94, J=.94, J=.94, A=.94, S=.92, O=.92, N=.90, D=.90	J=.70 ,F=.70, M=.7, A=.70, M=.70, J=.79, J=.70, A=.70, S=.70, O=.70, N=.70, D=.70
2	J=.73 ,F=.73, M=.73, A=.73, M=.73, J=.73, J=.73, A=.73, S=.73, O=.73, N=.73, D=.73	J=.90, F=.90, M=.9, A=.94, M=.94, J=.94, J=.94, A=.94, S=.92, O=.92, N=.90, D=.90	J=.90, F=.90, M=.9, A=.94, M=.94, J=.94, J=.94, A=.94, S=.92, O=.92, N=.90, D=.90
EFRDEP			
1	1.21	1.21	1.21
2	1.21	1.21	1.21
EVTR(1,2)	2	2	2
FPAW(1,2	0	0	0
CONST			
1	0.70	0.90	0.70
2	0.70	0.90	0.80

Variable	All Forest	All Grass	Riparian Grass
FOREST			
1	1	0	1
2	1	0	0
CO2TRA	0 (no)	0 (no)	0 (no)
TMPCUT(1,2)	1.0	1.0	1.0
IUNSAT(1,2)	1	1	1
LYSIM	0 (no)	0 (no)	0 (no)
QFRESP			
1	0.05	0.40	0.05
2	0.05	0.40	0.40
COFRU			
1	.005	0.020	0.005
2	0.020	0.020	0.020
SMDDEP			
1	0.40	0.34	0.40
2	0.40	0.34	0.40
IRUN			
1	1	1	1
2	1	1	1
ADJIMP			
1	.015	0.020	.015
2	.015	0.020	.015
DISIMP(1,2)	0.055	0.060	0.055
STOIMP(1,2)	1.00	1.00	1.00
COIAM(i)			
1	J=.25, F=.25, M=.25, A=.30, M=.30, J=.30, J=.35, A=.35, S=.30, O=.30, N=.25, D=.25	J=.30, F=.30, M=.30 A=.30, M=.30, J=.30, J=.30, A=.30, S=.30, O=.30, N=.30, D=.30	J=.25, F=.25, M=.25 A=.30, M=.30, J=.30, J=.35, A=.35, S=.30, O=.30, N=.25, D=.25
2	J=.25, F=.35, M=.35, A=.35, M=.35, J=.35, J=.35, A=.35, S=.35, O=.35, N=.35, D=.35	J=.30, F=.30, M=.30 A=.30, M=.30, J=.30, J=.30, A=.30, S=.30, O=.30, N=.30, D=.30	J=.30, F=.30, M=.30 A=.30, M=.30, J=.30, J=.30, A=.30, S=.30, O=.30, N=.30, D=.30
PEAK(1,2)	0 (no)	0 (no)	0 (no)
LAG(1,2)	1	1	1
SLOPE(1,2)	12.3	12.3	12.3
HYLEN(1,2)	146.	146.	146.
CNII	51.	51.	51.

Other related WRC reports available:

Improving the basis for predicting total evaporation from natural veld types in South Africa

Jarmain C; Govender M; Everson CS

Evapotranspiration or "green water" represents between 50 and 99 % of our natural water balance in South Africa. Hydrology, rain-fed agriculture and irrigation have in the past followed somewhat different methods to estimate evapotranspiration of plants and plant covers. This project aims at building a common base from which the integration of the various catchment management activities (afforestation, wetland rehabilitation and alien vegetation control) can be quantitatively understood and prioritised.

Report Number: 1219/1/04 **ISBN No: 1 77005 171 6**

TO ORDER: Contact **Publications** - Telephone No. 012 330 0340
Fax Number: 012 331 2565
E-mail: publications@wrc.org.za

9781770056138

Water Research Commission
Private Bag X03, Gezina, 0031, South Africa
Tel: +27 12 330 0340, Fax: +27 12 331 2565
Web: http://www.wrc.org.za

Designed by The Kashan Group K-2102 (www.kashangroup.com)